Vapour-Liquid Equilibrium Measurements at Moderate Pressures using a Semi-Automatic Glass Recirculating Still

Hitesh Lilwanth 206500452

Supervisor: Dr. P. Naidoo

Co-Supervisors: Prof. D. Ramjugernath

Prof E Eitelberg

This thesis has been submitted in fulfillment of the academic requirement for the degree of Master of Science in Engineering (MSc.Eng.) at the school of Chemical Engineering, University of Kwa-Zulu Natal

January 2014

Declaration

I, Hitesh Lilwanth, declare that:

(i) The research reported in this dissertation, except where otherwise indicated, is my original work.

(ii) This dissertation has not been submitted for any degree or examination at any other university.

(iii) This dissertation does not contain other persons' data, pictures, graphs or other information, unless specifically acknowledged as being sourced from other persons.

(iv) This dissertation does not contain other persons' writing, unless specifically acknowledged as being sourced from other researchers. Where other written sources have been quoted, then:

a. Their words have been re-written but the general information attributed to them has been referenced;

b. Where their exact words have been used, their writing has been placed inside quotation marks, and referenced.

(v) This thesis does not contain text, graphics or tables copied and pasted from the internet, unless specifically acknowledged, and the source being detailed in the thesis and in the References sections.

_____ _____

Hitesh Lilwanth Date

As the candidate supervisor, I, Dr. P. Naidoo, approved this dissertation for submission.

_____

Dr. P. Naidoo

As the candidate co-supervisor, I, Prof. D. Ramjugernath, approved this dissertation for submission.

_____

Prof. D. Ramjugernath

Acknowledgments

I would like to this opportunity to express my deepest gratitude and appreciation to the following people and organizations that have made a significant contribution to this project and my study career:

- My supervisors Dr. P. Naidoo, Prof D. Ramjugernath and Prof E Eitelberg.

- The workshop and laboratory staff at the University of KwaZulu-Natal, especially Ayanda Khanyile and Lindinkosi Mkhize

- My colleagues in Chemical Engineering, specifically Travis Pio Benecke, Renay Sewpersad, Kuveneshan Moodley, David Lokhat, Samuel Iwarere, Wayne Nelson and Prashant Reddy.

- The National Research Foundation (NRF) of South Africa for financial support.

- My parents, Raj and Nisha Lilwanth for their continuous support and motivation throughout this study.

Abstract

Vapour-liquid equilibrium (VLE) data of high accuracy and reliability is essential in the development and optimization of separation and chemical processes. This study focuses on satisfying the growing demand for precise VLE data at low to moderate pressures, by development of a computer-aided dynamic glass still which is semi-automated. The modified dynamic glass still of Joseph *et al.* (2001) was employed to achieve precise measurement of phase equilibrium data for a pressure range of 0 to 500 kPa.

The study involved the assembling and commissioning of a new moderate pressure dynamic still and various peripheral apparati. The digital measurement and control systems were developed in the object-oriented graphical programming language LabVIEW. The digital proportional controller with integral action developed by Eitelberg (2009) was adapted for the control of pressure and temperature. Pressure and temperature measurements were obtained by using a WIKA TXM pressure transducer and Pt-100 temperature sensor respectively.

The calculated combined standard uncertainties in pressure measurements were ±0.005 kPa, ±0.013kPa and ±0.15kPa for the 0-10 kPa, 10-100 kPa and 100-500 kPa pressure ranges respectively. A combined standard uncertainty in temperature of ±0.02 K was calculated.

The published data of Joseph *et al.*, (2001) and Gmehling *et al,*. (1995) for the cyclohexane (1) and ethanol (2) system at 40kPa and 1-hexene (1) + N-methyl pyrrolidone-2 (NMP) (2) system at 363.15 K respectively served as test systems. NMP is regarded as one of the most commonly used solvents in the chemical industry due to its unique properties such as low volatility, thermal and chemical stability. As a result the isothermal measurement of 1-hexene (1) + N-methyl pyrrolidone-2 (NMP) (2) system were conducted at 373.15 K constituting new VLE data. A further system comprising 1-propanol (1) and 2-butanol (2) was also measured at an isothermal temperature of 393.15 K.

The measured data were regressed using the combined and direct methods. The equations of state of Peng-Robinson (1976) and Soave-Redlich-Kwong (1972) combined with the mixing rules of Wong-Sandler (1992) in conjunction with a Gibbs

excess energy model was utilized for the direct method. The activity coefficient models namely Wilson (1964) and NRTL (Renon and Prausnitz, 1968) were chosen to describe the liquid non-idealities while the vapour phase non-ideality was described with the virial equation of state with the Hayden and O' Connell (1975) correlation. Thermodynamic consistency of the measured data was confirmed using the point test of Van Ness et al. (1973) and the direct test of Van Ness (1995).

Table of Contents

List of Figures

Chapter 2

Chapter 3

Chapter 4

Chapter 5

Chapter 6

Chapter 7

Chapter 8

Appendix C

List of Tables

Chapter 4

Chapter 7

Chapter 8

Nomenclature

English Letters

A_i	Constant in the Antoine equation
A_{12}	Parameters in the Van Laar Model (1910)
A_{21}	Parameters in the Van Laar Model (1910)
A^E	Excess Helmholtz free energy at infinite pressure
a	Intermolecular attraction force parameter of the Soave Redlich-Kwong (1972) equation of state or the Peng-Robinson (1976) equation of state
a_m	Mixture intermolecular attraction force parameter of the Soave Redlich-Kwong (1972) equation of state or the Peng-Robinson (1976) equation of state
a_c	Critical Parameter
a_{vdw}	Mixing parameter for the van der Waals (1873) mixing rules
B_i	Constant in the Antoine equation
B_{ii}	Second Virial coefficient of pure component i [cm^3/mol]
B_{ij}	Second Virial coefficient of interaction of species i - j interaction [cm^3/mol]
b	Parameter for the molecular size of component for Soave Redlich-Kwong (1972) equation of state or the Peng-Robinson (1976) equation of state
b_m	Mixture parameter for the molecular size for the Soave Redlich-Kwong (1972) equation of state or the Peng-Robinson (1976) equation of state
C_i	Constant in the Antoine equation
D	Summation term in the mixing rule of Wong Sandler (1992)
F_1, F_2	Response factors
f_i	Fugacity of component i [kPa]
$\hat{f}_i$	Fugacity of species i in solution

G	Molar Gibbs Energy [J/kmol]
$\overline{G_i}$	Partial molar Gibbs free energy [J/kmol]
G^E	Excess Gibbs Energy [J/kmol]
G_{ij}	The Non-Random-Two-Liquid (NRTL) model of Renon and Prausnitz (1968) parameter.
g_{ij}-g_{ii}	Energy interaction parameters between components in the NRTL model of Renon and Prausnitz (1968)
k_{ij}	Binary interaction parameter in the Wong-Sandler mixing rule.
n	Number of moles
P	System pressure [kPa]
Q	Summation term in the mixing rule of Wong Sandler (1992)
R	Universal Gas Constant [J/mol.K]
R_d	Mean radius of gyration [Å]
T	System Temperature [K]
U	Molar or specific internal energy [J/kmol]
V	Molar or specific volume [cm^3/mol]
x	Liquid phase mole fraction or composition
y	Vapour phase mole fraction or composition
Z	Compressibility factor

Greek Letters

α_{ij}	Non-randomness parameter in NRTL (1968) model.
γ	Activity coefficient
γ_i^{∞}	Activity coefficient at infinite dilution
Δ	Denotes residuals for the point test of Van Ness(1973)

δ_{ij}	Term reflecting the second virial coefficients.
ε_A	Tolerances used for object functions
μ_i	Chemical potential of component i
μ_d	Dipole moment
Φ	Ratio of fugacity coefficients and the Poynting correction factor
ϕ	Fugacity coefficient
$\hat{\phi}_i$	Fugacity coefficient in solution
Λ_{ij}	Wilson (1964) parameter
$\lambda_{ij} - \lambda_{ii}$	Molar interaction parameter for the Wilson (1964) equation
κ	Constant in the Peng-Robinson (1976) equation of state
τ_{ij}	Parameter in the NRTL (1968) model.
ω	Acentric factor

Subscript

1	Denotes component 1
2	Denotes component 2
c	Denotes critical property
i	Denotes component i
j	Denotes component j
r	Denotes reduced

Superscript

E	Denotes an excess property
id	Denotes an ideal solution

l	Denotes liquid phase
R	Denotes a residual property
sat	Denotes a saturated property
v	Denotes a vapour phase
π	Denotes a thermodynamic phase

Abbreviations

NMP	N-methyl pyrrolidone-2
RMS	Root mean square
VLLE	Vapour-liquid-liquid equilibrium
VLE	Vapour Liquid Equilibrium
PR-WS (NRTL)	Peng Robinson (1976) equation of state with the Wong Sandler (1992) mixing rule that includes the NRTL activity coefficient model
SRK-WS (NRTL)	Soave-Redlich-Kwong (1972) equation of state with the Wong Sandler (1992) mixing rule that includes the NRTL activity coefficient model.
HOC-NRTL	Hayden and O'Connell (1975) virial equation of state (vapour phase) with the NRTL activity coefficient.
HOC-WIL	Hayden and O'Connell (1975) virial equation of state (vapour phase) with the Wilson activity coefficient

1. Introduction

The most commonly employed industrial process for the separation of liquid mixtures is undoubtedly distillation. Distillation is preferred as it produces large volumes of product in an efficient and controlled manner. In recent times, the distillation process has evolved immensely through the use of complex computer aided process design/simulation and operation tools. These technological advancements require accurate vapour-liquid equilibrium (VLE) and in some cases vapour-liquid-liquid equilibrium (VLLE) data to perform their functions.

Although predictive tools for phase equilibrium are available to engineers, the measurement of VLE is still indispensable especially for non-ideal systems. Research (Seker and Somer, 1992) indicates that a theoretical approach in predicting phase equilibrium at conditions of interest with sufficient accuracy is not always possible due to the uncertainties in liquid behavior in mixtures and differences in chemical structures and compositions of compounds. Therefore considering the large capital investments and operating costs involved during design and operations, it is essential and profitable that accurate and reliable methods be employed in determining vapour-liquid equilibria, particularly regarding non-ideal systems.

Furthermore simulation packages such as Aspen are limited in application due to insufficient phase equilibrium data being published. Industrial companies such as SASOL also rely on publication of VLE data and physical properties to optimize chemical processes and facilitate measures in reducing effluents that could be potentially harmful to the environment. Currently extensive experimental work has been published with regards to low pressure and high pressure VLE however there seems to be a lack of experimental VLE data at moderate pressures. A recent survey conducted by Dohrn *et al.* (2010) confirms a growing interest in high pressure phase equilibria compared to low or moderate pressures.

The lack of VLE publications at moderate pressure conditions could be attributed to the difficulty in phase equilibria measurements and the time consuming experimental procedure associated with working at moderate conditions (30 kPa to 500 kPa).

However the mentioned range is of particular importance as a number of chemical and petroleum separation processes operate within this range (Reddy, 2006).

The overall research objective of this study is to determine whether it is possible to develop a semi-automated apparatus for VLE measurements, and to verify its capability by comparison of the VLE data measured with data from literature.

Additionally, insufficient experimental work has been conducted regarding systems containing the commonly used solvent N -methyl pyrrolidone-2 (NMP). An existing publication by Fisher *et al*. (1996) contains P-x data only; therefore the data was not subjected to rigorous thermodynamic consistency testing. NMP is a desired industrial solvent due to its selective affinity for aromatics, unsaturated hydrocarbons and sulfur, and performing measurements of this system would be valuable

This project comprises:

a. Assembling of the new apparatus (modified VLE glass still) and auxiliary equipment setup. The entire apparatus setup must allow for transition from low to medium pressure during isobaric and isothermal experimental measurements and must be automatic with regards to temperature and pressure control. The process control being fully automated is regarded as a major step in the advancement of VLE research.

b. Commissioning of the equipment by performing various tests.

c. Measurement of test systems to verify experimental procedures and confirm accuracy of equipment. The test system to be investigated is cyclohexane (1) + ethanol (2).

d. The new binary systems investigated which have limited/insufficient literature data available and are of particular economic importance to industrial partners:
    - ✓ 1-hexene(1) + N-methyl pyrrolidone-2(NMP) (2)
    - ✓ 1-propanol (1) + 2-butanol (2).

e. The correlation of VLE data to suitable phase equilibrium models and use of regression procedures to determine model binary interaction parameters. In addition, thermodynamic consistency tests will be performed to validate the experimental data.

2. Thermodynamic Principles for Vapour-Liquid Equilibrium

Phase equilibrium knowledge is essential for planning, development and operation of various separation processes within chemical industries (Grenner *et al.*, 2005). Separation processes such as distillation, extraction and absorption utilize differences in phase equilibrium properties, reported in vapour-liquid, liquid-liquid, vapour-solid or liquid-solid literature data to achieve desired stream purities.

Vapour-liquid equilibrium measurements are frequently performed for binary systems (Raal and Mühlbauer, 1998) and can be extended to predict multi-component system properties, valuable for industrial simulation packages. Vapour-liquid equilibrium measurements are both time consuming and expensive therefore the data obtained must be of the highest quality and maximum theoretical treatment of the data should be achieved. Theoretical treatment includes the extrapolation and interpolation of the measured data from experimental conditions to conditions experienced at industries.

In thermodynamics the term equilibrium state is defined as a static condition whereby the macroscopic properties of the system remain constant with respect to time, or when the chemical potentials of all species in each phase are equal. This is the fundamental basis on which vapour-liquid equilibrium is derived.

This chapter provides a brief review of the theoretical aspects and techniques of low to medium pressure VLE data reduction and analysis. Methods for the evaluation of fugacity and activity coefficients are proposed together with a discussion of the regression and correlation of experimental data. This comprises of the gamma-phi formulation (indirect method), the associated activity coefficient models and the phi-phi (direct) method of modeling using the equations of state (Clifford, 2004). A review of pertinent thermodynamic consistency tests for VLE concludes the chapter. For further in-depth knowledge regarding thermodynamic behavior the following texts are recommended Raal and Mühlbauer (1998), Smith *et al.* (2001) and Walas (1964).

2.1. The criterion for phase equilibrium

For any closed system, the canonical variables, temperature and pressure are related to the Gibbs energy by the following equation:

$$d(nG) = (nV)dP - (nS)dT \tag{2.1}$$

However considering a single-phase open system, where material can either enter the system from the surroundings or leave the system to the surroundings, the Gibbs energy now becomes a function of n_i the number of moles of a specific chemical species i within the system. The Gibbs energy is still a function of pressure and temperature. This is shown as:

$$nG = g(P,T, n_i) \tag{2.2}$$

The total differential of equation (2.1) will result in

$$d(nG) = (nV)dP - (nS)dT + \sum_i \mu_i dn_i \tag{2.3}$$

where:

$$\left[\frac{\partial(nG)}{\partial n_i}\right]_{P,T,n_j} = \mu_i \tag{2.4}$$

μ_i, referred to as the chemical potential of species i, has a unique significance in solution thermodynamics. Equation (2.4) is regarded as the fundamental property relation.

2.2. Fugacity and fugacity coefficient

The chemical potential μ_i, is used in the criterion for phase equilibrium but is defined in relation to immeasurable quantities for which their absolute values are unknown (Narasigadu, 2006). As a result, absolute values for chemical potential μ_i, are unavailable. Therefore a meaningful quantity fugacity f was introduced by G.N Lewis,

in units of pressure (Smith *et al.*, 2001). Fugacity can be related to the chemical potential μ_i at constant temperature by the equation

$$\mu_i = \Gamma_i(T) + RT \ln f_i \tag{2.5}$$

The fugacity coefficient of component *i*, represented as ϕ_i , is related to fugacity by the equation below (refer to Smith *et al.*, 2001 for derivation):

$$\phi_i = \frac{f_i}{P} \tag{2.6}$$

Similarly, the fugacity of species *i* in solution is given by $\hat{f}_i$, and the definition of the fugacity coefficient is extended to include the fugacity coefficient of species *i* in solution (Smith *et al.*, 2001), given by $\hat{\phi}_i$.

The expressions for the fugacity of the vapour and liquid in solution are as follows:

$$\hat{f}_i^V = \hat{\phi}_i y_i P \tag{2.7}$$

$$\hat{f}_i^L = x_i \gamma_i f_i \tag{2.8}$$

The γ_i in equation (2.8) is the activity coefficient of species *i* in solution and will be discussed in section 2.6.

2.3. Poynting correction factor

The exponential term known as Poynting correction factor, derived in Smith *et al.* (2001), corrects the fugacity arising from saturation conditions:

$$f_i = \phi_i^{sat} P_i^{sat} \exp\left[\frac{V_i^l \left(P - P_i^{sat}\right)}{RT}\right] \tag{2.9}$$

When the difference between the system pressure and the saturation pressure of the liquid is not considerable, normally at low to moderate pressures, the Poynting

correction becomes close to unity and can be omitted (but not applicable to polar compounds such as carboxylic acids and strongly associating compounds) Reddy (2006). By combining equations (2.7), (2.8) and (2.9) the following expression results:

$$y_i \Phi_i P = x_i \gamma_i P_i^{sat} \tag{2.10}$$

A simplifying term Φ_i is introduced and is quantified as follows:

$$\Phi_i = \frac{\widehat{\phi}_i}{\phi_i^{sat}} \exp\left[\frac{-V_i^l \left(P - P_i^{sat}\right)}{RT}\right] \tag{2.11}$$

The evaluation of the V_i^l in the Poynting correction can be achieved using the Rackett (1970) equation:

$$V_i = (V_c)_i (Z_c)_i^{[1-(T_r)_i]^{0.285}} \tag{2.12}$$

where for component *i*, Z_c is the critical compressibility factor and V_c the critical molar volume and $(T_r)_i$ is the reduced temperature defined as $\frac{T}{(T_c)_i}$ while $(T_c)_i$ critical temperature of component *i*.

2.4. Equations of State

Thermodynamic properties such as internal energy and enthalpy required for calculations of heat and work within industrial processes are often estimated from measurements of molar volume as a function of temperature and pressure, leading to pressure/volume/temperature (*PVT*) relations, which may be expressed mathematically as equations of state (Smith *et al.*, 2001). Equations of state provide a convenient way of describing properties of pure compounds and non-polar or slightly polar fluid mixtures. However, recently numerous papers (Focke, 2004, Mingjian *et al.*, 2007, Marco and Trebble, 1997) have been published extending equations of states to strongly polar compounds.

2.4.1. Virial equation of state

The virial equation of state was derived from a statistical mechanical framework, therefore on a theoretically basis capable of representation of properties of pure gases and mixtures (Reddy, 2006).

Perry and Green (1998) reiterates the opinions of many researchers (Prausnitz, 1969; Smith and Van Ness, 1987) that the truncated (after the second term), generalized, pressure explicit form of the virial equation of state (convenient form) is capable of accurately evaluating fugacity coefficients and compressibility's, from low to moderate pressures (up to 15000 kPa). The equation is as follows

$$Z = 1 + \frac{BP}{RT} \tag{2.13}$$

where, Z is known as the compressibility factor, *PV/RT*. *B,* second virial coefficient and is a function of temperature and composition. The composition dependence can be obtained from the following statistical mechanics based, mixing rule equation

$$B_{mixture} = \sum_i \sum_j y_i y_j B_{ij} \tag{2.14}$$

where *i* and *j* identify species and *y* represents the mole fractions in a gas mixture. The cross virial coefficient B_{ij} characterizes a bimolecular interaction between molecule *i* and *j* consequently therefore $B_{ij} = B_{ji}$.

For a binary system, equation (2.14) reduces to

$$B_{mixture} = y_1^2 B_{11} + y_1 y_2 B_{12} + y_2^2 B_{22} \tag{2.15}$$

where B_{11} and B_{22} terms represent the pure component virial coefficients and B_{12} term is the mixture cross coefficient.

Equation (2.1) is transformed as result of the assumption that the truncated virial equation of state describes the vapour phase. The following equation is obtained

$$\Phi_i = \exp\left[\frac{\left(B_{ii} - V_i^l\right)\left(P - P_i^{sat}\right) + P y_j^2 \delta_{ij}}{RT}\right] \tag{2.16}$$

where

$$\delta_{ij} = 2B_{ij} - B_{ii} - B_{jj} \tag{2.17}$$

Experimental methods can be used to determine second virial coefficients for pure substances B_{ii} and mixtures B_{ij} or alternatively it can be obtained from various experimental compilations such as Dymond and Smith (1980) and Cholinski *et al.* (1986). However due to the temperature dependencies and the difficulty in obtaining experimental data for a specific species, correlations were formed that enabled calculations of second virial coefficients. Some of these correlations include Tsonopoulos (1974), Nothnagel *et al.* (1973), O'Connell and Prausnitz (1967), Black (1958) and Hayden and O'Connell (1975).

This study only considers the Hayden and O'Connell (1975) correlation, as it provides an accurate, yet simple, method for predicting second virial coefficients for a large range of compounds using only the critical properties and molecular parameters.

2.4.1.1. Hayden and O'Connell Correlation

The established predictive method by Hayden and O'Connell (1975) was developed based on the various kinds of intermolecular forces between pairs of molecules which contribute to the second virial equation. The method takes into account strong association and solvation effects and incorporates the chemical theory of dimerization (Pillay, 2009).

The input parameters required for the correlation include critical temperature T_c, critical pressure P_c dipole moment μ, mean radius of gyration R_d, solvation and association parameters η.

The total second virial coefficient is considered to be the sum of numerous contributions:

$$B_{total} = B_{free} + B_{metastable} + B_{bound} + B_{chen} \tag{2.18}$$

where B_{free} refers to contributions by free pairs of non-polar and non-association molecules, $B_{metastable}$ and B_{bound} indicates the type of pair interactions as a result of potential energy and distance between molecular centers, metastable bound pairs and strongly bound pairs and B_{chen} refers to the chemical bonds of associating substances.

Due to the complexity of the method and the calculation procedure it will not be shown in detail here. The reader is referred to the publication by Hayden and O'Connell (1975) and Appendix A of Prausnitz *et al.* (1980).

The critical parameters can be obtained from Frendenslund *et al.*, (1977), Reid *et al.*, (1988), Prausnitz *et al.* (1980) and the Dortmund Data Bank (DDB, 2010). The dipole moments are available in McClellan (1974) or can be found using the method proposed by Smyth (1955). When the mean radius of gyration is unavailable, the method proposed by Harlacher and Braun (1970) together with the group contribution method of Reid *et al.* (1988) can be used. Harlacher and Braun (1970) formed a relationship between the mean radius of gyration and the property parachor, P' (calculated by the method of Reid *et al.* (1988)) as follows:

$$P' = 50 + 7.6R_d + 13.75R_d^2 \tag{2.19}$$

The positive root from equation (2.19) represents the real value of R_d. The association and solvation parameters for most systems are available in the tables published in Prausnitz *et al.* (1980) alternatively values of chemically similar systems may be used.

Hayden and O'Connell (1975) suggests that the association and solvation parameters may be set to zero for species that are chemically un-similar (are not in the same hydrocarbon group) and determined empirically for chemically similar systems.

2.4.2. Cubic Equations of State

Cubic equations of state are regarded as the simplest method of describing both liquid and vapour behavior. In 1873, J.D van der Waals introduced the first cubic equation that incorporated the non-zero size of molecules and the attractive force between them. The equation consists of two species specific parameters that allow calculation of

pressure as a function of volume for various values of temperature. However, due to the fact that the model parameters are not temperature dependent and its simplistic treatment of attractive forces, it makes the model inappropriate for non-ideal systems that require rigorous quantitative calculations. Through extensive research the general form of the van der Waals cubic equation has been significantly modified enabling better description of non-ideal systems. The first significant modification was that of Redlich-Kwong in 1949, which provided more accurate treatment of nonideal systems than previous models. However its limitations arise from the poor representation of liquid phase behavior. Among the many cubic equations of state available the Soave-Redlich-Kwong (SRK) equation of state and the Peng-Robinson (PR) equation of state are the most widely used to predict vapour-liquid equilibrium for non-polar or slightly polar systems. Through the incorporation of a suitable mixing rule these equations of states can also be extended to describe non-ideal chemical systems.

2.4.2.1. Soave-Redlich-Kwong (SRK) Equation of State

In 1972, Soave modified the temperature-dependent function of the original Redlich-Kwong equation with a more proficient function term involving temperature and the acentric factor namely *a (T, ω)*. The modification significantly improved the accuracy in predicting vapour pressures of pure substances and made the estimate of vapour-liquid equilibrium of mixtures feasible (Mingjian *et al.*, 2007). The SRK equation of state was regarded as the most successful modification of the Redlich-Kwong equation (Reddy, 2006) represented below as:

$$P = \frac{RT}{V-b} - \frac{a(T,\omega)}{V(V+b)} \tag{2.20}$$

where T is the absolute temperature, P and R, are pressure and universal gas constant respectively and V the molar volume. The *a* constant is a function of temperature and represents the force of attraction between molecules while the *b* constant corrects for the volume (Iwarere, 2009) and is temperature independent. The reader is referred to Appendix A for the complete set of equations.

The SRK alpha function, $\alpha(T,\omega)$ used for calculation is:

$$\alpha(T,\omega) = \left[1+\kappa\left(1-T_r^{0.5}\right)\right]^2 \tag{2.21}$$

with κ being a quadratic function of acentric factor ω,

$$\kappa = 0.480 + 1.574\omega - 0.176\omega^2 \tag{2.22}$$

Many researchers have revised the original SRK alpha function as it was found to be sensitive to critical properties. A recent article (Mingjian *et al.* 2007) introduced a new alpha function with reported improved accuracy in estimating vapour-liquid equilibrium compared to the original alpha function, with the greatest improvement shown for systems containing water. The formulation of the modification was based on the saturated vapour-pressure data of 31 pure substances.

Another noteworthy improvement of the alpha function is that of Twu *et al.* (1995), which gave better estimates of vapour pressures at low temperatures. The analysis and comparison of different alpha functions of the SRK equation of state undertaken by Mingjian *et al.* (2007) suggested that the proposed alpha functions of Grabosik and Daubert (1978) and Mathias and Copeman (1983) have no essential difference from the one of Soave and was therefore not considered.

The pure component fugacity coefficient is calculated as follows:

$$\ln\phi = Z - 1 - \ln(Z-B) - \frac{A}{B}\ln\left[\frac{Z+B}{Z}\right] \tag{2.23}$$

The SRK equation of state provides a good estimation of the phase behavior of non-polar or slightly polar substances. Although the SRK equation is seen as a great improvement, it still has the inherent weakness in generating accurate liquid density values. Furthermore it lacks the requirement of a binary interaction parameter that relates molecular parameters to the model (Reddy, 2006). This makes the equation, less capable of accurately representing vapour-liquid equilibria of polar systems.

2.4.2.2. Peng Robinson (PR) Equation of State

The Peng-Robinson (1976) equation of state improved on the predictions of liquid phase behavior through a more complex expression for the volume dependency than that of Soave. It also incorporated a binary interaction parameter to allow better treatment of mixtures. The generalized Peng-Robinson (1976) equation of state is as follows:

$$P = \frac{RT}{V-b} - \frac{a(T,\omega)}{V(V+b)+b(V-b)} \tag{2.24}$$

The *b* constant adjusts for molecular size and is temperature independent while the, *a* constant is temperature dependent and relates to the intermolecular forces of attraction.

$$a(T,\omega) = a_c \alpha\ (T,\omega) \tag{2.25}$$

$$b = 0.07780\left(\frac{RT_c}{P_c}\right) \tag{2.26}$$

The correlation of Stryjek and Vera (1986) extended the applicability of the Peng-Robinson (1976) equation of state, to mixtures that exhibit non-polar and associating properties. The reader is referred to Appendix A, for the complete set of equations.

Peng-Robinson (1976) also included a set of mixing rules:

$$a_m = \sum_i \sum_j x_i x_j a_{ij} \tag{2.27}$$

$$a_{ij} = (1-\delta_{ij})(a_i a_j)^{0.5} \tag{2.28}$$

$$b_m = \sum_i x_i b_i \tag{2.29}$$

δ_{ij} is the binary interaction parameter determined empirically for each unique binary system. The parameter is determined from regression of vapour-liquid data and it

should be noted that $\delta_{ij} = \delta_{ji}$. A discussion on application of mixing rules is covered in section 2.5.

2.5. Mixing Rules

Equations of states can be extended from a pure-component form into a multi-component mixture form through the use of an appropriate mixing rule. The mixing rule incorporates the additional interactions between the different components present in the mixture into the equation of state, for example in a binary system the *ij* interaction between molecule *i* and *j* would be incorporated together with the pure component interaction *ii*.

According to Raal and Mühlbauer (1998) two methods exist for applying cubic equation of state to mixture:

- Pseudo-critical properties (T_{cm}, P_{cm} …) of the mixture are determined first via suitable combining rules, and these are used to calculate the a_m and b_m parameters of the employed equation of state. This method is referred as method A combing rules by Walas (1985) and will not be further discussed.
- The more commonly applied, method B mixing rules by Walas (1985), uses the mixing rule to express the a_m and b_m parameters as some function of composition and pure-component a_i and b_i parameters.

Mixing rules have developed and improved exponentially throughout the years, from the simplest van der Waals one-fluid-theory classical mixing rule to the complex mixing rules of Wong and Sandler (1992) and Twu and Coon (1996). The root motivation for all these developments is the quest for accurate representation and prediction of multi-component vapour-liquid equilibrium. This study focuses on the application of the Wong and Sandler (1992) mixing rules. A more comprehensive review of mixing rules is available in Raal and Mühlbauer (1998).

2.5.1. Wong-Sandler mixing rules

The Wong and Sandler (1992) density-independent mixing rules is widely recognized for its incorporation with cubic equations of state in correlating vapour-liquid equilibria data for strongly non-ideal systems over wide temperature and pressure ranges. Wong and Sandler improved the short-comings of the Huron-Vidal mixing rule essentially

through the use of the excess Helmholtz free energy (A^E) instead of the excess Gibbs free energy (G^E) during the formulations of their mixing rules. The use of A^E, ensured the quadratic composition dependence for the second virial coefficient therefore maintaining consistency with statistical mechanics (Raal and Mühlbauer, 1998). Furthermore it enables the Wong-Sandler mixing rules to be correct at low or high densities without being density dependent.

Wong and Sandler (1992) presented the a_m and b_m (m denotes mixture properties) as follows:

$$\frac{a_m}{RT} = \frac{QD}{(1-D)} \tag{2.30}$$

$$b_m = \frac{Q}{(1-D)} \tag{2.31}$$

with Q and D given by

$$Q = \sum_i \sum_j x_i x_j \left(b - \frac{a}{RT} \right)_{ij} \tag{2.32}$$

$$D = \sum_i x \frac{a_i}{b_i RT} + \frac{A_\infty{}^E}{cRT} \tag{2.33}$$

Wong and Sandler (1992) used the principle that the excess Helmholtz free energy, A^E is a weak function of pressure, which validates the excess Helmholtz at infinite pressure to be equated to the excess Gibbs free energy, G^E at low pressure (Marco and Trebble, 1997). Thus allowing predictions of high pressure vapour-liquid equilibrium from low pressure vapour-liquid equilibrium; furthermore any expression for excess Gibbs free energy can be substituted for excess Helmholtz free energy at constant temperature shown below. The reader is referred to Smith *et al.* (2001), for additional equations and derivations on this mixing rule.

In this study the NRTL Gibbs excess energy model was selected to describe A^E as follows:

$$\frac{A_{\infty}^{e}}{RT} = \sum_{i} x_i \left(\frac{\sum_{j} x_j \tau_{ji} g_{ji}}{\sum_{k} x_k g_{ki}} \right) \tag{2.34}$$

$$\ln \gamma_i^{\infty} = \frac{\sum_{j} x_j \tau_{ji} g_{ji}}{\sum_{k} x_k g_{ki}} + \sum_{j} \frac{x_j g_{ij}}{\sum_{k} x_k g_{kj}} \left(\tau_{ij} - \frac{\sum_{l} x_l \tau_{lj} g_{lj}}{\sum_{k} x_k g_{ki}} \right) \tag{2.35}$$

The cross parameter is calculated as follows:

$$\left(b - \frac{a}{RT} \right)_{ij} = \frac{\left(b_i - \frac{a_i}{RT} \right) + \left(b_j - \frac{a_j}{RT} \right)}{2} \left(1 - k_{ij} \right) \tag{2.36}$$

The adjustable parameter k_{ij} in equation (2.36) is acquired through the regression of binary vapour-liquid equilibrium experimental data. The use of the NRTL Gibbs excess energy model also brings three additional parameters, bringing the overall number of interaction parameters used to four.

2.6. Activity Coefficient

The concept of activity coefficient was introduced to characterize the deviations from ideality associated with the liquid phase. The activity coefficient (according to Prausnitz *et al.*, 1980) can be fully defined only if the standard-state fugacity is clearly specified. The reference point is the ideal solution, with deviations from ideality described through the use of excess functions. The activity coefficient for component *i* in solution is defined as: (the reader is referred to Smith *et al.* (2001) for the derivation)

$$\gamma_i = \frac{\hat{f}_i}{x_i f_i^{o}} \tag{2.37}$$

$$\overline{G}_i^{E} = RT \ln \gamma_i \tag{2.38}$$

By the derivations illustrated in Smith *et al.* (2005) which introduce an alternative form of the fundamental excess property relation that relates the excess thermodynamic properties to the activity coefficients, the following can be written:

$$\ln \gamma_i = \left[\frac{\partial \left(nG^E / RT \right)}{\partial n_i} \right]_{P,T,n_j} \tag{2.39}$$

In general G^E / RT are a function of canonical variables P, T and the mole numbers. Since the natural logarithm of the activity coefficient is a partial molar property with respect to G^E it therefore obeys the summability relationship, Smith *et al.* (2005)

$$\frac{G^E}{RT} = \sum_i x_i \ln \gamma_i \tag{2.40}$$

and the Gibbs Duhem equation can be related to excess properties as:

$$\sum_i x_i \, d \ln \gamma_i = \frac{\overline{V}^E}{RT} dP - \frac{\overline{H}^E}{RT^2} dT \tag{2.41}$$

At constant pressure and temperature equation (2.41) reduces to an important relation used in thermodynamic consistency as shown below:

$$\sum_i x_i \, d \ln \gamma_i = 0 \quad \text{(constant T, P)} \tag{2.42}$$

2.7.Excess Gibbs Energy Models - Activity Coefficient

Currently there exist numerous liquid phase activity coefficient models that account for the non-idealities associated with the liquid phase. The complexity of these models depends on the difficulty associated with trying to describe the system behavior. According to Raal and Mühlbauer (1998) the most complex system behaviours are for components that differ greatly in molecular size and chemical nature.

Some of the most recognizable models include the Margules, Van Laar, Wilson, NRTL (Non-Random Two Liquid) and the UNIQUAC. In this study the Wilson and NRTL

were utilized since a recent work by Hirawan (2007) on similar systems to this project revealed that the Van Laar and NRTL dominated over the other models and allowed for good correlation of experimental data. Furthermore the NRTL model and Wilson are well-known for representing complex and simple systems.

2.7.1. The Van-Laar model

In 1910, Van Laar developed a model to account for the size differences of molecules:

$$\frac{G^E}{RT} = \frac{A_{12}A_{21}}{A_{12}x_1 + A_{21}x_2} \tag{2.43}$$

In terms of activity coefficients:

$$\ln \gamma_1 = A_{12}\left(\frac{A_{21}x_2}{A_{12}x_1 + A_{21}x_2} \right)^2 \tag{2.44}$$

$$\ln \gamma_2 = A_{21}\left(\frac{A_{12}x_1}{A_{12}x_1 + A_{21}x_2} \right)^2 \tag{2.45}$$

where the A_{12} and A_{21} are adjustable parameters. The Van Laar model is a quite simple model with relatively little theoretical basis and is most often applied to non-polar liquids. The constants of the Van Laar equations are purely empirical suggesting that a more complex model is required for representing interactions of liquid components.

2.7.2. The Wilson model

A significant breakthrough in excess Gibbs energy models was formulated in 1964 by G.M. Wilson. This marvelous development introduced the concept of local composition within a liquid solution. Smith *et al,* (2001) states that the local compositions are presumed to account for the short-range order and nonrandom molecular orientations that result from differences in molecular size and intermolecular forces. These differences are due to a variation between the interaction energy of the central molecule with the molecules similar to it namely *i-i* interactions and with the molecules dissimilar to it namely *i-j* interactions (Focke, 2004)

The Wilson equation for a binary system is as follows:

$$\frac{G^E}{RT} = -x_1 \ln\left(x_1 + \Lambda_{12} x_2\right) - x_2 \left(x_1 \Lambda_{21} + x_2\right) \tag{2.46}$$

The activity coefficients are obtained as follows:

$$\ln \gamma_1 = -\ln\left(x_1 + \Lambda_{12} x_2\right) + x_2 \left[\frac{\Lambda_{12}}{x_1 + \Lambda_{12} x_2} - \frac{\Lambda_{21}}{\Lambda_{21} x_1 + x_2} \right] \tag{2.47}$$

$$\ln \gamma_2 = -\ln\left(x_2 + \Lambda_{21} x_1\right) - x_1 \left[\frac{\Lambda_{12}}{x_1 + \Lambda_{12} x_2} - \frac{\Lambda_{21}}{\Lambda_{21} x_1 + x_2} \right] \tag{2.48}$$

where Λ_{21} and Λ_{12} are Wilson adjustable parameters that are related to pure component liquid volumes by the general equation:

$$\Lambda_{ij} = \frac{V_i}{V_j} \exp\left[\frac{\lambda_{ij} - \lambda_{ii}}{RT} \right] \tag{2.49}$$

Aspen Plus® can also be used to determine the Wilson adjustable parameters as purely a function of temperature, ignoring the liquid molar volumes. The study by Van Dyk (2005) recommends this alternative for a better fit to VLE data:

$$\Lambda_{ij} = \exp\left[a_{ij} + \frac{b_{ij}}{T} + c_{ij} \ln T + d_{ij} T \right] \tag{2.50}$$

The binary parameters a_{ij} and b_{ij} shall be determined from VLE data regression c_{ij} and d_{ij} were set to zero. Some of the shortcomings of the Wilson model highlighted in literatures Prausnitz (1969), Renon (1968) and Pillay (2010) were:

- It is not suited for predicting partially miscible systems of two liquid phases.
- It cannot be used for systems that exhibit maxima and minima when the natural logarithm of the activity coefficients is plotted against x_i.
- Systems that experience positive deviations from ideality are represented better, than systems that experience negative deviations from ideality.

The initial guesses for the Wilson parameters Λ_{21} and Λ_{12} used during calculations, are difficult to determine as it is not unique and a range of values will fit the data equally well (Pillay, 2010).

2.7.3. Non-Random Two Liquid (NRTL) model

A substantial improvement in local composition models was achieved through the introduction of the Non-Random Two Liquid model by Renon and Prausnitz (1968). The model has the ability to describe partially liquid miscible systems and completely miscible systems. The formulation of the NRTL equation is based on the two-liquid model of Scott (1956) and an assumption of non-randomness. The NRTL equation has become a favorable and widely used equation among researchers in describing complex system behaviors. The equation is as follows:

$$\frac{G^E}{RT} = \frac{\tau_{21}G_{21}}{x_1 + G_{21}x_2} + \frac{\tau_{12}G_{12}}{x_2 + G_{12}x_1} \tag{2.51}$$

with

$$G_{12} = \exp\left(-\alpha_{12}\tau_{12}\right) \tag{2.52}$$

$$G_{21} = \exp\left(-\alpha_{12}\tau_{21}\right) \tag{2.53}$$

The τ_{12} and τ_{21} are related to the energy parameters g_{ij} by:

$$\tau_{12} = \frac{g_{12} - g_{22}}{RT} \tag{2.54}$$

$$\tau_{21} = \frac{g_{21} - g_{11}}{RT} \tag{2.55}$$

The activity coefficients are found from the following expressions:

$$\ln \gamma_1 = x_2^2\left[\tau_{21}\left(\frac{G_{21}}{x_1 + x_2G_{21}}\right)^2 + \frac{\tau_{12}G_{12}}{\left(x_2 + x_1G_{12}\right)^2}\right] \tag{2.56}$$

$$\ln \gamma_2 = x_1^2\left[\tau_{12}\left(\frac{G_{12}}{x_2 + x_1G_{12}}\right)^2 + \frac{\tau_{12}G_{21}}{\left(x_1 + x_2G_{21}\right)^2}\right] \tag{2.57}$$

The NRTL equations consist of three adjustable parameters namely (g_{21}-g_{22}), (g_{12}-g_{11}) and α_{12}. The (g_{21}-g_{22}) and (g_{12}-g_{11}) are energy parameters that characterize the molecular interactions between species i and j. The parameter α_{12} is a constant that represents the non-randomness of the mixture. In the case of α_{12} being zero it indicates that the mixture is completely random. Typical acceptable values for α_{12} fall between 0.2 and 0.47. Seader and Henley (2006) recommend α_{12} values of:

- 0.2, mixtures of saturated hydrocarbons and polar, non-associated species.
- 0.30, mixtures that exhibit deviations from Raoult's law.
- 0.47, for mixtures of an alcohol or other strongly self-associated species with nonpolar species.

However Raal and Mühlbauer (1998) suggest that the α_{12} value should be determined from experimental data reduction.

2.8.Data Regression

An abundant amount of techniques have been proposed for the reduction of phase equilibrium data with each technique comprising unique advantages and drawbacks in application. In general data reduction involves the condensing of large amount of data into a useable and convenient form. This is achieved by correlating the data to predictive thermodynamic models (liquid phase activity coefficients models or equation of state models) yielding a set of specific interaction parameters for the system. The reduction of data further allows for interpolation and extrapolation from experimental conditions to desired conditions. The reduction techniques selected for this project were the combined method (gamma-phi approach ($\gamma_i - \Phi_i$)) and the direct method (phi-phi approach ($\Phi_i - \Phi_i$))

2.8.1. Combined method (gamma-phi approach) regression

The combined method employs an activity coefficient model to describe the non-idealities of the liquid phase and a suitable equation of state to describe the non-idealities of the vapour phase.

An appropriate procedure or algorithm for obtaining model parameters via regression must be selected. The least squares method developed by Marquardt (1963) and Gess *et al.* (1991) is one such algorithm; however software programs such as Matlab or Aspen have built-in functions to accomplish this with ease. The regression technique involves minimizing the error between the experimental and model values for a particular quantity. The difference between the experimental and model values for a particular quantity is termed residual and symbolized as δ. Any of these quantities: pressure, vapour composition, activity coefficients, excess Gibbs energy are usually selected for minimization. The regression procedure is run until the set minimum value of the objective function is reached (Van Ness and Abbott, 1982).

One such objective function is of the form:

$$S = \sum (\delta P)^2 \tag{2.58}$$

Other objective functions such as δy, $\delta \gamma$, $\delta(G^E/RT)$ will produce a variety of model parameters for VLE data that maybe thermodynamically not perfect. Research conducted by Van Ness (1995) suggests that the objective function form of equation (2.8.1) is simplest and gives results that are equally as good as any other. Aspen Plus® provides additional options for objective function namely: maximum-likelihood, ordinary least squares and Barker's method.

The regression algorithms for isothermal and isobaric data are presented in Figures 2.1 and 2.2. For available isothermal data, pressure and vapour composition values are determined by a bubble point pressure iteration. For available isobaric data, temperature and vapour composition values are determined by a bubble point temperature iteration. This is done for each experimental point.

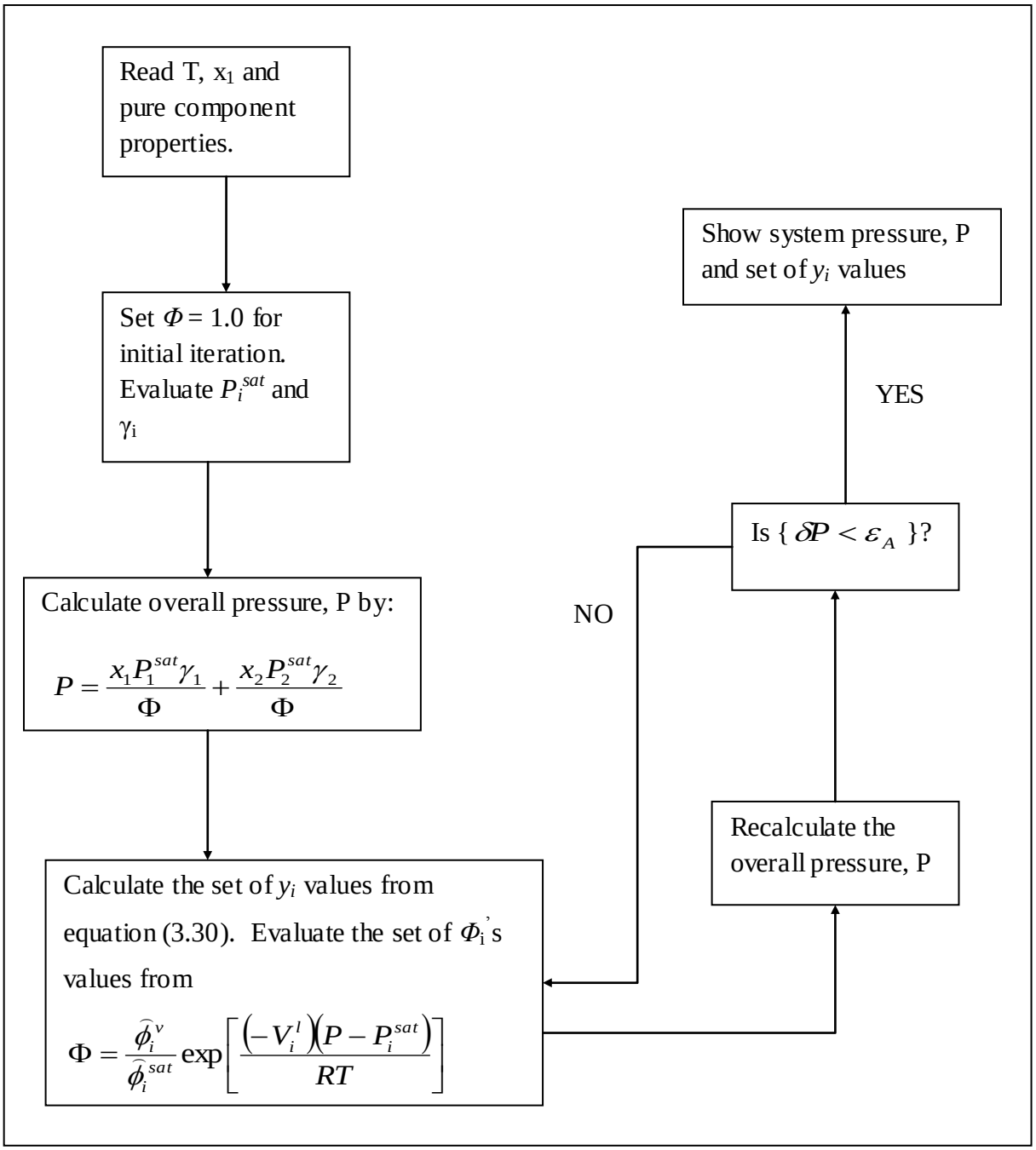

Figure 2.1 Flow diagram for bubble-point pressure iteration (Combined method, Clifford, 2003)

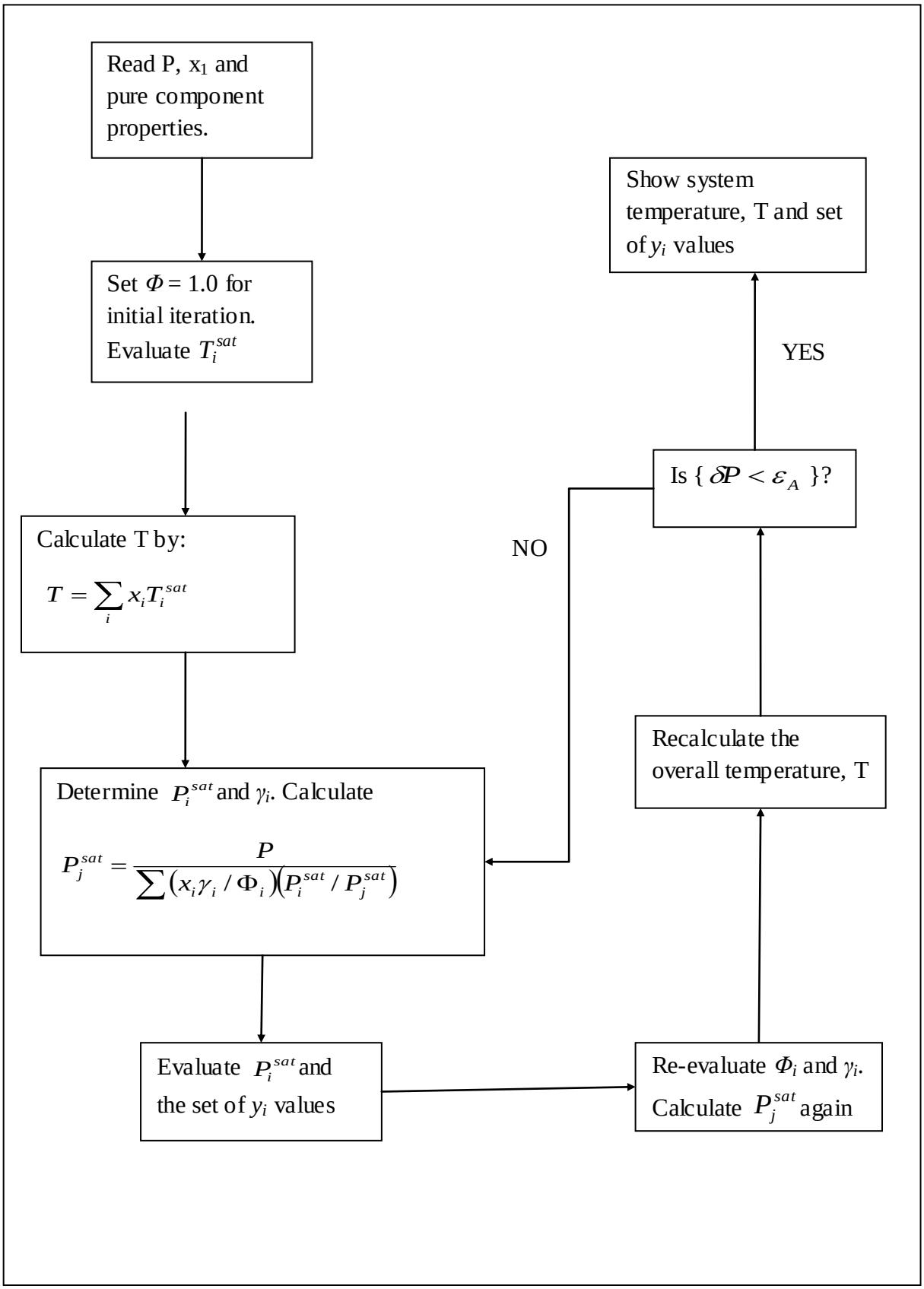

Figure 2.2: Flow diagram for bubble-point temperature iteration (Combined method, Clifford, 2003)

2.8.2. Direct method (phi-phi approach)

In this approach an equation of state represents both the vapour and liquid non-idealities through the use of fugacity coefficients. The equilibrium criterion of equation (2.3) is expanded to:

$$x_i\hat{\phi}_i^l = y\hat{\phi}_i^v \tag{2.59}$$

A suitable equation of state should be selected for the fugacity coefficients $\hat{\phi}_i^L$ and $\hat{\phi}_i^V$. Similarly as for the combined method a good regression procedure needs to be selected to correlate the experimental data. The flow diagram for the bubble pressure iteration and bubble temperature iteration for the direct method are presented in Figures 2.3 and 2.4.

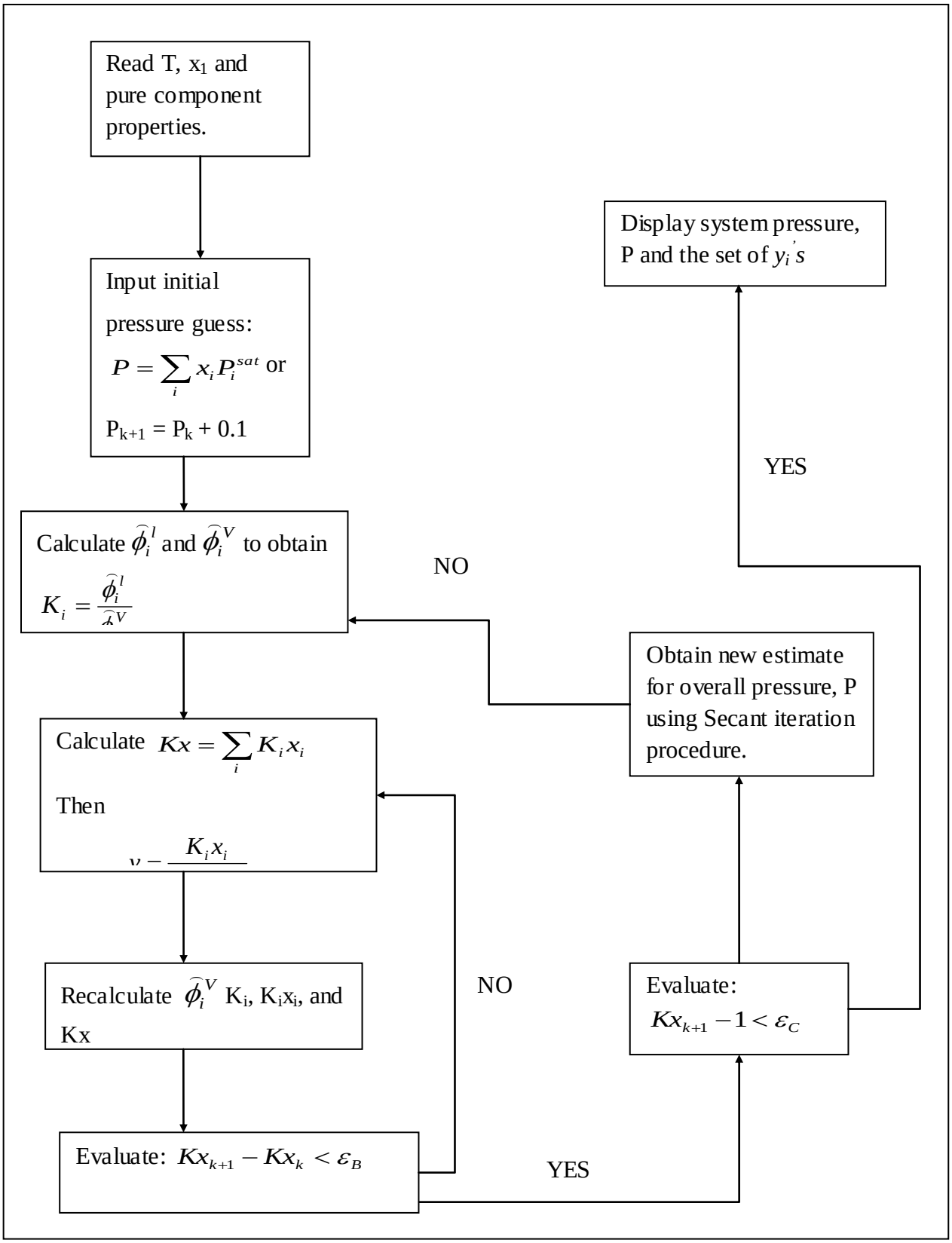

Figure 2.3: Flow diagram for bubble-point pressure iteration (Direct method, Clifford, 2003)

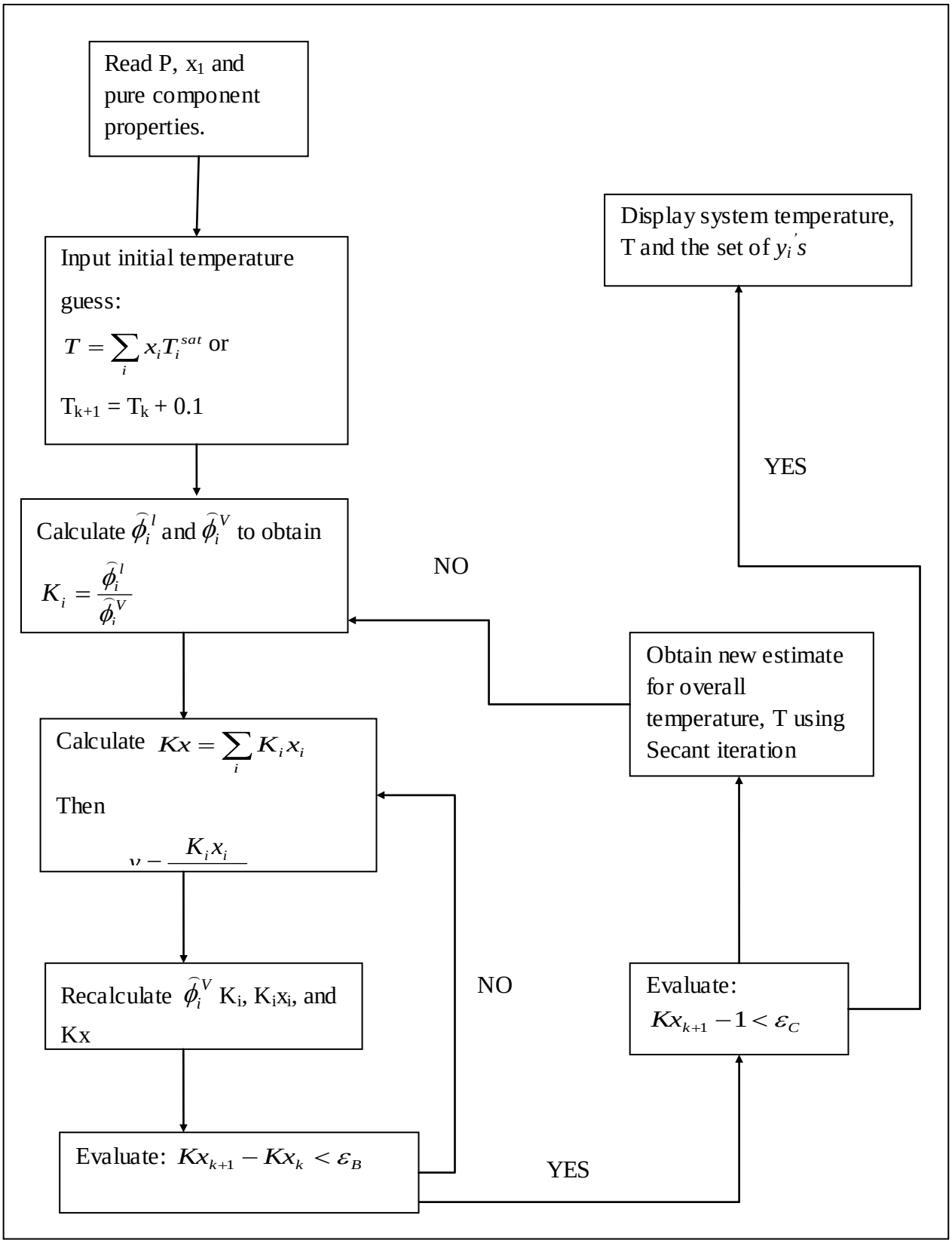

Figure 2.4: Flow diagram for bubble-point temperature iteration (Direct method, Clifford, 2003)

2.9.Thermodynamic consistency testing

Checking the reliability of published experimental phase equilibria data has always been an integral part of thermodynamics. Consistency test serve the purpose of ensuring that published data is of an acceptable quality and can be used with confidence. The development of thermodynamic consistency tests were based on the Gibbs-Duhem equations. Measurements of temperature, pressure, liquid composition and vapour composition for a VLE system is termed "over-specification". As stated in Smith *et al.* (2001) the calculation of any one these variables can be determined from the other three variables using the Gibbs-Duhem equations.

2.9.1. Point test

Van Ness *et al.* (1973) introduced a thermodynamic consistency test that improved on the shortcomings of previous tests such as the area test proposed by Redlich and Kister (1948). The point test is based on the over-specification of variables, allowing any one variable to be calculated from data regression and compared to the actual experimentally measured variable. In most cases the vapour compositions variable is selected as it introduces the most errors. Danner and Gess (1990) introduced a quantitative criterion stating that the absolute average deviation, Δy_{AAD} should be less than 0.01 for the data to be thermodynamic consistent.

The point test is suitable for thermodynamic models that accounts for liquid phase activity coefficients and vapour phase equations of state.

$$\Delta y_{ad} = \frac{1}{n}\sum\left|\left(y_{\exp} - y_{calc}\right)\right| \tag{2.60}$$

where n is the number of experimental points, y_{exp} and y_{calc} are the experimentally measured and calculated vapour composition respectively.

2.9.2. Direct test

Van Ness (1995) developed a simple and efficient consistency test. The method is regarded as a direct measure of deviations from the Gibbs/Duhem equation using residuals. The defining equation for the Direct test is:

$$\delta \ln \frac{\gamma_1^*}{\gamma_2^*} = x_1 \frac{d \ln \gamma_1^*}{dx_1} + x_2 \frac{d \ln \gamma_2^*}{dx_2} - \varepsilon \qquad (2.61)$$

The right hand side of equation (2.61) is the residual that should be exactly equal to zero for consistent data. The extent to which values of this residual fail to scatter about zero measures the departure of the data from thermodynamic consistency. (Van Ness, 1995). The value of the ε term depends on whether the data is isobaric or isothermal. The direct test is primarily applied for activity coefficient models and is inadequate for systems that exhibit association effects (Pillay, 2009).

Van Ness (1995) established a scale to indicate the quality of a data set. The measure is based on the root mean square (RMS) value of the $\delta\left[\ln \frac{\gamma_1^*}{\gamma_2^*}\right]$ term. The scale, termed consistency index starts at 1 for highly consistent data and goes to 10 for very poor quality. For complete understanding and derivation of this test, the reader is referred to Van Ness (1995).

3. Review of Vapour-Liquid Equilibrium measurement techniques

The complexity of determining phase equilibria prompted the development of various measuring techniques and equipment all possessing unique capabilities and limitations. Reddy (2009) attributes the broad spectrum of VLE equipment to its use, were no single type of VLE still is suitable for all temperature and pressure ranges, chemical systems and type of data required. Therefore it is imperative that a general classification be used. The methods for the direct determination phase equilibria can be classified into the following groups (Seker and Somer, 1993):

a) Dynamic techniques
b) Static techniques
c) Dew/Bubble point techniques

The most common techniques are the static and dynamic methods. The dynamic method principally involves the circulation of either the vapour phase, liquid phase or both phases of the boiling mixture through an equilibrium chamber. Alternatively the static method is operated isothermally with both liquid and vapour phases not being circulated. Simply, the static method involves a static cell that contains an agitated liquid mixture in equilibrium with its vapour. The dew and bubble point method reviewed by Malanowski (1982) is normally only employed for high pressure VLE measurements.

Comprehensive literature reviews such as Hala *et al.* (1967), Abbott (1986), Raal and Mühlbauer (1998) and Grenner *et al.* (2005) regarding the different VLE techniques are readily available. In the subsequent sections, emphasis shall be given towards the operations of dynamic circulating stills and to lesser extent static stills as per the intent of this work.

3.1.Static technique

The static method is normally employed for isothermal measurements at high pressures. A static equilibrium cell of constant or variable volume is charged with a degassed liquid mixture and allowed to reach phase equilibrium.

Magnetic stirrers or rocking equipment are employed to agitate the liquid mixture to promote the attainment of equilibrium. However excessive agitation (Raal and Mühlbauer, 1998) creates temperature gradients within the equilibrium cell leading to significant errors in measurements.

The static technique is commonly sub dived into analytic and synthetic static methods. The static analytic technique normally involves the sampling of the liquid phase; while the vapour phase composition is calculated with the measured P-x data. The static synthetic method requires no sampling of phases. A mixture of known composition is prepared and transferred into an equilibrium cell. The temperature and pressure are adjusted until the contents of the cell form a homogenous phase (Nagahame, 1996). Since the starting amounts of each substance within the cell are known, the composition of the homogenous phase can be calculated.

A major concern in the static cell is the degassing of components. Essentially, degassing is the removal of impurities (dissolved gases) from the liquid component. If not executed correctly, these impurities would significantly impact on the accuracy of VLE data as stated by Wilson (2008). The sampling of the equilibrium phases is another concern by many researchers. The process of withdrawing of a sample from the cell may cause a change of the equilibrium state pressure, temperature and composition resulting in the vapour phase partially condensing or the liquid phase partially evaporating. Furthermore during the sampling of the liquid phase, there is a propensity for the more volatile component in the sample to flash if exposed to a lower pressure. Subsequently equilibrium phases sampled are not homogenous and composition analysis is erroneous.

Some of the other disadvantages of the static synthetic technique include the difficulty in precise identification of the incipient phase formation especially dew-points, which

may lead to inaccuracy in measurement of pressure and temperature as stated by Nagahama (1996). The full set of measured VLE data are unavailable (P, T, x and y) but rather calculated using thermodynamic equilibrium relations. As a result, the data cannot be tested for thermodynamic consistency.

3.2.Dynamic technique

The use of dynamic equilibrium stills according to Raal and Mühlbauer (1998) accounts for the largest portion of published VLE measurements. The operation is based on the boiling of a liquid mixture, followed by the continuous separation of vapour and liquid within the equilibrium chamber. The separated vapour is condensed and returned to the boiling chamber were it mixes with the boiling liquid. The separated liquid from the equilibrium chamber is also circulated. The composition of both liquid and vapour phase change with time until a steady state is reached. Measurements of pressure, temperature, liquid and vapour compositions are recorded at steady state as these should differ insignificantly from true equilibrium values for properly designed stills as stated by Marsh (1988).

One of the early dynamic VLE designs was that of Sameshima (1918), involving the circulation of the vapour phase only. Othmer (1928) improved on this design by condensing the vapour generated and returning the condensate to the boiling chamber. The design of Othmer (1928) also permitted the sampling of both phases. Numerous modifications pertaining to this design exist but researchers Raal and Mühlbauer (1998) advise against its use, due to its numerous limitations.

Circulation of both the vapour and liquid phases was accomplished using the dynamic VLE still of Gillespie (1946) based on earlier work of Lee (1931). Gillespie (1946) also incorporated the Cottrell pump of Cottrell (1919) to facilitate the circulation of phases shown in Figure 3.1 below:

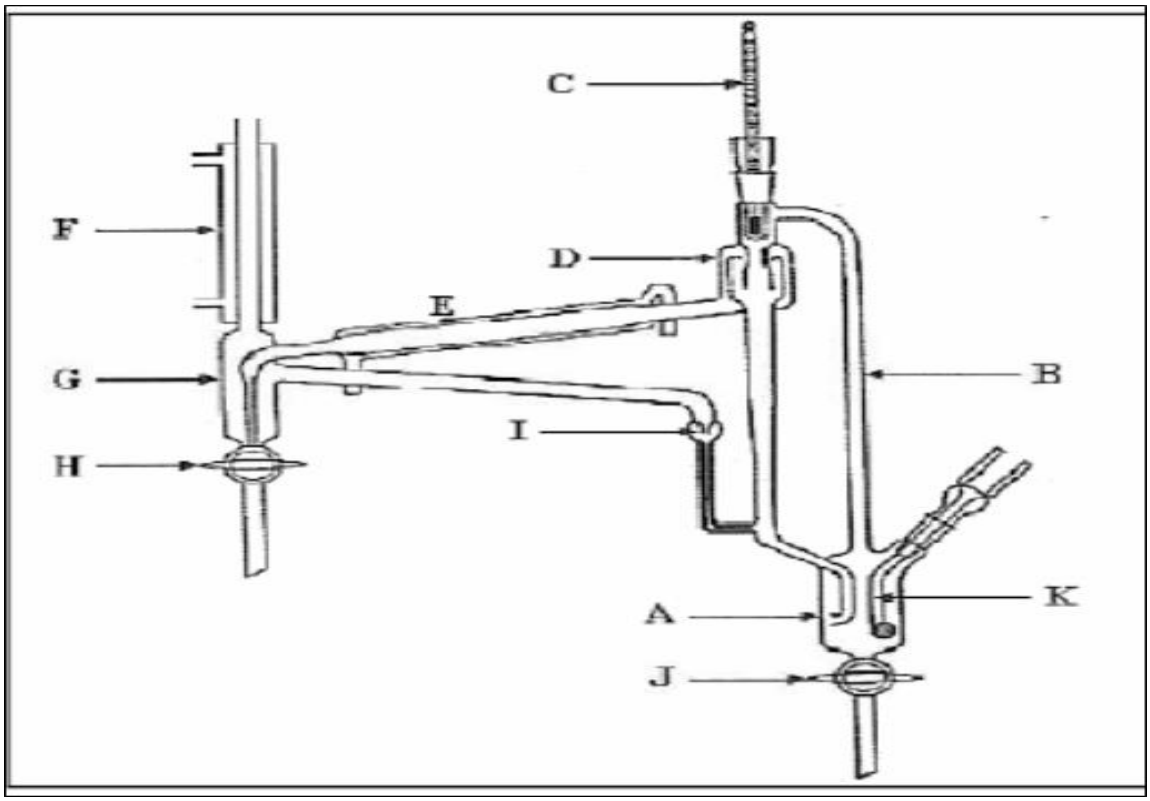

Figure 3.1 Apparatus of Gillespie (1946)

[A: Boiling Chamber; B: Cottrell tube; C: thermometer; D: Vapour-liquid separating chamber; E, F: Condensers; G: Condensate receiver; H: Condensate sample cock; I: Droplet counter; J: Liquid sample cock; K: Internal heater]

Although the VLE still of Gillespie (1946) achieved better quality results than earlier stills, it still contained limitations discussed by Coulson (1946). These were subsequently dealt with by the VLE stills of Yerazunis *et al.* (1964) and later Raal and Mühlbauer (1998).

The dynamic glass still of Raal and Mühlbauer (1998) permitted excellent measurements of low pressure VLE data, some of the exceptional features of this still include:

- A packed equilibrium chamber for better mass transfer and packing material of an open structure reducing pressure drop.
- The entire upper portion of the still which includes the equilibrium chamber and Cottrell tube is insulated with a vacuum jacket. This insulates the equilibrium chamber from possible heating effects caused by upward flowing vapour-liquid mixture.

- The unique feature of the central Cottrell tube design is that the equilibrium chamber is angularly symmetric therefore no preferred radial direction for concentration or temperature gradients to develop.
- The boiling chamber and the condensate receiver have stirring through the use of magnet stirrers.
- An interesting feature is the use of internal and external heaters in the boiling chamber.

A contributor to the design of the moderate pressure dynamic VLE glass was the dissertation of Reddy (2006). The dissertation provided insight on operating at moderate conditions and the subsequent problems. Reddy (2006) designed a dynamic stainless steel still that had improved on the initial design of Harris (2004) through these important features:

- The thicknesses of the walls were sufficient to withstand pressures, but still thin enough to ensure heat transfer to reach internal thermal equilibrium within a reasonable timeframe.
- The still is easily assembled and disassembled.
- Temperature and pressure control is fully automated and the respective sensors need to be placed at strategic points for accurate measurements.
- The fluid flow characteristic and rate of flow of the vapour-liquid mixture through the Cottrell tube is visible. The nature of the flow of the phases within sample traps should also be visible.

Other limitations encountered with moderate pressures include the attainment and realization of steady state, pressure and temperature control, the accuracy and speed of recording measurements of thermodynamic properties at steady state. Some of these limitations have been reduced through the use of sophisticated digital controller strategies such PID control algorithms. The journal publications of Joseph *et al.*, (2001) and Grenner *et al.*, (2005) describe the use of digital control strategies for performing automative isothermal measurements. The central idea is the development of a control algorithm which varies the pressure (adjustments in computer controlled solenoid valves) to attain the desired temperature. This has significantly improved the accuracy and efficiency of obtaining isothermal VLE data by dynamic equilibrium stills.

3.3.Automation Considerations

3.3.1. Review of automated dynamic VLE apparati

The ability for digital control became possible as result of the cost of digital computing decreasing and its speed of operation increasing Alia and Abuzalata (2004). The publication of Grenner *et al.* (2005) describes the use of computer-aided equipment for undertaking precise measurements of vapour-liquid equilibrium data at normal and low pressures. A circulation still developed by Röck and Sieg (1955) forms the central apparatus with which VLE measurements are obtained as shown Figure 3.2. A brief summary for the operation of the VLE still is as follows:

- Firstly the components within the boiling flask (1) are boiled. The vapour generated, travels past the Cottrell-pump (2).
- The vapour and liquid phases are separated at the liquid passing sample point (8).
- The vapour is condensed within the cooler (6) and the condensed vapour enters the sampling point (7).
- Both liquid and vapour streams flow back into the boiling flask dependent on the pestle's (5) position.

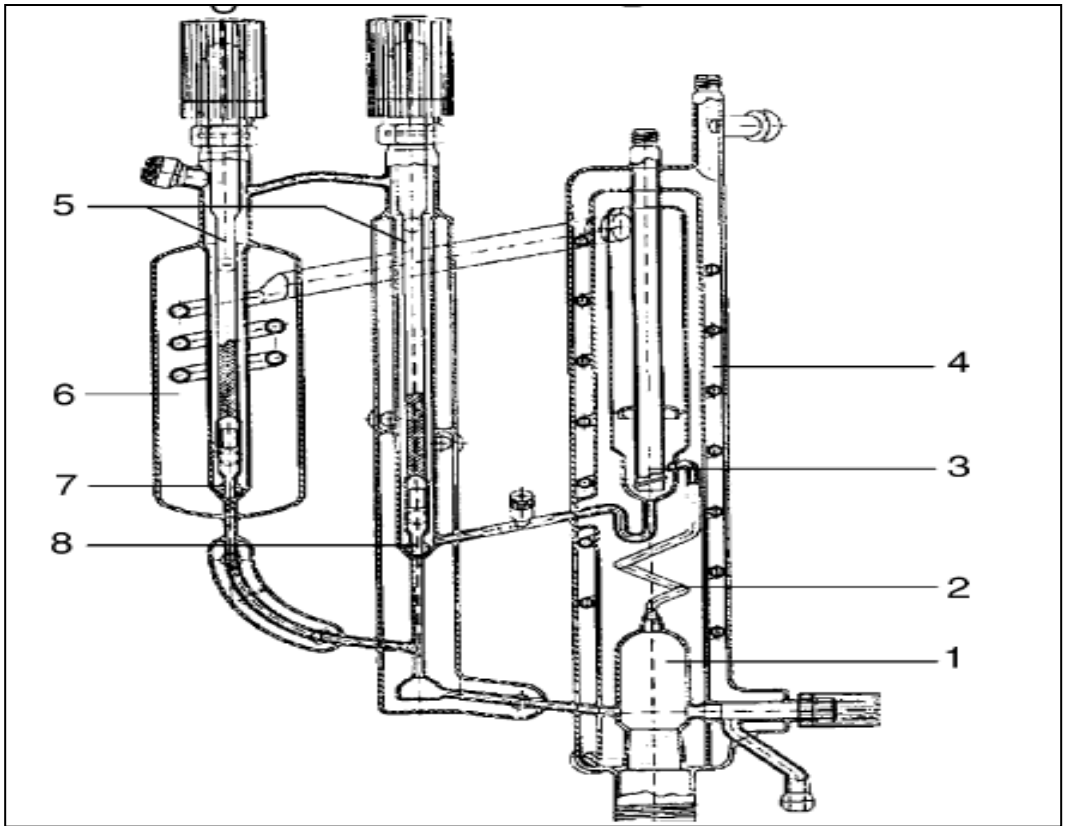

Figure 3.2 Röck and Sieg circulation still (Grenner *et al.*, 2005)
[1: Boiling Flask; 2: Cottrell pump; 3: Temperature measuring point; 4: Silicone oil jacket; 5: Pestle; 6: Cooler; 7: Sampling point, condensed vapour; 8: Sampling point, liquid]

A Pt-100 resistance sensor and Keithley Multimeter 2700 was used to record temperatures. A MKS690 Q pressure transducer and MKS 270 D signal conditioner measured pressure. All the data were transferred via a IEEE-card to the PC. A Druck Incorporated DPI 520 was employed for pressure control while the programming environment of TestPoint® was utilized for performing isobaric and more difficult isothermal measurements.

During isothermal operation, the TestPoint® software calculates the required pressure for the set temperature. The pressure controller will receive the calculated pressure and control accordingly. However the challenge was ensuring that the algorithm is not substance or mixture dependent and caters for system instability resulting from extreme pressure changes to attain a desired temperature. Furthermore no definite relation between temperature and pressure for mixtures is known.

To overcome these shortcomings, Grenner *et al.*, (2005) proposed the use of the Clausius-Clapeyron equation to approximate the necessary pressure changes. The approximation is a calculation of the mixture enthalpy of vapourization using a linear mixing rule of individual component vapourization enthalpies and mole fractions. Grenner *et al.* (2005) improved the approximation by developing equation 3.1 and employing the equation in the control logic.

$$P_{new} = P_{present} \left[1 + \left(1 - \frac{P_2}{P_1}\right) 0.05\right] \tag{3.1}$$

where, P_2 is the current pressure and P_1, is the calculated pressure determined using the Clausius Clapeyron equation. The reported accuracies in measurements were ± 0.06 kPa between a pressure range of 5 – 100kPa and ± 0.03K between a temperature range of 273–373K. The measured VLE data compared satisfactorily with literature data and were proven to be thermodynamically consistent by the methods of Van Ness (1995) and Christiansen and Fredenslund (1975), indicating an efficient set of equipment and correct measurement technique.

Another notable computer driven dynamic still is that completed at the University of Oldenburg: Germany (Gmehling, 2012). The automated VLE still obtains VLE data up to atmospheric pressure, activity coefficients at infinite dilution and pure component vapour pressure data. An ebulliometer is the central apparatus for VLE measurement. A platinum resistance thermometer (Conatex Pt 100) measures temperature inside the cell and a Druck RPT 301 is used for pressure measurements. A Windows program named "Computer-Aided-Ebulliometer-Measuring–System performs all VLE measurements operations except for the filling of components to the cell.

Automation of temperature and pressure control is commonly accomplished by commercial controllers due to its accessibility and affordability. An example of a commercial pressure controller used in VLE measurements is the experimental setup of Ndlovu (2005). Pressure was measured using a Wika model P10 pressure transmitter and controlled with a BUCHI model B-721 pressure controller. A Pt-100 and a Wika model: 4003 $4^1/_2$ digital meter was used for temperature measurement and display

respectively. The reported accuracy for pressure measurement was ±0.03kPa and control to within 0.01 kPa for isobaric operation. The reported accuracy in temperature measurement was within ±0.02K and accuracy of manual temperature control was between ±0.01K and ±0.05K during isothermal operation. The shortfall of the apparatus of Ndlovu (2005) is the dependence on human involvement for phase equilibrium identification and adjustments to heat input required for boiling.

3.3.2. Laboratory Virtual Instrument Engineering Workbench (LabVIEW)

LabVIEW is a product of National Instruments that uses an object-oriented graphical programming language called G that has a style, syntax and data flow, as opposed to text-based programming languages such a C, Pascal or FORTRAN, Hambley (2005). Higher programming languages like such as LabVIEW make programming easier, less error prone and allow the use of floating-point math, (Alia and Abdu Zalata, 2004).

A LabVIEW program called virtual instrument, consists of a front panel and block diagram. The front panel is the user-interface for entering parameters, displaying of results and allows for changes of user-specified parameters during operations. The block diagram is the programming platform and shows how the instrument analyzers sensor data and input from the front panel.

Digital implementation of controller algorithms can be accomplished efficiently by LabVIEW. According to National Instruments (2002) productivity using LabVIEW is (5-10) times better than with other conventional languages such as C.

The flexibility of advanced computer based software control such as LabVIEW allows for on-line controller tuning, for instances during operation, controller gain can be altered in order to minimize system overshoot and response time, keeping at the same time a zero steady-state offset (Alia and Abdu Zalata, 2004).

4. Equipment description and review

The dynamic equilibrium glass still used in this work for measurement of VLE data is a modification of the glass still designed by Joseph *et al.*, (2001). The still of Joseph *et al.* (2001), based on Raal and Mühlbauer (1998), has produced excellent low pressure VLE data and was therefore selected to be modified for moderate pressure measurements (0 to 500 kPa). These modifications were undertaken by the researchers of the Thermodynamics Research Unit of the University of KwaZulu Natal while the assembly and commissioning of the apparatus and peripheral equipment, followed by automation of the dynamic technique are the purposes of this project.

4.1. Modified VLE still of Joseph *et al.* (2001)

The schematic diagram of the moderate pressure VLE glass still commissioned in this project is illustrated in Figure 4.1.The reboiler is charged with a liquid mixture that is brought to the boil by external and internal heaters (I). The external heater consists of nichrome wire wrapped around the boiling chamber which compensates for heat losses to the environment. The internal heater (positioned within the boiling chamber in a glass sheath) consists of a heater cartridge which provides the actual driving force for boiling. The internal heater provides nucleation sites for smooth boiling, improving the circulation rate. The vapour liquid mixture formed moves upward through the vacuum-insulated Cottrell tube (G) and is discharged onto the packing within the equilibrium chamber. The packing in the equilibrium chamber consists of 3mm rolled stainless steel wire mesh cylinders (A) which provide large interfacial areas for increased contact between the liquid and vapour. A Pt-100 (C) sensor is placed within the packing of the equilibrium chamber for accurate reading of the equilibrium temperature. The small holes at the bottom of the equilibrium chamber allows for the disengagement of liquid and vapour. The liquid flows into the liquid trap (S1) and the vapour flows upwards and around the equilibrium chamber thereby acting as thermal lagging. The vapour enters the condenser forming condensate that collects in the condensate receiver (S2). The overflow of condensate returns to the boiling chamber via a standpipe leg.

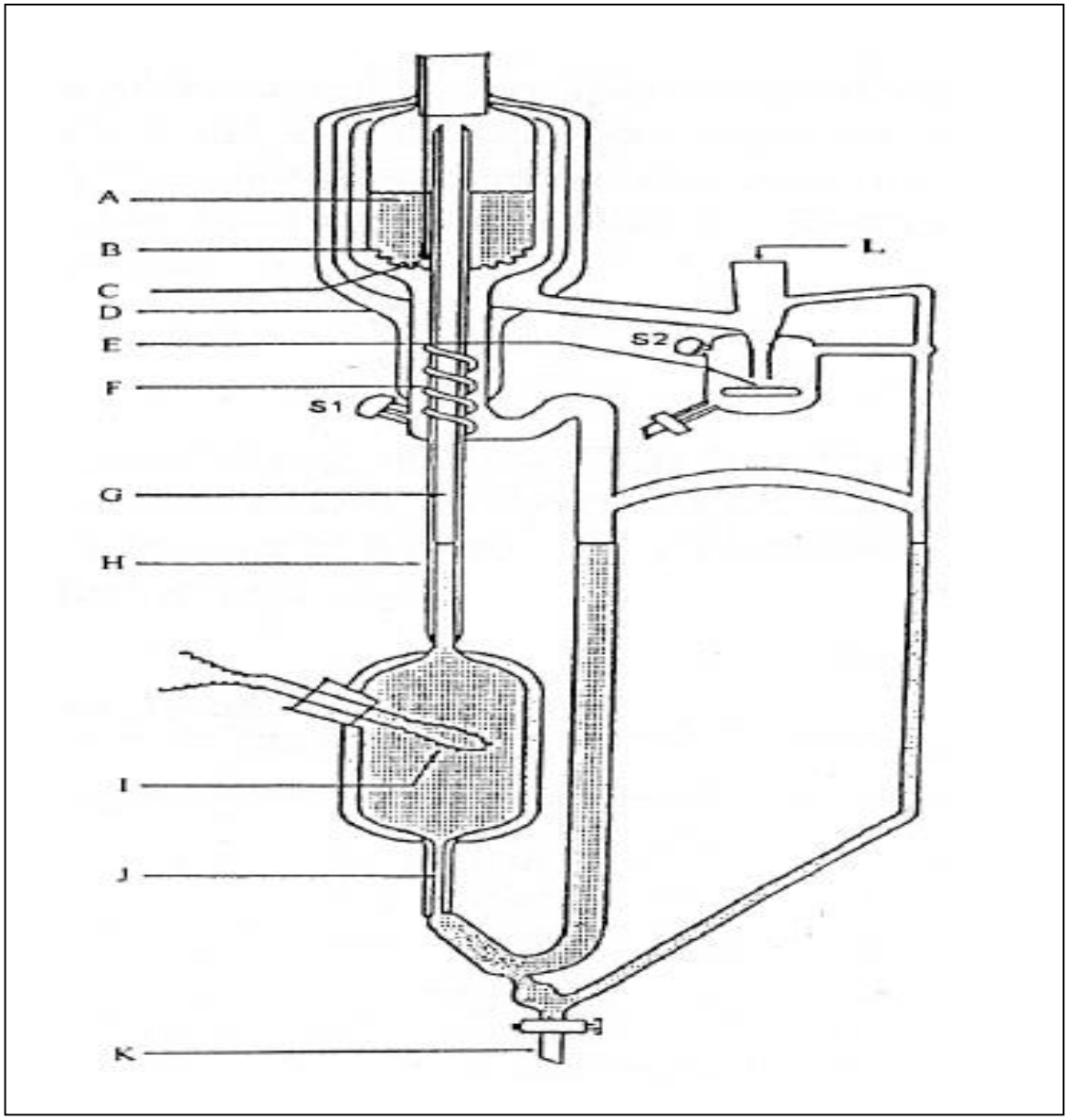

Figure 4.1 Schematic diagram of VLE still (Clifford, 2003)

[A: Stainless steel wire mesh packing; B: Drainage holes; C: Pt-100 sensor; D: Vacuum jacket; E: Magnetic stirrer; F: Stainless steel mixing spiral; G: Insulated Cottrell pump; H: Vacuum jacket; I: Internal heater; J: Capillary leg; K: Drainage valve; L: Condenser attachment; S1: Liquid sampling septum; S2: Vapour sampling septum]

During the construction of the VLE still, the glass thickness was increased by an average of 3mm from that of Joseph *et al.* (2001), improving the tensile strength of the structure. Thus the VLE still although constructed of glass, was designed to operate at pressures from 0 to 500 kPa.

The vapour and liquid septum holders were constructed of plastic and teflon rated for use for temperatures up to 493.15 K. The glass holder for the internal heater cartridge (I) was secured by additional clamps to prevent dislodgment. A clear plastic shield was installed in front of the VLE still. The shield serves as protective barrier against injuries resulting from mechanical failures of the equipment, especially during operation at above atmospheric conditions.

4.2.Peripheral equipment installation

The operation at low to moderate pressures requires the following auxiliary equipment (refer to Figure 4.2):

- Edwards Speedivac Vaccum pump
- Wika TXM 0-5 bars pressure transducer
- 113L Ballast tank
- Two Pt-100 temperature sensors
- Water bath with ethylene glycol and water solution as the cooling medium
- Temp bath controller with pump
- Two 50 ohms precision resistors
- Dual Core Computer (2.13 GHz)
- Three solenoid valves and 6 manual valves
- Delta programmable power supplier (0-75V,0-2A)
- Power suppliers
- National Instruments (NI) Modules N19263, N19216 and NI9203.
- cRIO-9073 eight slot chassis
- DC motor brushes
- Nitrogen gas cylinder with a regulator
- Laboratory Virtual Instrument Engineering Workbench (LabVIEW) BASIC software package.

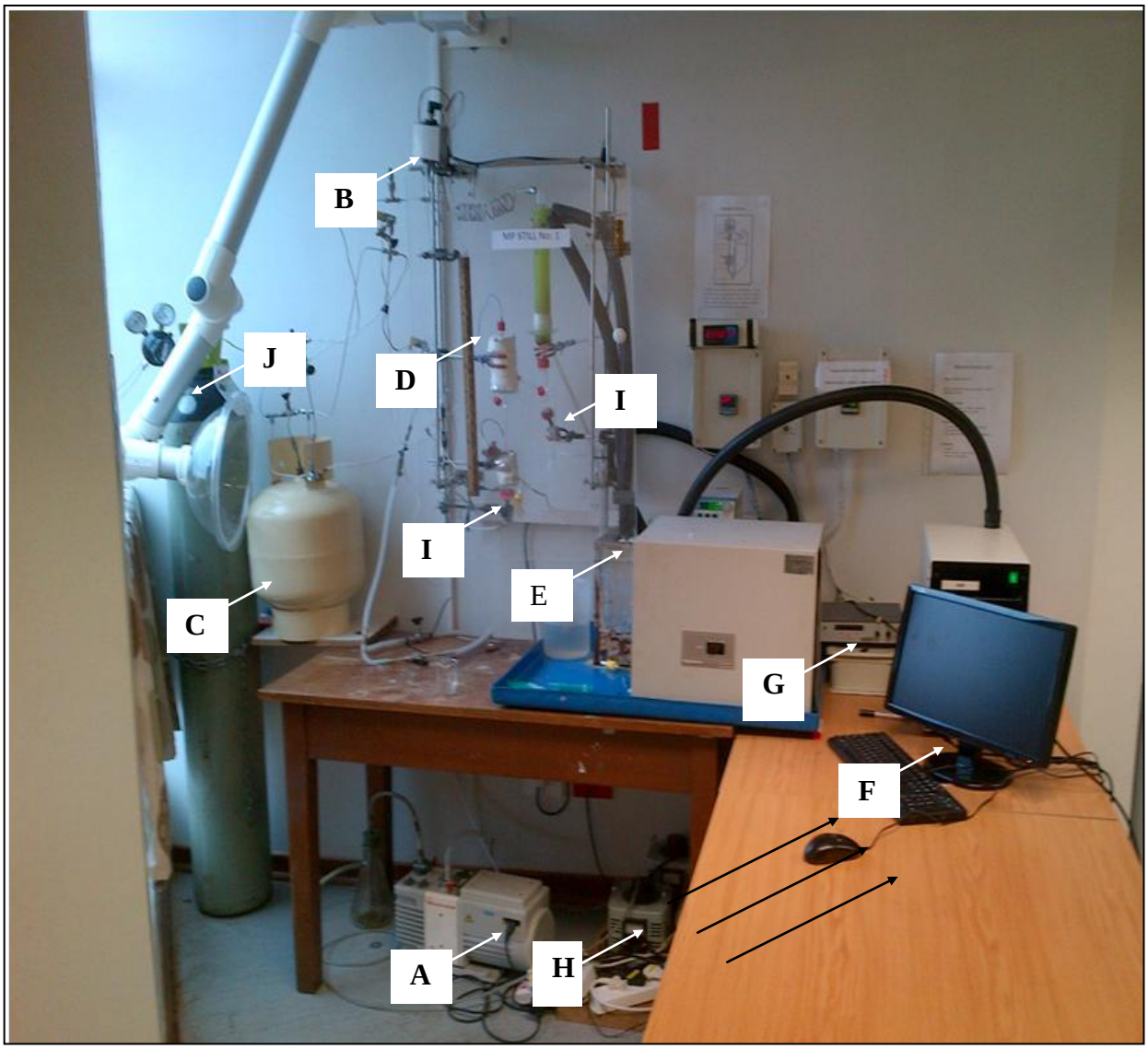

Figure 4.2 Schematic of the semi-automated equipment and layout

A: Edwards Vacuum pump; B: Wika pressure transducer; C: 113L Ballast tank; D: Pt-100 temperature transmitter; E: Water Bath; F: Computer; G: Delta programmable power supplier; H: Power suppliers; I: Magnetic stirrers; J: Nitrogen tank

The equipment layout incorporated ergonomic principles for easier equipment use, demonstrated in Figure 4.2. Initially best practices of manual operability and functionality testing were conducted on instruments such as modules and power suppliers. Figure 4.3 illustrates all instrument (Input/Output) interfaces with equipment and PC.

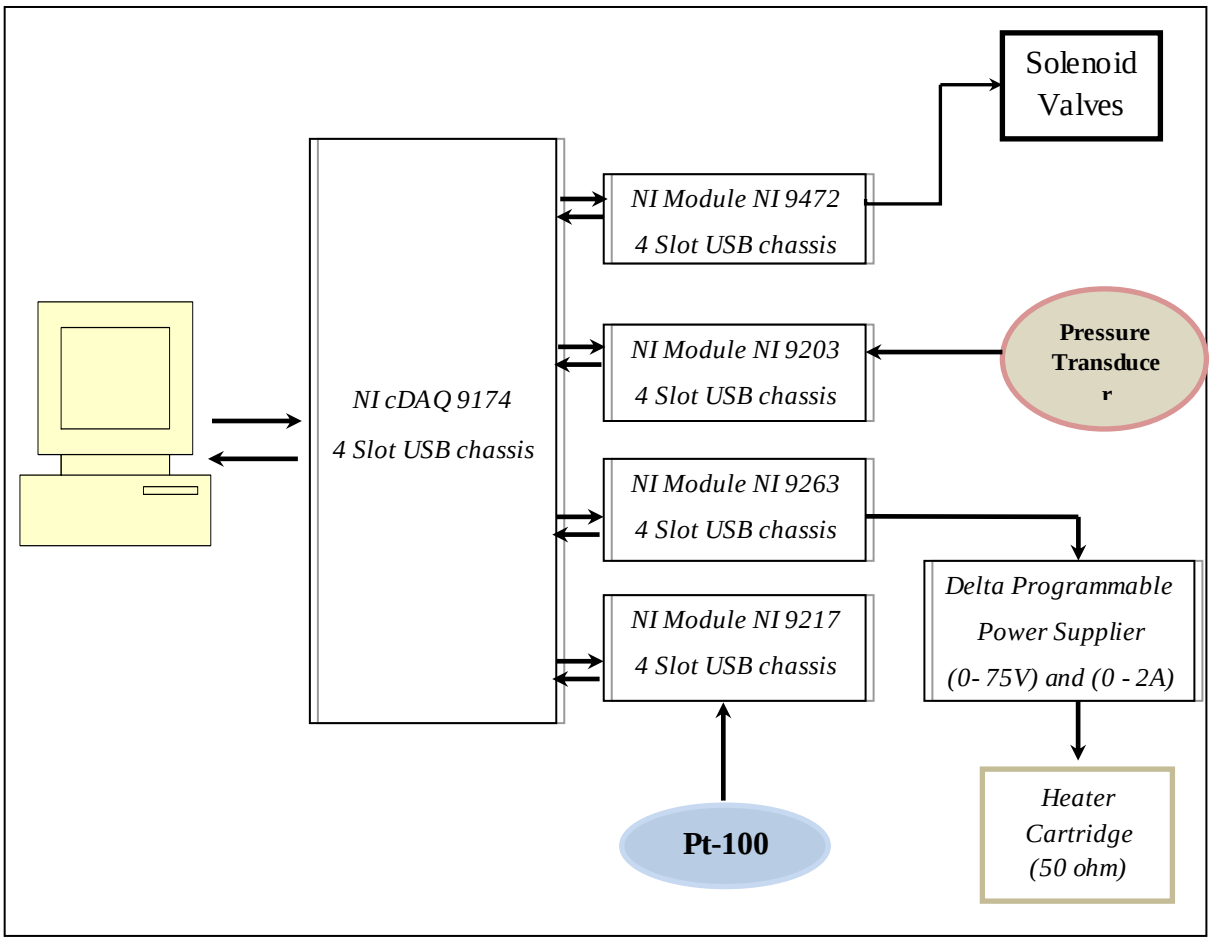

Figure 4.3 Interface (Input/Output) diagram

The automation of the dynamic technique was complex; therefore it was split into development stages. These development stages included:

- Standalone LabVIEW pressure controller (VI) program.
- LabVIEW program for automation of vapour pressure measurements at low to medium pressures.
- LabVIEW program for semi- automation of isobaric measurements
- LabVIEW program for temperature control.
- LabVIEW program for semi-automation of isothermal measurements.

4.3.Design and development of the digital pressure controller

Pressure measurements were obtained using a Wika TXM pressure transducer via a National Instrument (NI) 9203 module to a LabVIEW user interface program. The pressure transducer is housed within an aluminum heated block so as to maintain a constant temperature.

The pressure transducer (4-20) current signal was highly susceptible to outside interference caused by surrounding equipment. These interferences were observed on an oscilloscope as having frequencies and amplitudes ranging from 300 kHz to 500 kHz and 0.1 Volts to 0.05 Volts respectively. To eliminate some of the high frequency noises and still allow for rapid pressure measurements a 100 F capacitor was installed across the analog signal supplied to the NI 9203 module.

The use of a dual core Lexmark computer with a processing speed of 2.13 GHz made possible a sample rate 15ms. The analog-filtered (4-20) current signal was converted to a pressure scale, with a pressure range of 0-500 kPa within LabVIEW. The pressure regulation over this range is achieved by the operation of three 24 volt solenoid valves namely VS1, VS2 andVS3 installed as per Figure 4.4 these valves were powered by a 8 channel NI 9472 voltage module. These solenoid valves operate as fully open/close with a response time of 5-10ms. The flow relationships are:

- 14 l/min (0 to 1.8 bar)
- 15 l/min (1.8 to 5 bar)

Table 4.1 depicts the three pressure ranges and interactions of these valves to attain the desired pressure. Valve VS2, is the common valve, used at above and below atmospheric conditions to attain pressure control. The region close to atmospheric conditions was regarded by Reddy (2005) as difficult for pressure regulation and a similar trend was experienced within this project.

Valves VS1 and VS3 are installed on pressure lines connected to the vacuum and high pressure nitrogen cylinders respectively as illustrated in Figure 4.4. During operation of these valves for pressure control, the system is exposed to sudden excessive pressure surges. To compensate for pressure instabilities a 113*l* ballast tank was installed to act as a pressure buffer.

Manual valves V5 and V6 installed as per Figure 4.3 assist in accomplishing better accuracy in pressure control. By throttling the flow upstream, it prevents large pressure variance across the solenoid valves especially since the solenoids are unable to open partially.

The failure mode selected for each valve is that: V1 and V3 Fail-Close, and V2 Fail-Open. Therefore in the event of process upset or equipment failures, pressure within the system shall stabilize to atmospheric conditions. The greatest concern is on over pressure within the system therefore adjustable spring operated safety relief valve was installed. with a set relief pressure of 500 kPa.

Table 4.1: Pressure Regulation Operation.

Pressure Description	**Pressure Range (kPa)**	**Valves [W = Working, C = Closed, O=Open]**		
		VS1	**VS2**	**VS3**
Above atmosphere	102 - 500	W	W	C
At atmosphere	98.5 - 102	W	O	W
Below atmosphere	0 – 98.5	C	W	W

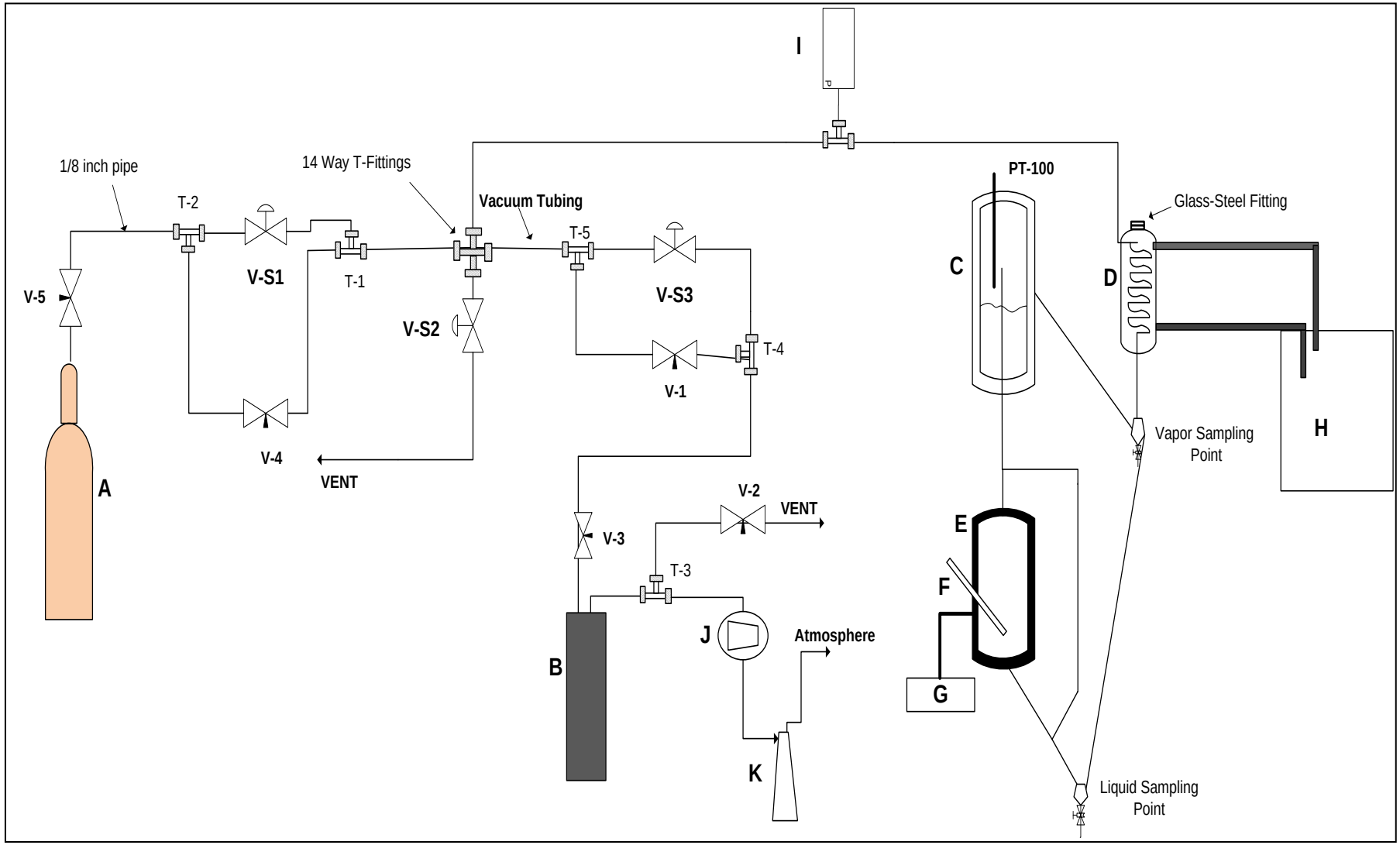

Figure 4.4 Process Flow Diagram of the VLE setup

A: Nitrogen Cylinder; B: Ballast Tank; C: Insulated Equilibrium Chamber; D: Condenser; E: Boiling Chamber; F: Internal heater; G: External Heater; H: Cold Bath; I: Wika pressure transducer; J: Edwards Vacuum pump; K: Vacuum Flask; V-1 to V-5: Manual Ball Valves; V-S1 to V-S3: Solenoid Valves; T-1 to T-8: Mechanical Fittings

The development of the pressure control program algorithm was based on the literature of Eitelberg (2000). The digital series controller with protection against reset wind up, developed by Eitelberg, (2000) was employed as illustrated in Figure 4.5.

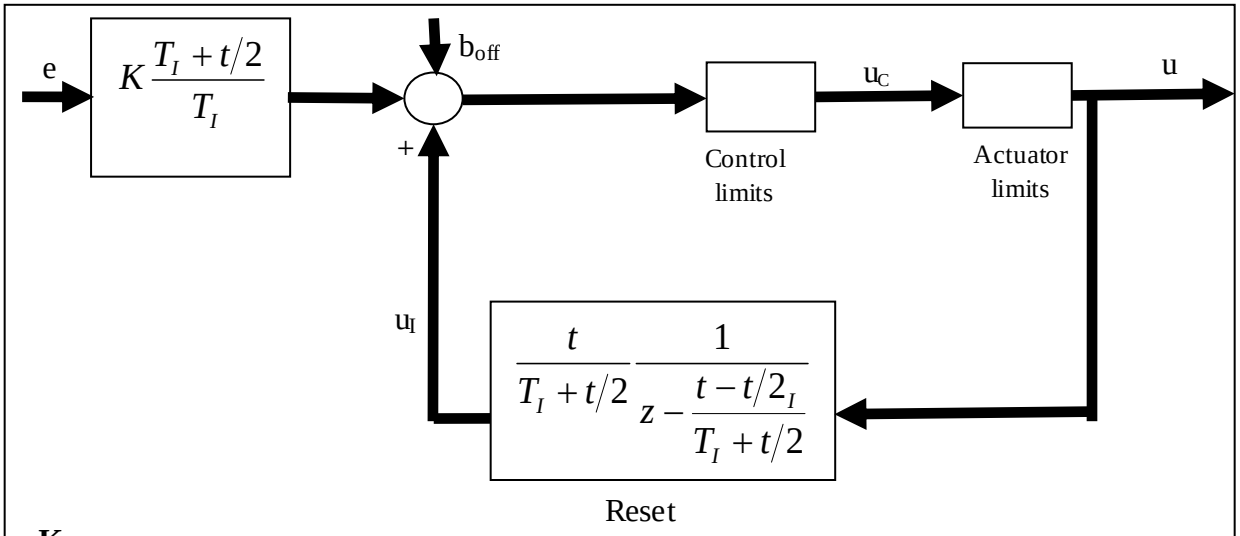

Key

$e = P^{SP}-P^{PV}$, T: Sample time interval, T_I: integral time, b_{off}: pressure bias, u_C: controller output, u; actuator output, u_I: integral output, K: proportional gain factor

Figure 4.5 PI controller with reset feed from actuator output (Eitelberg, 2000)

The selected controller with proportional and integral action assists with achieving the following design requirements:

- Control system pressure by manipulating three solenoid valves as per Table 4.1 via the NI 9472 voltage module.
- Set-point to be defined within the program or remotely by other LabVIEW programs.
- Pressure control to within 0.01kPa.

The controller promotes the use of an initial value for the integrator to assist against instability, when the control system is switched from manual to automatic operation. The reset function of the controller, shown in Figure 4.5, is a counter measure to system wind-up. As discussed by Eitelberg (2000), it prevents wind-up during start-up, shutdown and upset system conditions by generating the integral component u_I from the

actuator output u instead of the controller output u_c. A more comprehensive review on the controller capabilities is available in Eitelberg (1994; 2000).

The LabVIEW program logic and sequence for executing and operating the controller algorithm and solenoid valves respectively are depicted in Figure 4.6. LabVIEW's numeric, time and Boolean function palettes were utilized. A *while* loop with a sample rate 35ms was utilized within the program. Digital signal conditioning was required for pressure measurements due to its inherent dynamic nature. A digital low-pass filter as per equation 4.1 below was used.

$$P(i+1) = 0.965P(i-1) + 0.034P(i) \tag{4.1}$$

The low pass filter coefficients were determined by the trapezoidal technique of Eitelberg (2001), derived in Appendix C. This method can be used for digital filtering when dealing with discrete time intervals as in this case.

One of the most common and simple methods for PI controller tuning is that developed by Ziegler and Nichols (1942). The methods were based on two ideas: to characterize process dynamics by two parameters that are easily determined experimentally and to calculate controller parameters from the process characteristics by a simple formula (Hägglund and Åström, 2004). During the controller tuning for the PI controller, initial estimates were identified using the Ziegler and Nichols (1942) method, followed by on-line tuning. The tuning parameters determined are depicted in Table 4.2.

Pressure control is used for all of the measurements performed within this study, namely vapour pressure, isothermal and isobaric measurements. Therefore the LabVIEW pressure control was designed as a standalone program with the option of remote P^{SP} input. This successful design supports simple integration with other programs.

The completed LabVIEW front panel and block diagram for pressure controller are depicted in Figures 4.7 and 4.8 respectively.

Table 4.2: Tuning parameters for the pressure controller

Controller Parameter	Value	Range
Controller Gain	0.001	0.0005-0.015
Integral Time	10	40

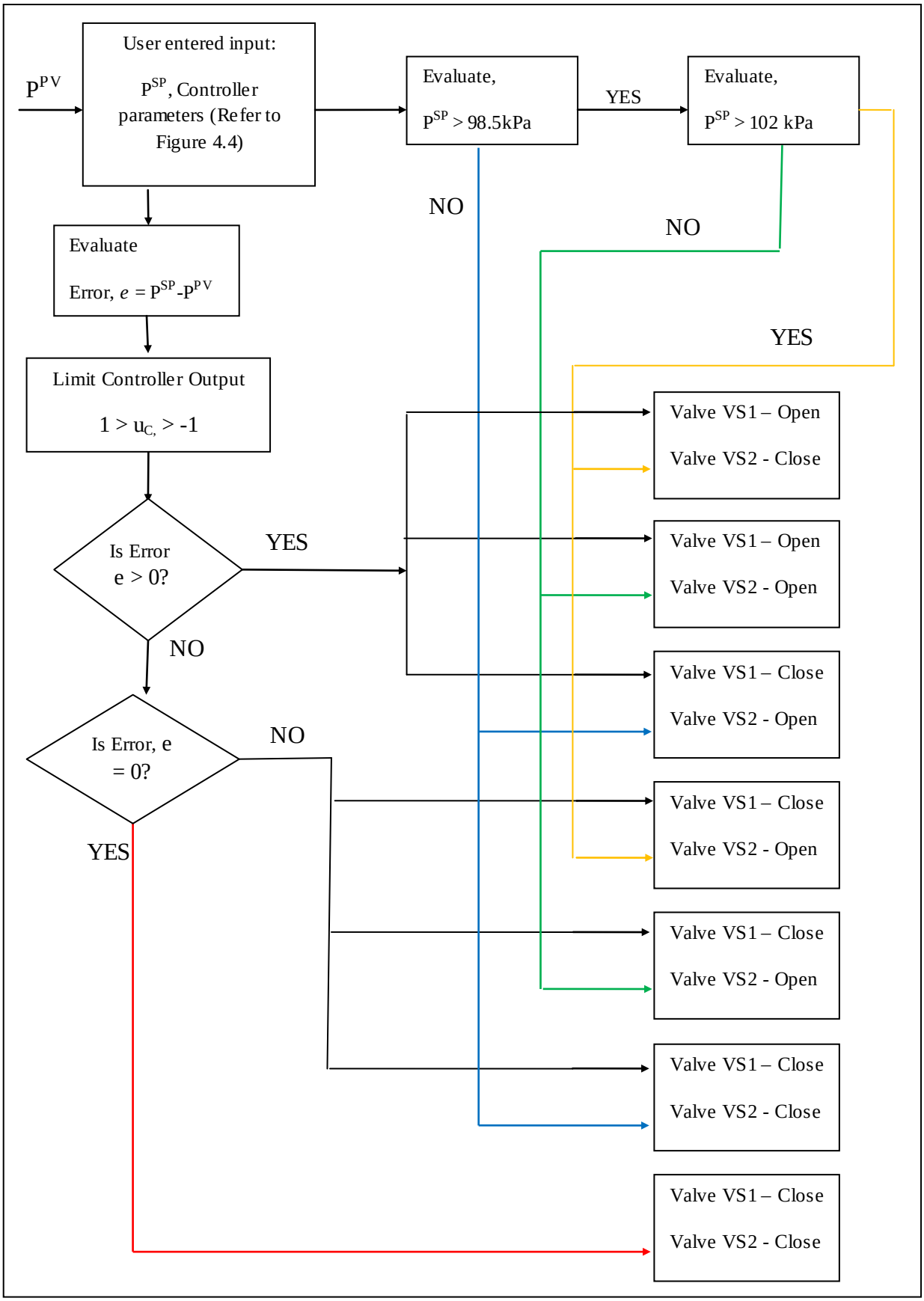

Figure 4.6: The algorithm for pressure control using LabVIEW

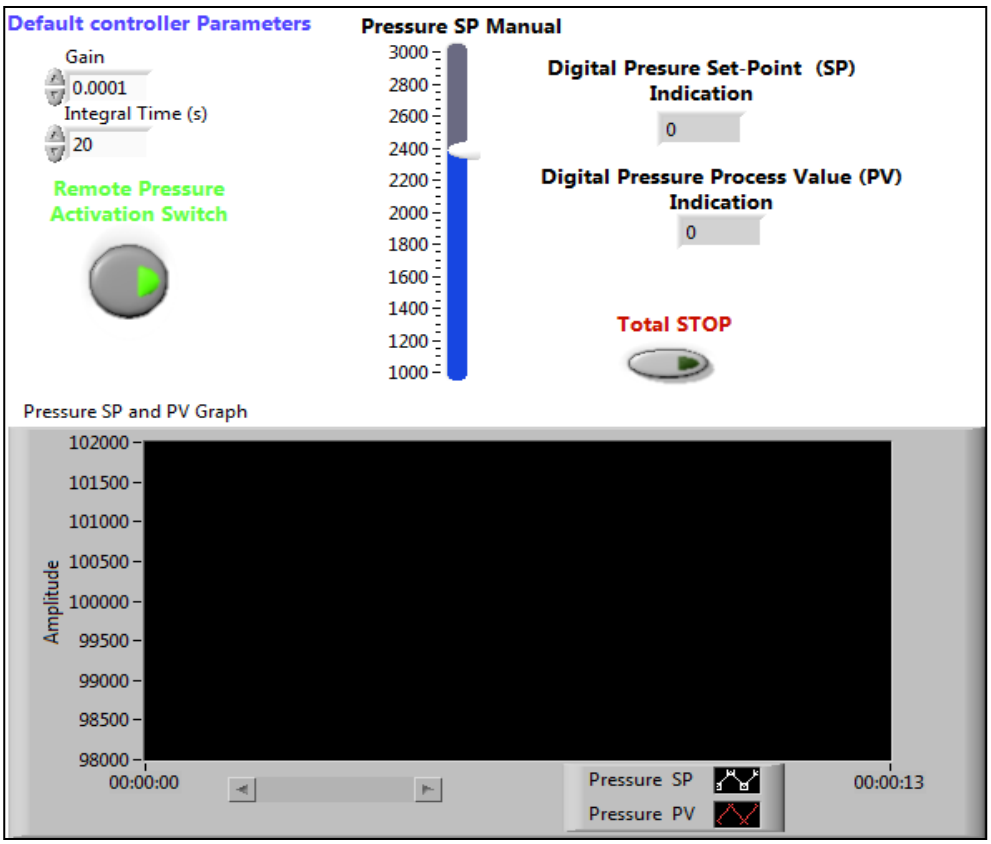

Figure 4.7: The Front Panel for Pressure Control using LabVIEW

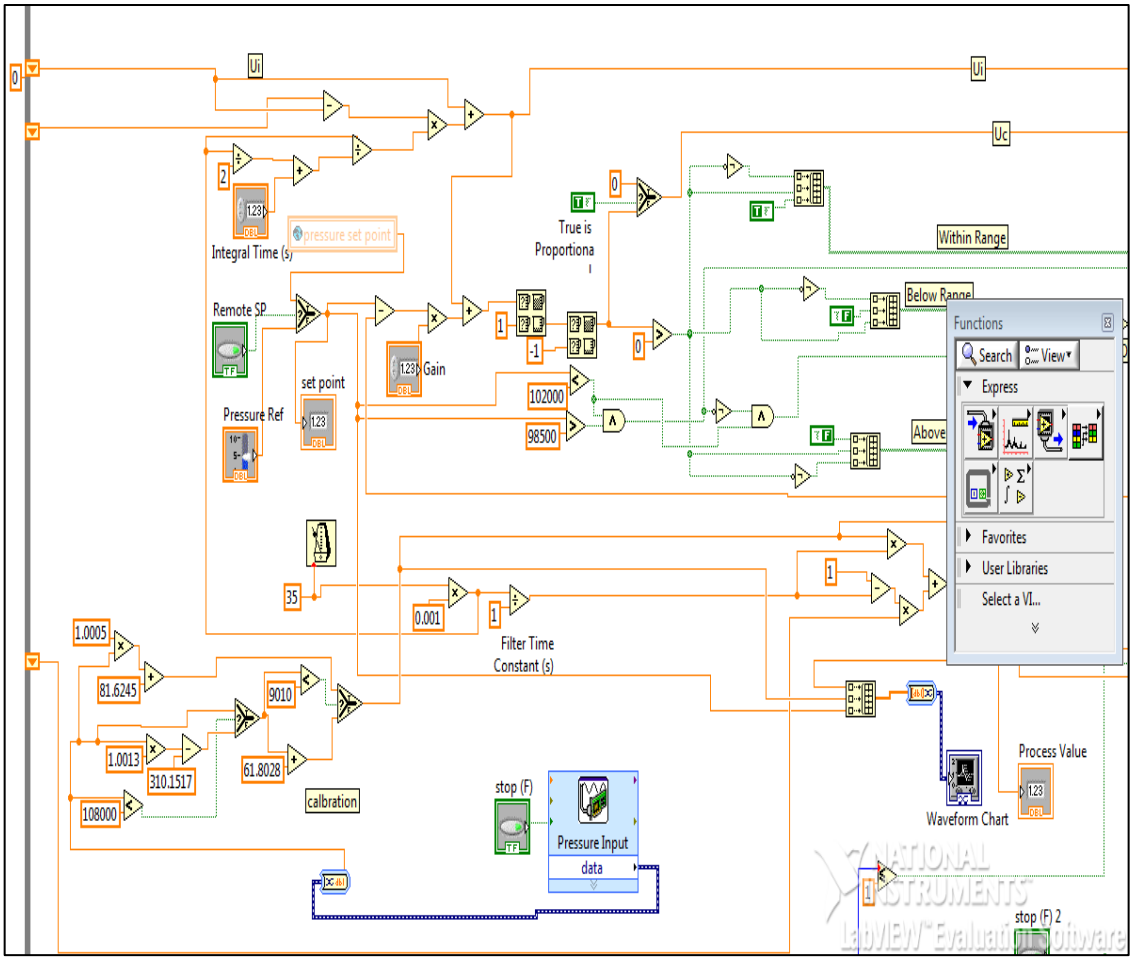

Figure 4.8: The Block Diagram for Pressure control using LabVIEW

4.4.Design and development of the digital temperature controller.

A 4-wire 1/10 DIN Pt-100 sensor (received by Wika Instruments) supplies the measured temperature resistance analog signal to a NI 9217 module for conversion into a temperature digital signal for use by any LabVIEW program.

A definite relationship between temperature and pressure for all mixtures or binary system does not exist or is very complex. Therefore a conventional mathematical modeled control scheme is undesirable. A simpler approach is to rely on technological advancements in the PID controllers as chosen in this study, for temperature control. A cascade temperature-pressure control scheme based on the thermodynamic relationship of increasing temperature results in increasing pressure was employed. The objective of the program design was the control of system's temperature to within 0.01K by altering the system's pressure.

The controller strategy was progressive in implementation, in other words, proportional action was first tested alone, and thereafter integral and derivative actions were included. Upon performance testing the best option was the PI digital series controller with protection against reset wind up and bias input, Eitelberg (2000). This is similar to the pressure control strategy except for the additional bias input. The bias ensured the controller output, u_C always remained positive for controller stability.

Figure 4.9 illustrates the construction of the controller strategy within LabVIEW. A *while* loop with a 500ms sample rate was utilized to implement the control strategy. The LabVIEW block diagram for temperature control is shown in Figure 4.10. The controller parameters were initially estimated using the Ziegler and Nichols (1942) method, followed by on-line controller tuning (Table 4.3)

Table 4.3: Tuning parameters for the temperature controller

Controller Parameter	Value	Range
Controller Gain	10	500
Integral Time	20	40

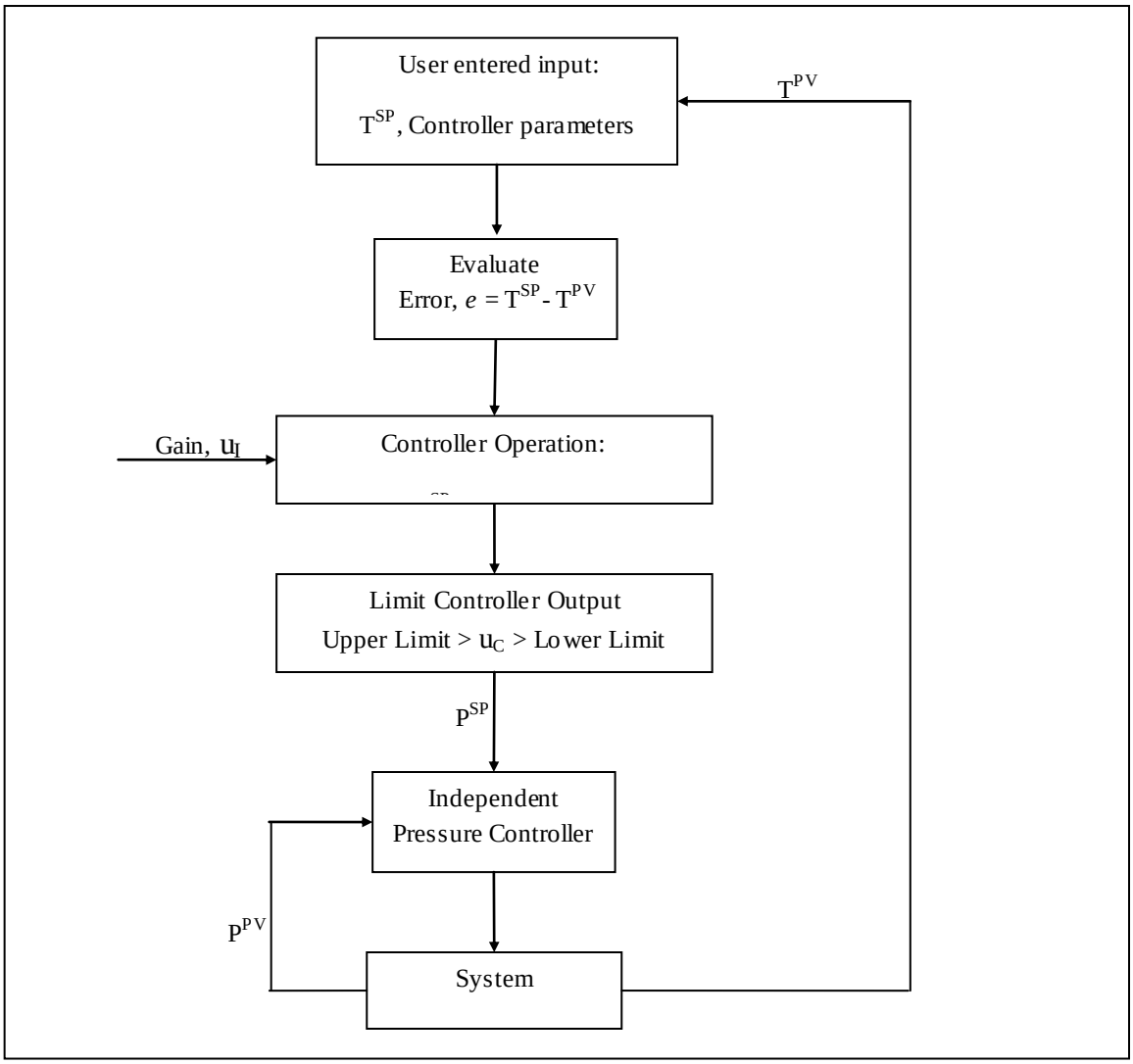

Figure 4.9: The algorithm for Temperature Control using LabVIEW

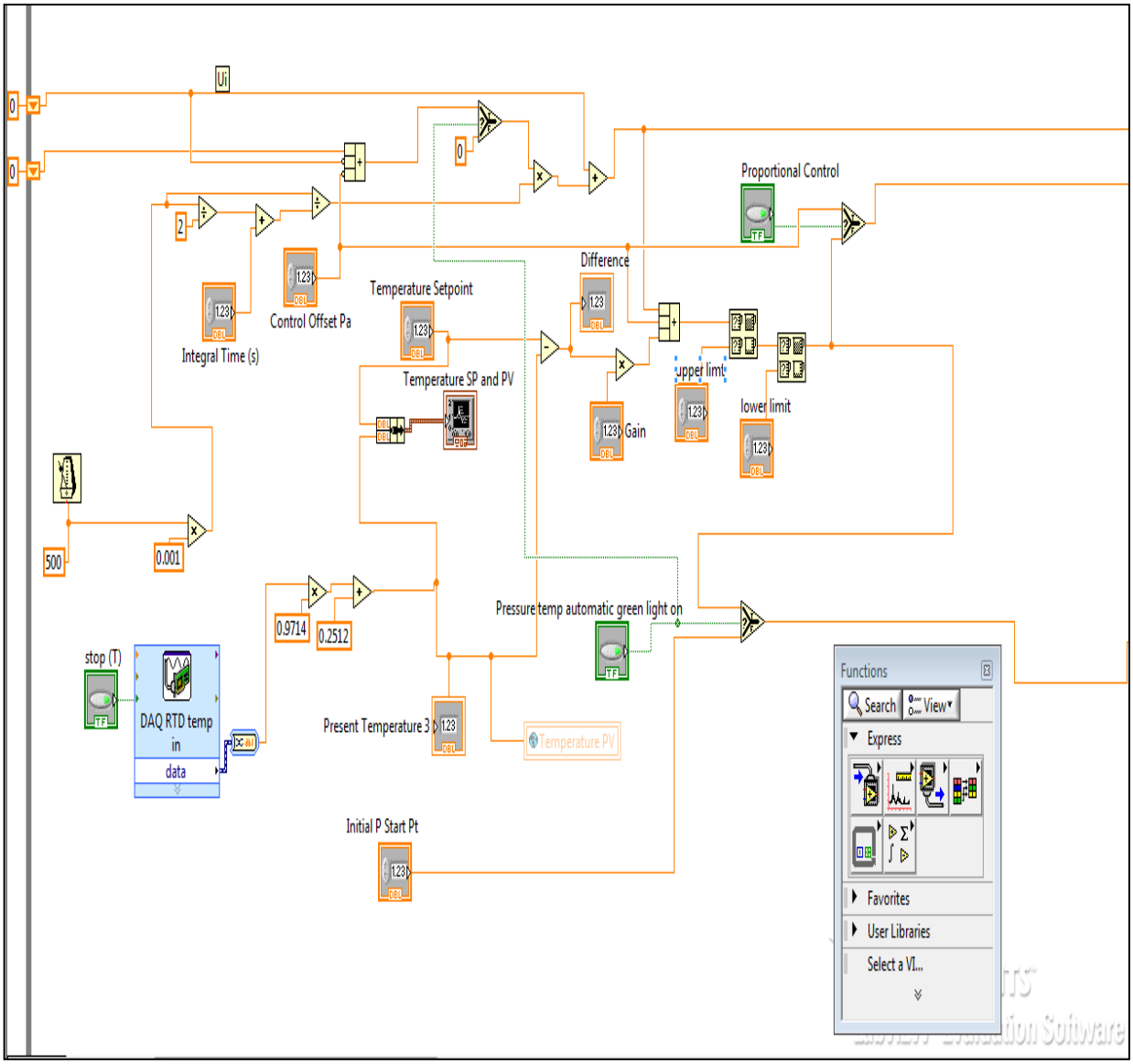

Figure 4.10: LabVIEW block diagram for Temperature control

4.5.Automation of isobaric and vapour pressure measurements

The isobaric LabVIEW program objectives were semi-automation of the manual isobaric and vapour pressure measurements, controlling heat input into the system, determining the true equilibrium point and capturing of VLE data. The equipment required to achieve the tasks includes a programmable power supplier, heater cartridge, computer, NI modules connected as shown in Figure 4.3

As mentioned earlier, a heater cartridge supplies the heat input within the boiling chamber. The liquid boils and the resulting vapour-liquid mixture separates at the equilibrium chamber where temperature measurements are obtained at constant pressure (isobaric measurement). However to obtain true equilibrium temperature the measurement must occur within the plateau region stated by Kniesl et al., (1989). The plateau region is known as a region where an increase in heating input does not change the operating temperature. During VLE measurements, the plateau region is identified as the flat profile on a plot of heat input versus measured temperature. The plot is constructed by incremental adjusting of the heating input and capturing the temperature at each heating increment.

This laborious and repetitive process was automated within LabVIEW. The LabVIEW program alters the heating input supplied to the still via the NI 9263 module interfaced to a Delta programmable power supplier connected to the heater cartridge shown in Figure 4.2. The heat input is varied by voltage steps obeying Ohms Law (current remains constant) while the Pt-100 connected to the computer via the NI 9217 module captures temperature.

The program comprises of two loops viz. an inner loop (heat stage) and an overall outer loop. The purpose of the heating stage is the continuous measurement of temperature from the Pt-100 and capturing of temperature, pressure, voltage and elapsed time measurement. These measurements are stored in a predetermined user text file.

The heat stage can only be completed once thermal equilibrium is reached within the still. In-order to satisfy this condition the program utilizes the following constraint: all measurements are captured after a minimum time of thirteen minutes provided that

three sequential temperature measurements have a deviation between them of less than 0.03 K or after a maximum time of eighteen minutes.

The outer loop requires the user to enter the start and end voltages before the program is executed but allows the user to change the increments as he/she wishes. The heating voltage range was limited to 0-75 V by the Delta programmable power supply. A 50 ohm heater cartridge resistor was utilized instead of the commonly used 120 ohms to provide sufficient heat leading to larger amounts of heat being dissipated for smaller changes in voltages, which can be harmful when considering that the dynamic still is constructed from glass. Further it influences the program's ability to achieve appropriate power versus temperature graph since the program assumes that thermal equilibrium is achieved within eighteen minutes of a voltage change but if the voltage increment is very large, than thermal equilibrium might take longer than expected.

A difficulty experienced with the program was fluctuations in temperature measurement caused by the dynamics of the system involving the circulation of vapour and to a smaller extent the liquid, pressure fluctuations and the chosen sampling rate for the capturing of measurements. To reduce these disturbances a first order digital low pass was used. The selection of a digital filter is dependent upon the characteristic of the system to be controlled. The system can be considered as a closed system with heat transfer with its surroundings. Heat leaves the system primarily from the condenser and enters the system via the boiling chamber. A simple overall heat balance performed by the author revealed that the system can be modeled as a first order equation. Considering that the heat input into the system is computer controlled and is step changed, it follows that temperature will vary as a first order equation. Therefore the first order digital low pass filter was implemented as per equation:

$$T(i+1) = \frac{2}{31}T(i-1) + \frac{29}{31}T(i) \tag{4.2}$$

The equation coefficients were determined by the trapezoidal technique of Eitelberg (2000), derived in Appendix C. The method is used for digital filtering when dealing with discrete time intervals as in this case.

A sampling time of 8 sec and a time constant of 120 sec were selected, incorporating the minimum time of 13 minutes before an increment, the time constant allows for 6.5 complete cycles. Further the digital filtering is completely a multiple and does not affect the final value. Digital filters provide a higher degree of freedom in manipulating signal's frequency spectrum, as well as a higher degree of programmability all leading to better performance as opposed to its analog counterpart.

Another feature of the program included the decrease of heating input gradually to prevent sudden temperature changes especially as the material of construction of the equipment is glass.

The isobaric program is regarded as semi-automatic as it requires the user to re-start the program at plateau conditions for obtaining equilibrium liquid and vapour samples. These samples are obtained manually as discussed in the experimental procedure.

The vapour pressure measurement program was created as an extension of the isobaric program. The only difference was an additional loop that alters system pressure in incremental steps selected by the user. At each step the complete isobaric cycle mentioned is performed. On completion of program a text file is generated containing all values.

4.6.Automation of Isothermal measurements

The automation of the isothermal process was achieved by extending the temperature control program to incorporate heating of the still and capturing of VLE data within the plateau region, similar to the isobaric case.

Like the isobaric case, two *while* loops viz. an inner loop (heat stage) and an overall outer loop were employed for the program. Continuous measurement of pressure occurred within the heating stage and upon completion temperature, pressure, voltage and elapsed time measurements were captured in a predetermined user text file.

Thermal equilibrium was achieved after a minimum of 15 minutes and when three sequential pressure measurements had a deviation between them of less than 0.04kPa or

after a maximum time of 20 minutes. The outer loop controlled the automotive voltage increase as per user requirements and generated the text upon completion.

4.7. Process Safety Features

The measurement of VLE data above atmospheric conditions poses significant process hazards. Therefore the following passive and reactive safety features have been incorporated (Ramjugernath, 2000):

- The VLE still was constructed with breakage points that allow for safe release of pressure with minimal damage to the still. The condenser glass cap will pop off; the return line from the vapour sampling point to the boiling chamber will break, before the more significant sections like the equilibrium and boiling chambers breaks.
- The failure modes of the solenoid valves V1, V2, V3 and the installation of an adjustable spring operated relief valve ensures a safe condition during process upsets or failures.
- As part of the shutdown process the LabVIEW program is designed to gradually reduce heat input to the still to prevent thermal cracks.
- Nitrogen being inert is used as the pressurizing gas.
- A clear plastic shield installed in front of the VLE still protects the user against injuries, in the event of the still exploding.
- An adjustable spring operated pressure relief valve was installed
- The Delta programmable power supplier (0-75 V, 0-2 A) supplies the heat energy into the still via the internal heater cartridges. In the event of a major process safety incident the user must switch the power supplier off.

5. Systems Investigated

The selection of binary systems depends on the capabilities of the VLE apparatus used. The diverse array of thermophysical and chemical properties of mixtures often dictates the incorporation of specialized features within the VLE apparatus, like corrosive mixtures of acetic acid and water at elevated temperatures or high relative volatility mixtures (Reddy, 2009). In this study the following systems were selected to fully test the capabilities of the apparatus:

- Cyclohexane (1) and ethanol (2) at 40kPa (Joseph, 2001)
- 1-hexene (1) + NMP (2) at 363.61 K, 373.15 (Fischer and Gmehling, 1995)
- 1-propanol (1) and 2-butanol (2) at 393.15 K.

The systems selected are compatible with the material of construction and operating range of the apparatus. These systems exhibit non-ideal behaviour and are readily available at high purities. Further the VLE data for the test systems originate from a reputable published literature source.

The cyclohexane (1) and ethanol (2) binary system is highly non-ideal with an existence of an azeotrope within the investigated VLE range. Cycloalkanes, such as cyclohexane are unreactive, non-polar and most often reasonably stable hydrocarbons. Alcohols are characterized by the presence of a hydroxyl group (–OH) within the compound, illustrated in Figures 5.3 and 5.4. The hydroxyl group (–OH) polarizes the C-O bond increasing its reactivity. The (-OH) group also changes the physical properties of the compound like increasing the boiling point. Alcohols also have associating properties due to their hydrogen bonding ability. Therefore alcohol mixtures with cycloalkanes give rise to nonidealities and may form azeotropes. The VLE data of Joseph *et al.*, (2001) has been recommended and used by many researchers such as Harris, (2001), Reddy (2009) as a test system.

The second system was the 1-hexene (1) + N -methyl pyrrolidone-2 (NMP (2) at 363.61 K (Fischer and Gmehling, 1995). NMP is a powerful, aprotic solvent with a low volatility. The polar properties of the NMP molecule (Figure 5.1) can be attributed to dipole-dipole oligomers that induce associative interactions (Letcher et al., 1998). As a result of these properties, the system of 1-hexene and NMP reflect negative deviations

from ideal volume. The 1-hexene molecule (Figure 5.1) is regarded as an alpha –olefin, due to the presence of a double bond on the primary carbon atom. The large difference in boiling points and molecular interaction of both these compounds also contributes to the difficulty of measuring this system. Further pressure range for the 1-hexene (1) and NMP (2) system of 2kPa to 220 kPa tests the capability of the apparatus to handle transition across atmospheric pressure.

NMP is a desired solvent for separation of aromatics from non-aromatics, recovery of butadiene's from C4 mixtures and pentadienes from C5 mixtures (Moodley, 2012). NMP is also used in the manufacture of various compounds, including pigments, cosmetics, drugs, insecticides, herbicides and fungicides. The wide spread use of NMP encouraged the measurement of 1-hexene (1) and NMP (2) at 373.15 K, which constitutes a new isothermal data.

The final system of 1-propanol (1) and 2-butanol (2) is of great importance within the petrochemical industry. The large scale industries like SASOL require VLE data of alcohols for purification of downstream products originating from its Fischer-Tropsch process. The molecule structures of both chemicals have been included in Figures 5.3 and 5.4.

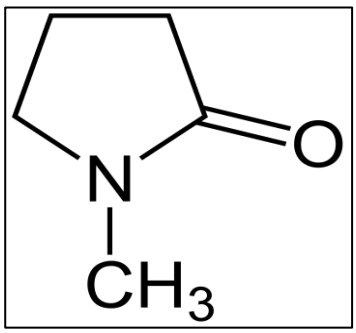

Figure 5.1: Chemical structure for NMP (Dyrkacz, 2001)

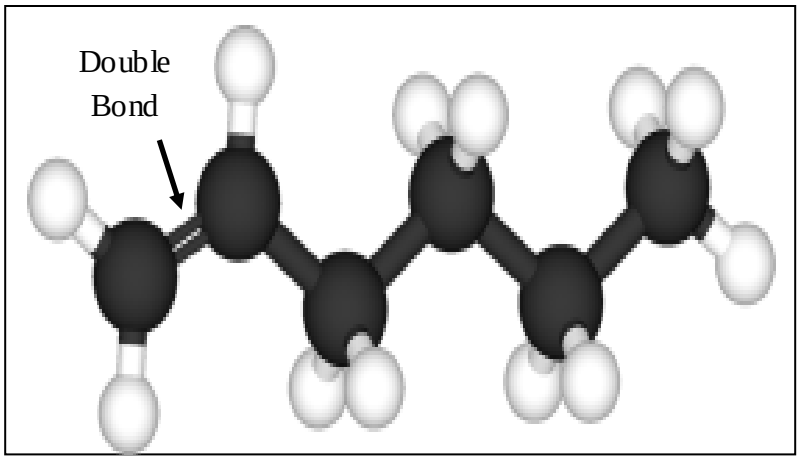

Figure 5.2: Chemical structure for 1-hexene (Weast, 1972)

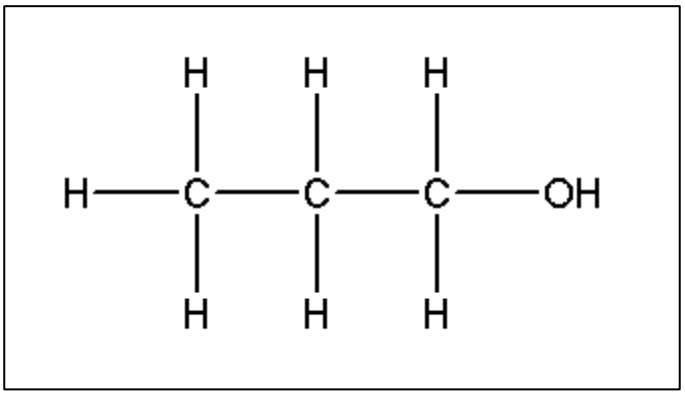

Figure 5.3: Chemical structure for 1-propanol (Weast, 1972)

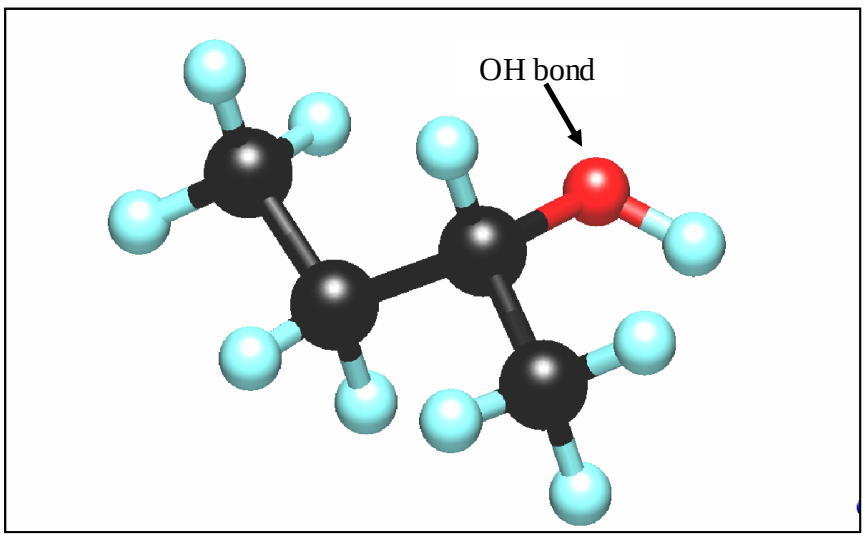

Figure 5.4: Chemical structure for 2-butanol (Budavari and O'Neil, 1989)

6. Experimental Procedure

It is essential to develop an accurate and reproducible experimental method for the attainment of precise and reliable phase equilibrium data. The sections below describe the preparation and operation of the equipment for measurements.

6.1. Leak Test

The apparatus is pressurized to 500 kPa and a surfactant based liquid (SNOOP®) is applied to the various fittings and seals. If the surfactant (on the areas applied) starts bubbling it indicates that a leak is present. After the leak test, a suitable solvent (acetone or pentane) should be circulated in the system to remove any contaminants.

6.2.Pressure Calibration

The Wika TXM 0-500 kPa pressure transducer was calibrated using the standard SENSOTEC Super TJE pressure transducer connected in series, to the VLE still. The pressure was varied across the experimental range and readings were taken at each point from both transducers. The pressure calibration was performed for a pressure range of 1.8 kPa to 500 kPa. The pressure calibration was repeated twice yielding three sets of calibration data points.

The standard pressure from the SENSOTEC Super TJE pressure transmitter was plotted against the displayed pressure from LabVIEW to obtain the linear pressure equation. The uncertainty in reproducibility is observed by the deviation of measured points from the trend line.

6.3.Temperature Calibration

Temperature calibration for the Pt-100 sensor located in the equilibrium chamber was accomplished using a standard Pt-100 reference probe connected to a Wika CTH 6500 display unit.

Both Pt-100 probes were submerged into the Wika 9100 oil bath filled with silicon oil. Temperature within the oil bath was varied, across the measuring range (273.15 K – 423.15 K) and temperatures of both probes were recorded.

A plot of standard temperature (from the Wika CTH 6500 display unit) versus displayed temperature (from LabVIEW) was produced and fitted to a linear trend.

6.4. Gas chromatograph (GC) Calibration

A Shimadzu (GC-2010) thermal conductivity detector was utilized for composition analysis. The area ratio method by Raal and Mühlbauer (1998) was employed for the calibration of the GC. Standard mixture samples were prepared in suitable sized vials to prevent flashing. The amount of sample injected into the GC ensured that the column was not overloaded. The area ratio method was used to determine response factor ratio as this method is independent of the amount of sample injected. The area ratio for a binary system is:

$$\frac{n_1}{n_2} = \left(\frac{A_1}{A_2}\right)\left(\frac{F_1}{F_2}\right) = \frac{x_1}{x_2} \tag{6.1}$$

A_1 and A_2 refer to the peak areas obtained from the GC for components 1 and 2 respectively. The response factor ratio F_1/F_2, is found from the plot of A_1/A_2 versus x_1/x_2 over the full composition range and should extrapolate through the origin. Equation (6.1) indicates that the response factor ratio F_1/F_2 is the slope of a linear plot of A_1/A_2 versus x_1/x_2 and should be constant. It is also apparent the slope of the inverse plot of A_2/A_1 versus x_2/x_1 should equal F_1/F_2. The acceptable average deviation between response factors ratios is 1%, to consider a linear relationship between the area ratios and mole fractions.

6.5.Isobaric Operation of the Still (P ≤ 98.5kPa)

First the cooling coil and Labotech unit for the circulation of the ethylene glycol solution from the water bath to the condenser are switched on. A suitable condenser temperature to ensure total condensation of the chemicals being measured must be established before commencing experiments.

The computer, NI modules and Delta programmable power supplier are switched on. One of the components of the binary system should be charged into the cleaned still. The boiling chamber should be filled to a level approximately 3 cm above the top of its outlet. This allows the chemicals to be forced up the Cottrell tube and assists in nuclear boiling. Manual valves V-2, V-4 V-6 are closed and V-3 open. The LabVIEW pressure control program is opened and set to remote. The LabVIEW isobaric front panel is opened as per Figure 6.1. The program is run twice, once for determining the plateau region and the other for withdrawing samples at that point.

The required entry of information for the isobaric front panel is listed in sequence below and referenced on Figure 6.1:

1. Insert voltage start and end points (Volts).
2. Insert voltage increments (Volts).
3. Insert pressure set point (kPa).
4. Set to zero (Used for vapour pressure measurements)
5. Run

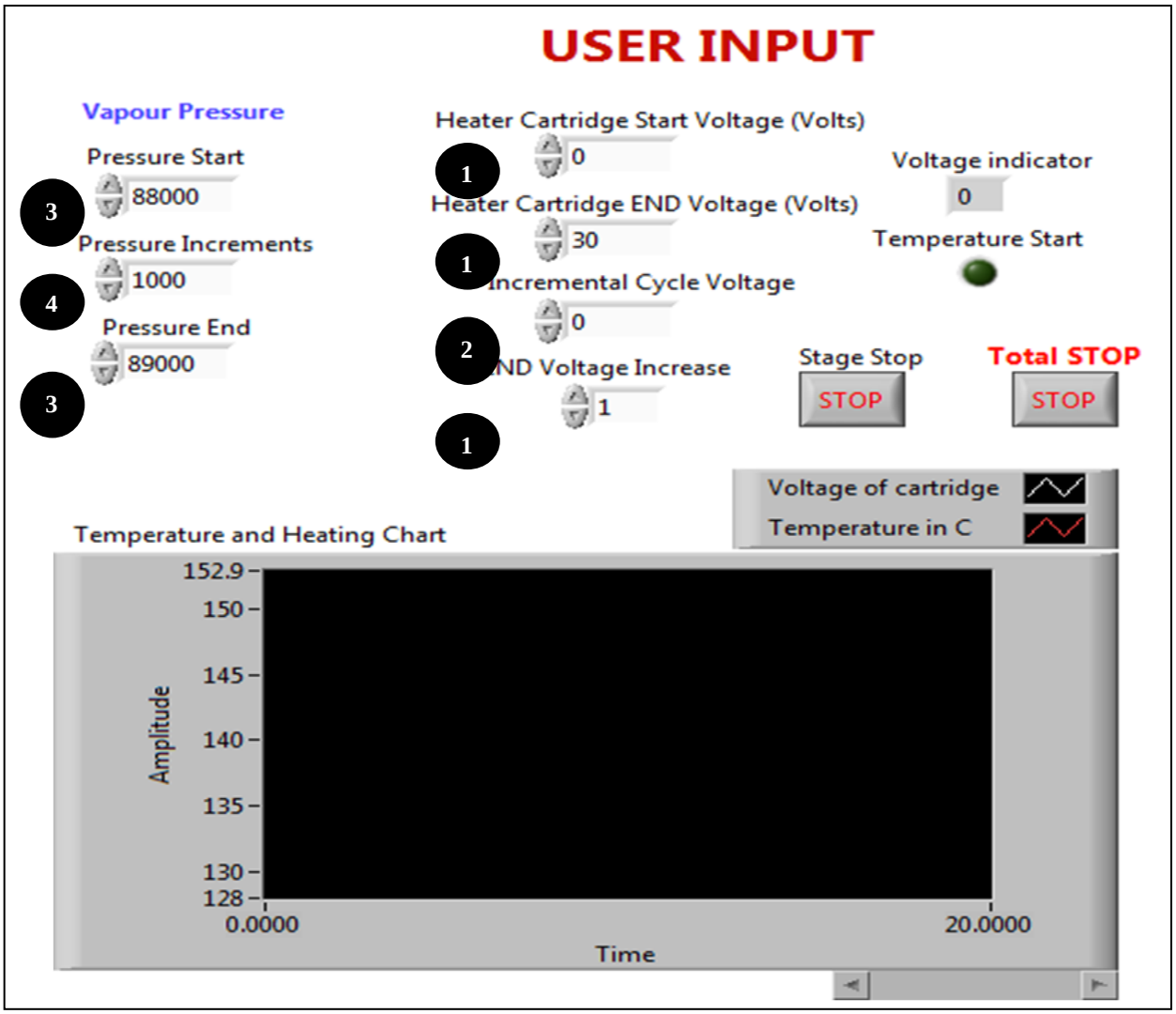

Figure 6.1 Screen shot of the LabVIEW Isobaric front panel settings

(Measurement of the plateau region)

The external heaters for the boiling chamber are switched on. The vacuum pump is switched on, and bypass valve V-1 can be opened for rapid de-pressurizing to desired pressure and closed thereafter. When the program run is completed the user identifies the plateau region from a plot of heat input versus measured temperature.

The program is re-initialized and programmed as per numbering reference on Figure 6.2 and below:

1. Insert plateau voltage (Volts).
2. Insert pressure set point (kPa).
3. Set to zero
4. Run

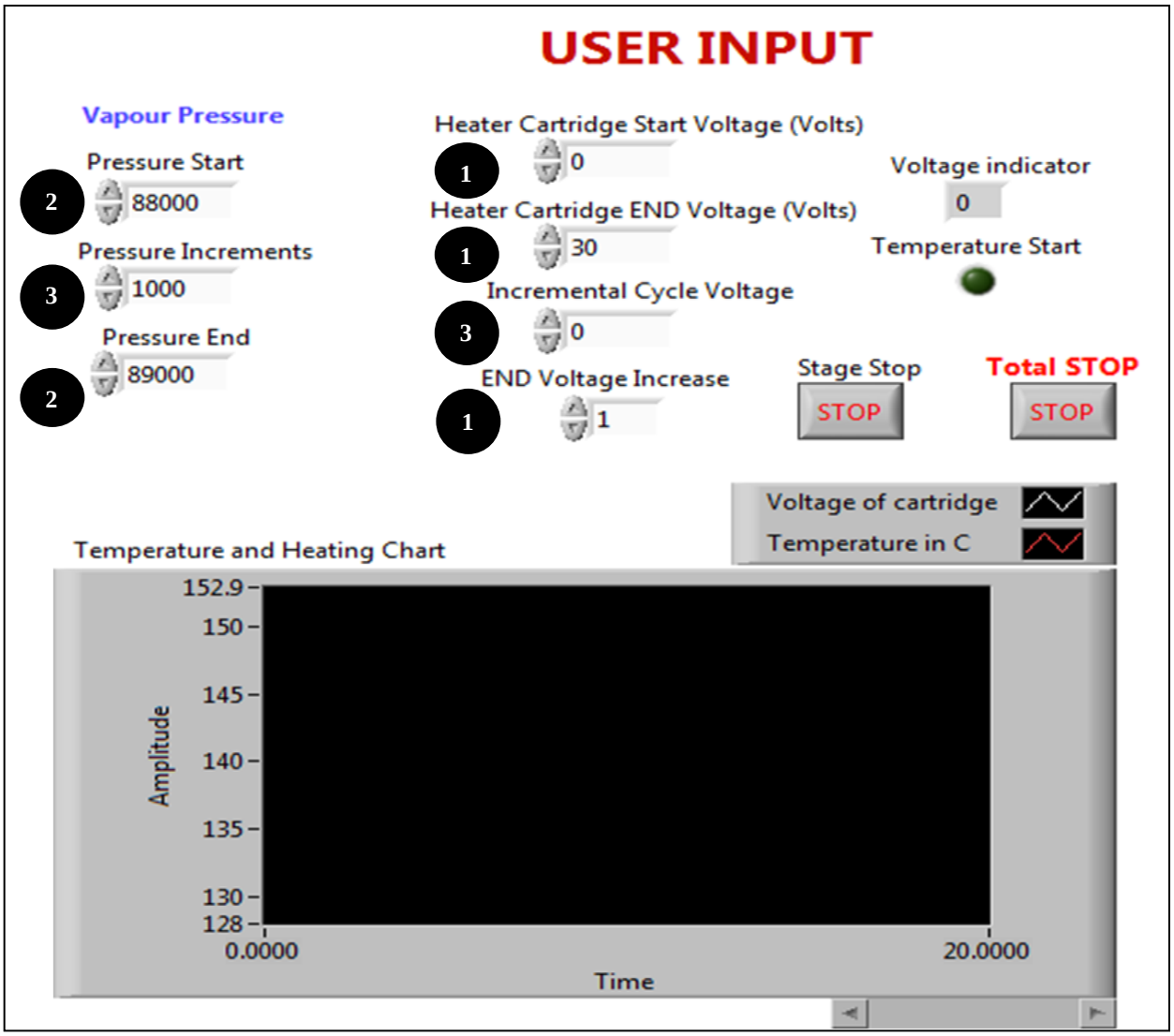

Figure 6.2 Screen shot of the LabVIEW Isobaric front panel settings (Measurement of VLE phase compositions)

An estimate of 50 minutes is allowed for the establishment of equilibrium in the plateau region. At equilibrium, samples are removed from the vapour and liquid sampling ports using a GC syringe. Three injections into the GC per phase are completed to ensure reproducibility. An average deviation for the area ratios considered acceptable was a tolerance of ± 0.002. Thereafter, approximately 1.5 to 2 ml of sample is removed from either the liquid or vapour port and replaced by the more dilute component to establish another system composition. The whole process is repeated beginning at the determination of plateau region.

The process is repeated until the halfway point on the composition range is reached. Thereafter the still is drained, cleaned and filled with the second pure component. The process described above is repeated for the other half of the phase equilibrium curve.

6.6.Isobaric Operation of the Still (98.5kPa ≤ P ≤ 500kPa)

For operating of the equipment within this range the nitrogen regulator and manual valves V-1, V-3, V-4 are opened. If the pressure is above 103 kPa the vaccum pump can be switched off and the bypass valve V-4 can be temporary opened to speed up pressurization within the still.
The withdrawal of samples within this pressure region is performed using 10 ml liquid syringes as a pressure gradient exists between the syringe and the system. The liquid is transferred to 2ml vial, followed by GC analysis.

6.7.Isothermal Operation of the Still

The isobaric start-up procedure covering equipment preparation and switching on sequence is followed. The LabVIEW pressure control program is open and set to remote. The LabVIEW isothermal front panel is opened as per Figure 6.3. The program is run twice, once for determining the plateau region and the other for withdrawing samples at that point.

The required entry of information for the isothermal front panel is listed in sequence below and referenced on Figure 6.3:

1. Insert voltage start and end points (Volts).
2. Insert voltage increments (Volts).
3. Insert temperature set point (°C).
4. Estimate pressure limits based on pure component vapour pressures (kPa)

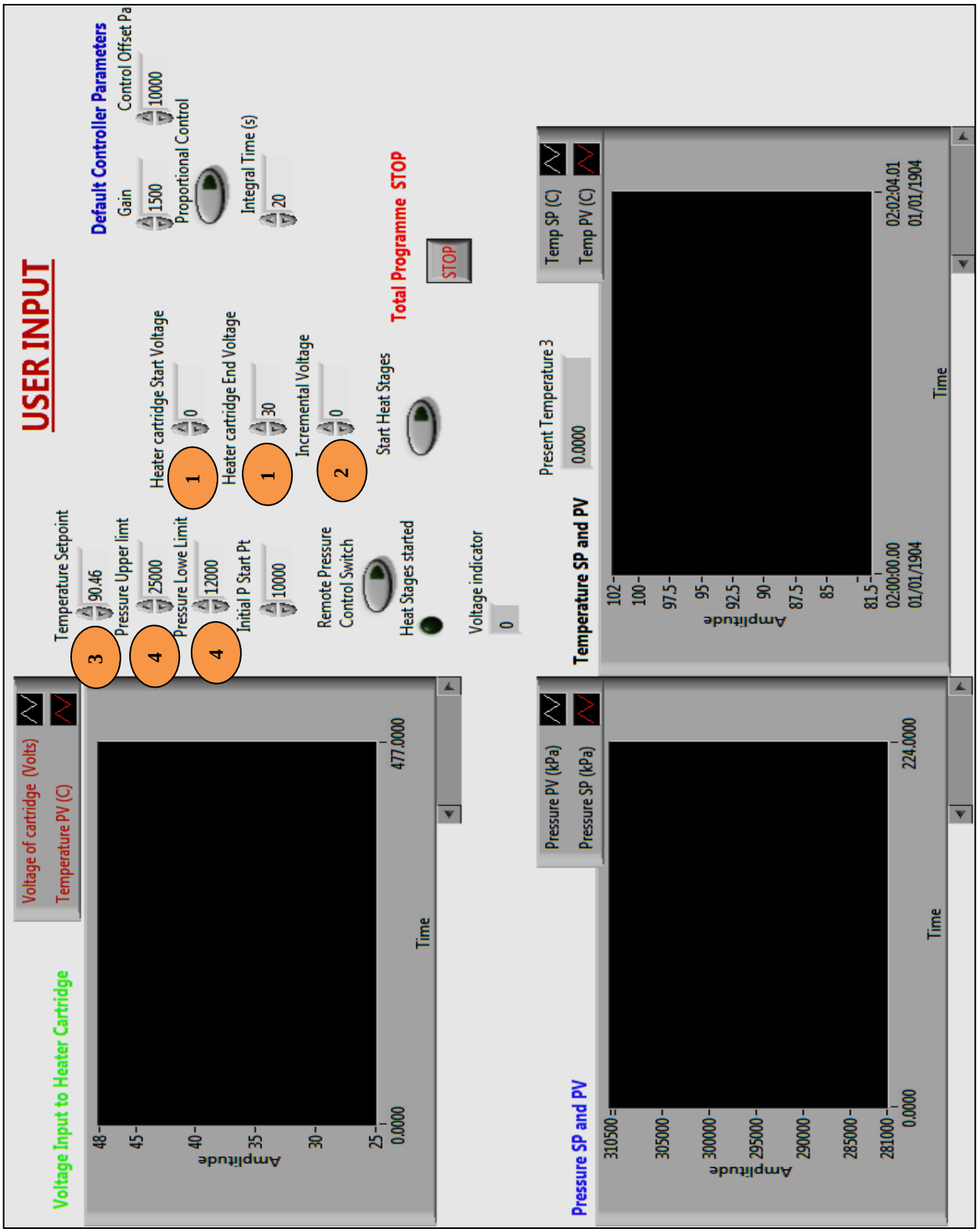

Figure 6.3 Screen shot of the LabVIEW Isothermal front panel settings

(Measurement of the plateau region)

Depending on the pressure ranges, the vacuum pump or nitrogen regulator is switched on/off or open/closed respectively (especially concerning the need for a vacuum pump). Similar to the isobaric case, when the program run is completed the user identifies the plateau region and initializes the program by entering the required information as per sequence listed below and referenced on Figure 6.4:

1. Insert plateau voltage (Volts).
2. Insert temperature set point (°C).
3. Set to zero.
4. Estimate pressure limits based on pure component vapour pressures (kPa)
5. Run

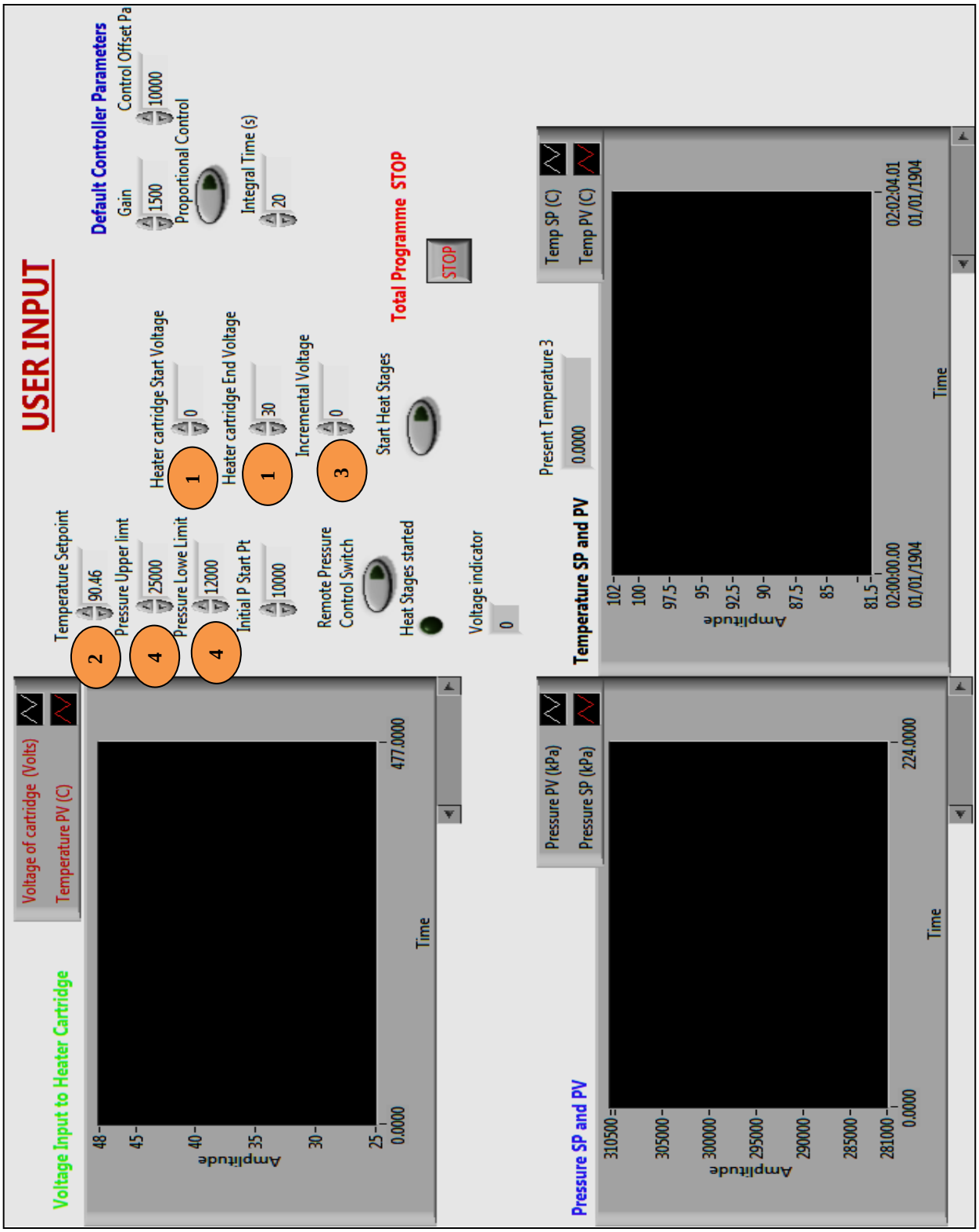

Figure 6.4 Screen shot of the LabVIEW Isothermal front panel settings

(Measurement of VLE phase compositions)

An estimated 50 minutes is allowed for the establishment of equilibrium in the plateau region. At equilibrium, samples are removed from the vapour and liquid sampling ports using a GC syringe and analyzed (as discussed previously). The process is repeated until the measurement of the VLE data across the composition range is completed.

7. Experimental Results

7.1.Purity of chemicals

The accuracy and reliability of reported results is reliant on the chemicals used. The manufacturer's stated purities were confirmed via GC analysis and refractive indices measurement.

Refractive indices were measured using ATAGO RX-7000α refractometer with a manufacturer stated uncertainty of ±0.00011. Table 7.1 lists the suppliers stated chemical purities, GC analyses and refractive indices (literature and measured). No significant impurities were identified, hence no further chemical purifications were necessary.

Table 7.1: List of chemicals used and their respective purities

Chemical (IUPAC name)	Supplier	Refractive Index		GC Analysis (Peak Area %)[b]	Supplier purity specified (Mass %)
		Exp at 298.15 K	Literature		
Ethanol	Merck	1.36178	1.3611[a]	99.9	≥ 99.5
Cyclo-hexane	Merck	1.42390	1.4235[a]	99.9	≥ 99.5
1-Propanol	Sigma-Aldrich	1.38511	1.3850 [a]	99.9	≥ 99.5
2-Butanol	Sigma-Aldrich	1.39750	1.3978[a]	99.9	≥ 99.5
1-Hexene	DLD Scientific	1.38789	1.385[a]	99.9	≥ 99.5
N-methyl-2-pyrrolidone	Merck	1.46775	1.4679[a]	99.9	≥ 99.5

[a] Poling *et al*. (2001) at 298.15 K.

[b] GC conditions as per section 7.4.

7.2.Temperature calibration

The calibration plot for the Pt-100 temperature sensor is presented in Figure 7.1 as per the method described in section 5.2. The plot of the temperature deviation is shown in Figure 7.2 and reveals the maximum deviation to be 0.027 K.

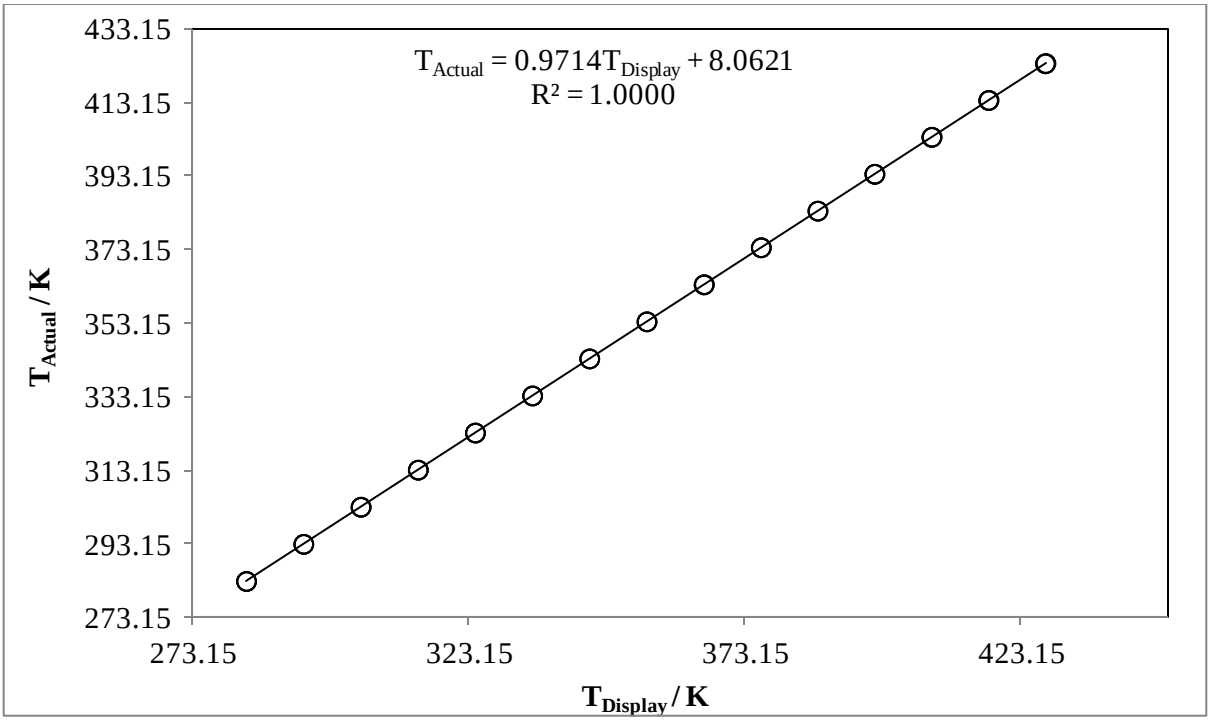

Figure 7.1: Calibration of the Pt-100 probe (Undertaken three times)

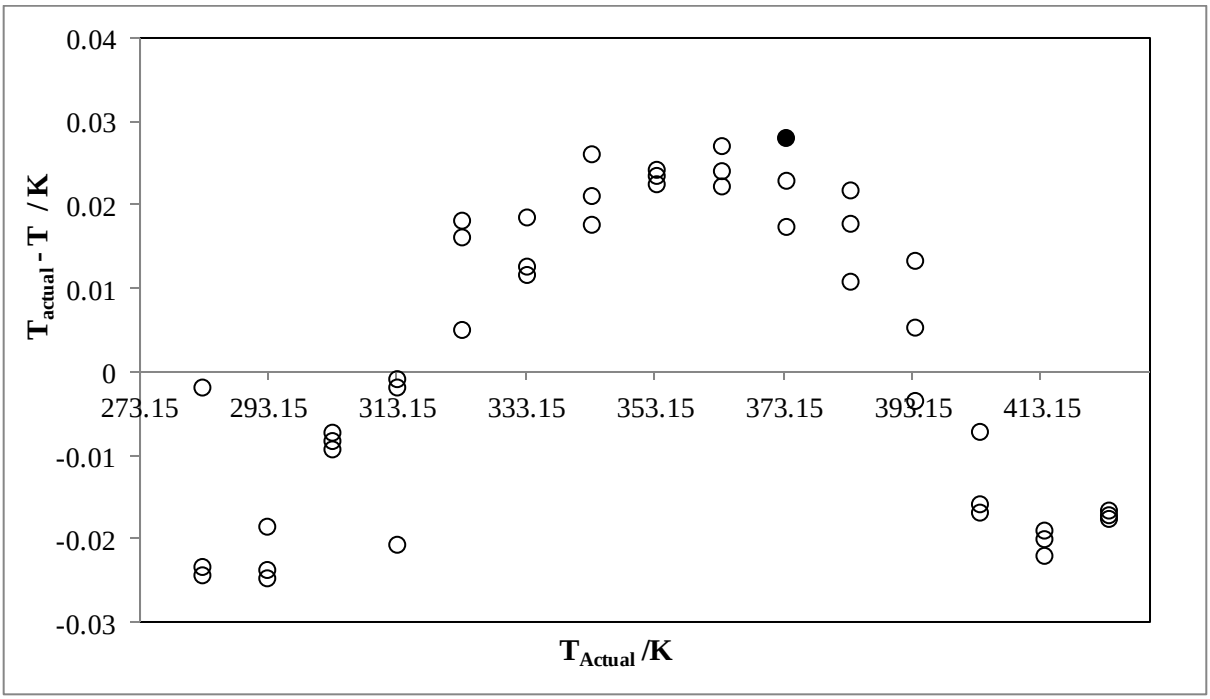

Figure 7.2: Plot of temperature deviations from actual temperature, ● maximum deviation.

7.3. Pressure calibration

Three pressure calibrations were completed for the operating pressure range of 0-500 kPa namely 0-10 kPa, 10-100 kPa and 100-500 kPa illustrated in Figures 7.3 - 7.5. The

plots for the pressure deviations are presented in Figures 7.6 - 7.8 and reveals maximum absolute deviations of 8.96 Pa, 13.56 Pa and 188.57 Pa respectively.

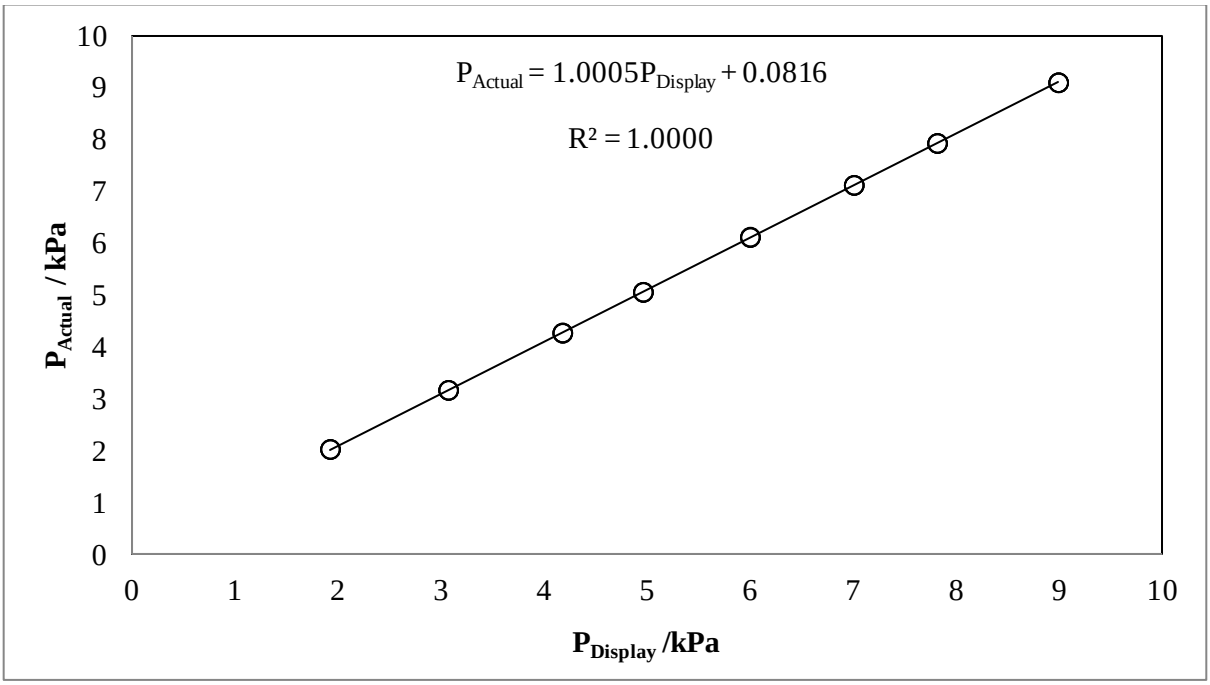

Figure 7.3: Pressure transducer calibration (0-10 kPa)

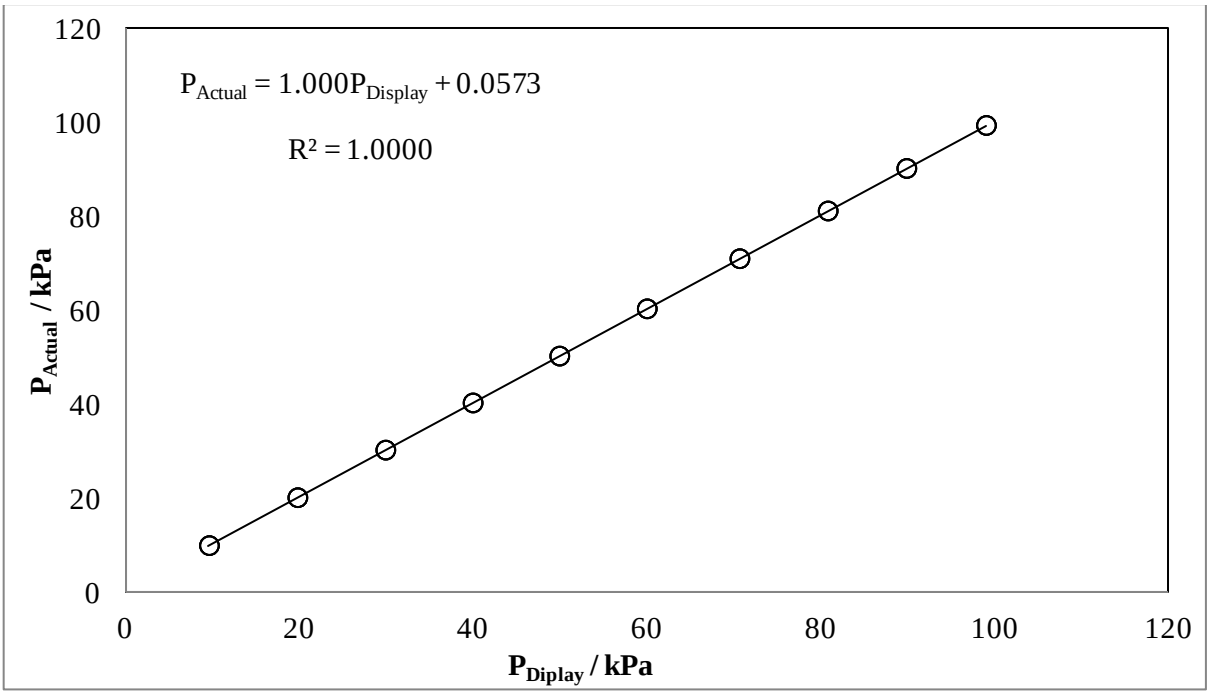

Figure 7.4: Pressure transducer calibration (10-100 kPa)

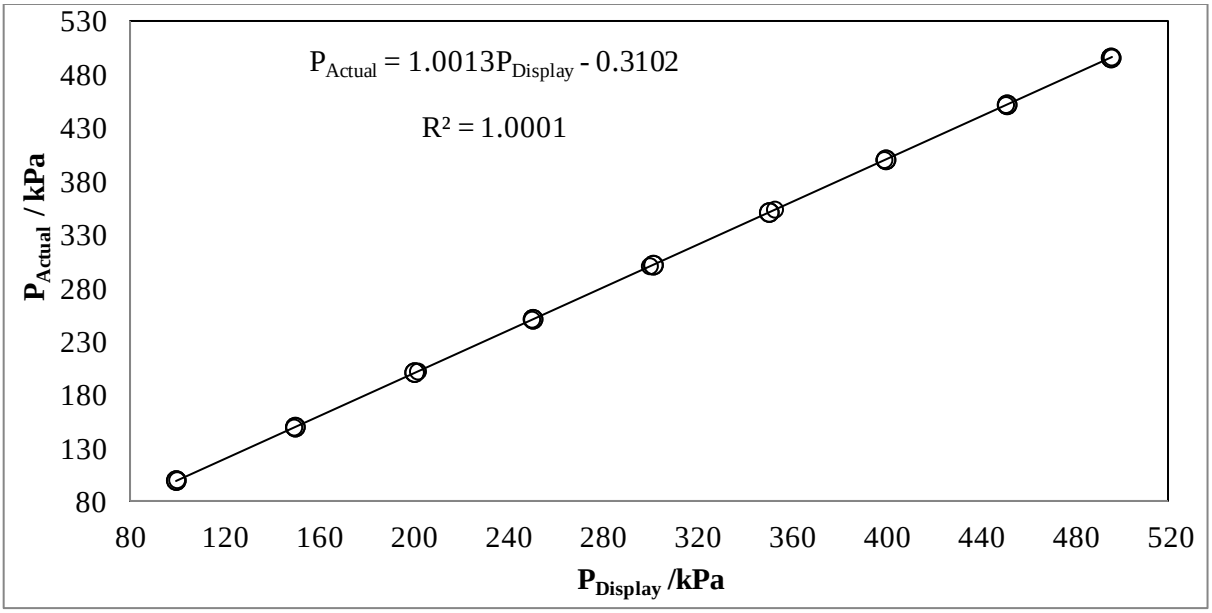

Figure 7.5: Pressure transducer calibration (100-500 kPa)

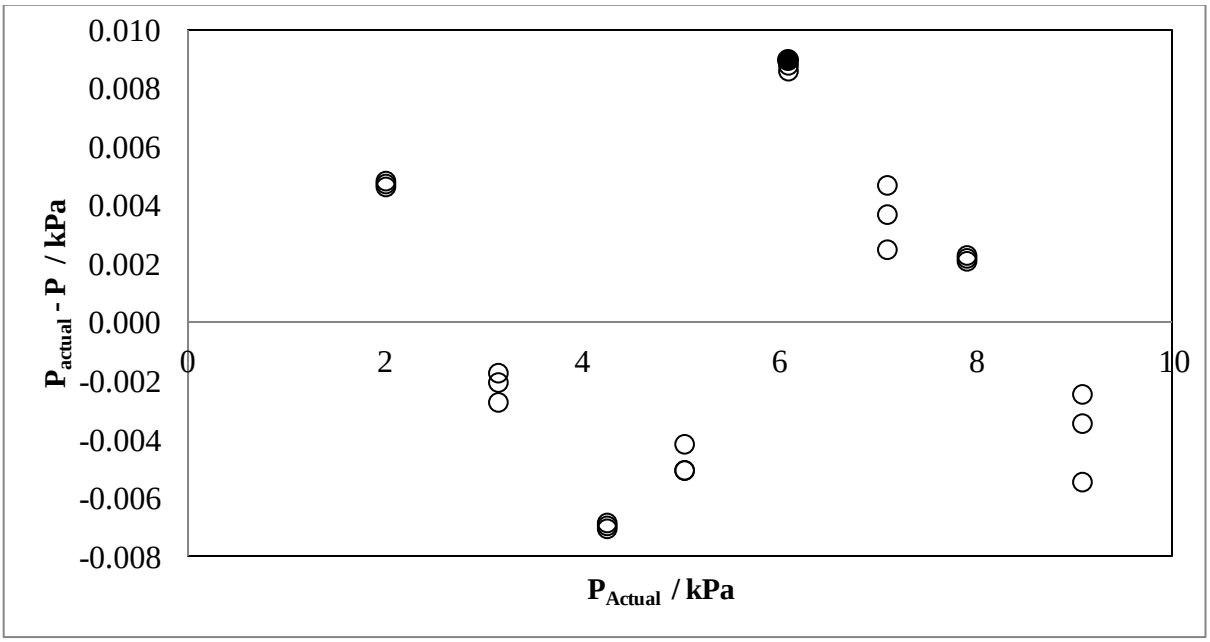

Figure 7.6: Plot of the pressure deviation (0-10 kPa), ● maximum deviation.

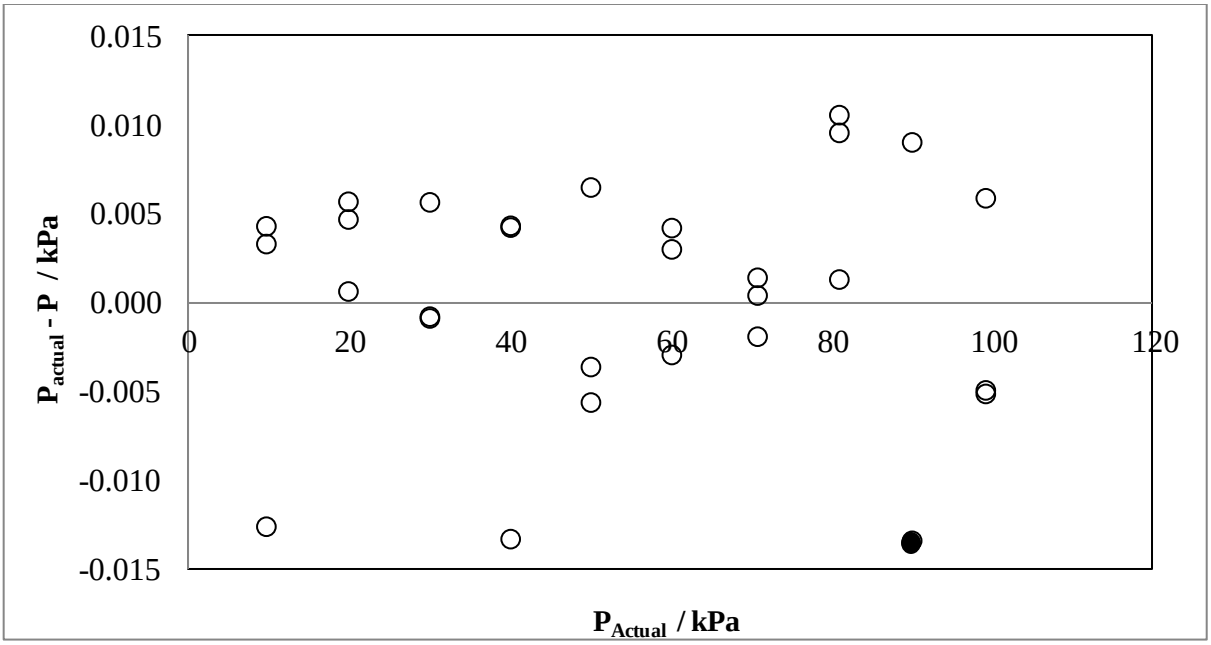

Figure 7.7: Plot of the pressure deviation (10-100 kPa), ● maximum deviation.

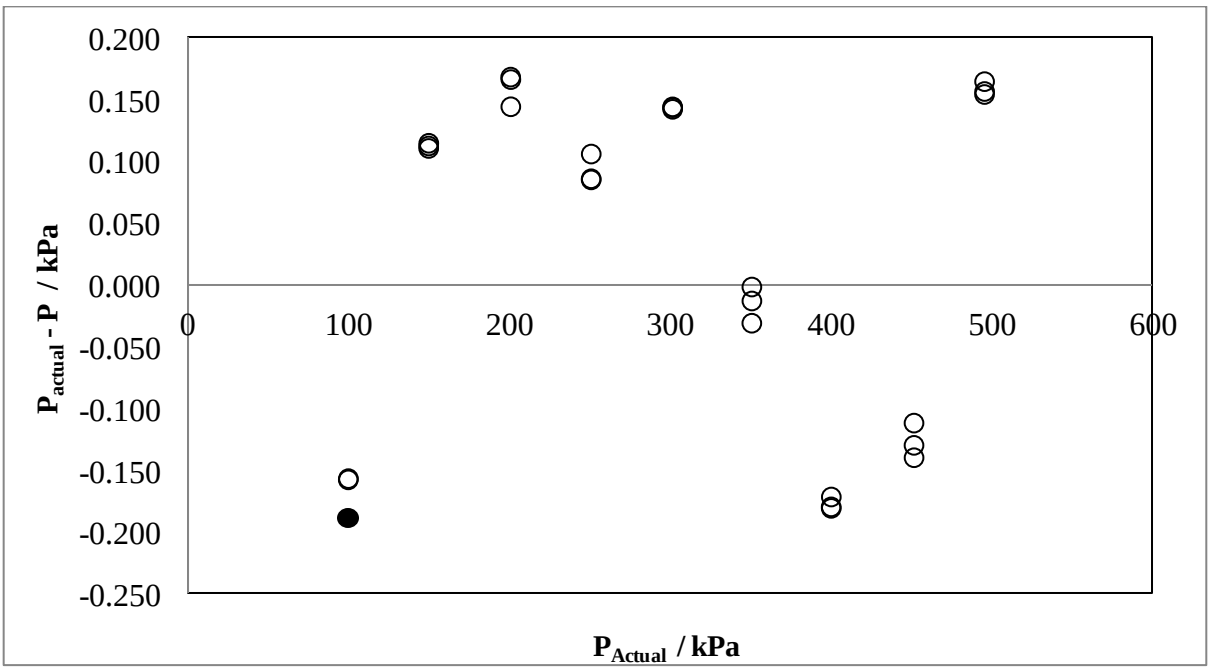

Figure 7.8: Plot of the pressure deviation (100-500 kPa), ● maximum deviation

7.4. **Uncertainty in Measurements**

Uncertainty is regarded as the doubts that arise from the measurement and can be quantified as an interval within which the specific quantity subject to measurement

(measurand) may be presumed to lie with a given probability (Bell, 1999 and Birch, 2003).

Individual uncertainties from different sources are calculated, and an overall uncertainty for the measurement referred to as the combined standard uncertainty is determined as follows:

$$u_c(\vartheta) = \pm\sqrt{\sum_i u_i(\vartheta)^2} \tag{7.1}$$

where $u_i(\theta)$ is the uncertainty from any possible sources, such as the temperature or pressure calibration.

7.4.1. Uncertainty in Temperature and Pressure

Uncertainties for these variables are attributed to calibration defects and repeatability deviations of a single transducer reading. The combined standard uncertainty in temperature or pressure is estimated as:

$$u_c(T) = \pm\sqrt{u_{calib}(T)^2 + u_{rep}(T)^2} \tag{7.2}$$

where *calib* and *rep* denotes calibration and repeatability respectively.

Calibration imperfections are determined by the Type B, random calculation method and repeatability deviations are extracted from manufacturer's manuals. The Type B (random uncertainty) for a rectangular distribution approach is:

$$u_{calib} = \frac{b}{\sqrt{3}} \tag{7.3}$$

where b is the average length between the upper and lower limits of the calibration plots.

7.4.2. Uncertainty in Molar Composition

The uncertainties for molar composition are attributed to an imprecision in the detector calibration, imperfections of the scale (balance) used for preparation of standard solutions and the standard deviation from the averaging of repeated samples. The study of Soo (2011) supports neglecting the errors arising from the mass balance and repeatability, as the sum of these uncertainties only contribute to 1% of the final total

uncertainty. As a result, a less rigorous but still more than sufficient, combined standard uncertainty (analogous to temperature) was utilized:

$$u_c(x_i) = \pm\sqrt{u_{calib}(x_i)^2 + u_{rep}(x_i)^2} \tag{7.4}$$

The repeatability of the measurements $u_{rep}(x_i)$ via:

$$u_{rep} = \frac{\sigma}{\sqrt{n}} = \sqrt{\frac{1}{n(n-1)}\sum_{i=1}^{n}\left(x_i - \bar{x}\right)^2} \tag{7.5}$$

where $\bar{x}$ is the mean, σ is the standard deviation and n is the number of repeated measurements.

The calculated combined standard uncertainties for temperature and pressure are presented in Table 7.2. These uncertainties indicate reliable results. The uncertainty in the molar composition was averaged over the entire data set and is presented in Tables 7.9.

Table 7.2: Experimental temperature and pressure combined standard uncertainties

	Range	u_C
Temperature/ K	273.15 – 433.15	±0.02 K
Pressure/ kPa	0-10	±0.005 kPa
	10-100	±0.013 kPa
	100-500	±0.15 kPa

7.5. Vapour pressure measurements

The correct estimation of plateau conditions via the LabVIEW program was one of the outcomes of the project. The temperature response curve for acetone at 40.33 kPa (Figure 7.9) clearly depicts the plateau region permitting accurate measurement of vapour pressures. Similar curves were completed for determining the vapour pressures of all chemicals used in this study.

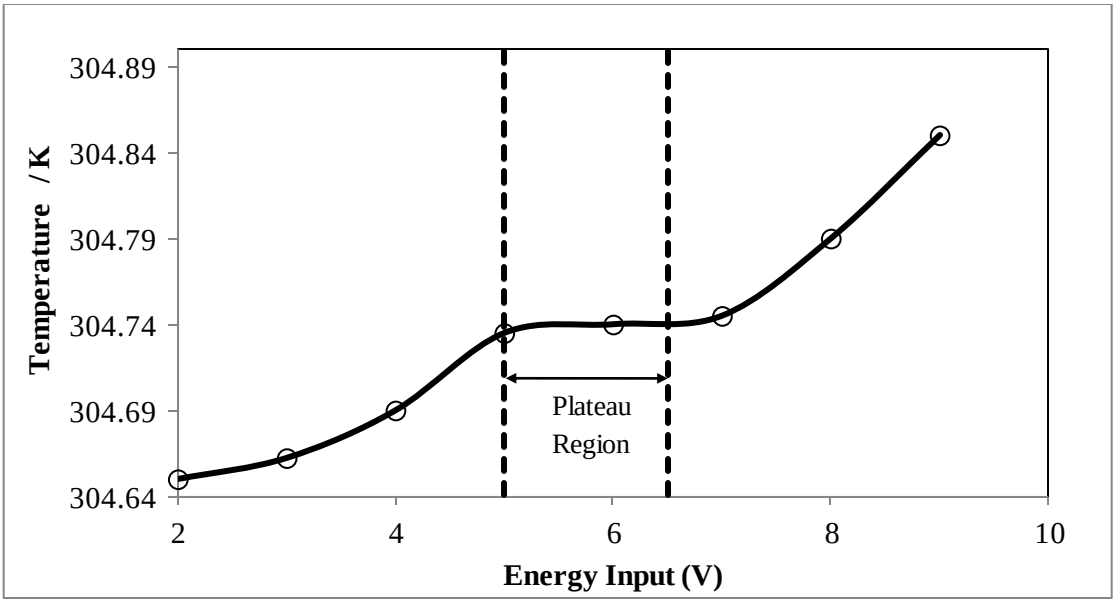

Figure 7.9: Temperature response curve for Acetone at 40.33 ±0.013 kPa.

Measured vapour pressures reported in Tables 7.3-7.8 serve as a preliminary test of all equipment functionality and confirms sensor calibrations. Vapour pressure measurements were conducted at low pressure and preceded to medium pressures.

The deviations between literature data and experimental measured data are quantified by adopting the following equations within the mentioned tables.

Deviation of ΔX (Temperature/Pressure)

$$\Delta X = X^{Exp} - X^{Lit} \tag{7.6}$$

Percentage Deviation of ΔX% (Temperature/Pressure)

$$\Delta X(\%) = 100 * \frac{X^{Exp} - X^{Lit}}{X^{Exp}} \tag{7.7}$$

Average absolute difference $\%\Delta X_{AAD}$ (Temperature/Pressure)

$$\%\Delta X_{AAD} = \frac{100}{n} * \sum_{i}^{n} \frac{X_i{}^{Exp} - X_i{}^{Lit}}{X_i{}^{Exp}} \tag{7.8}$$

Root mean square value of the $\delta\left[\ln\frac{\gamma_1^*}{\gamma_2^*}\right]$:

$$RMSD = \sqrt{\frac{\sum_{i=1}^{n}\left(\ln\frac{\gamma_1^{Exp}}{\gamma_2^{Exp}} - \ln\frac{\gamma_1^{Calc}}{\gamma_2^{Calc}}\right)^2}{n}} \qquad (7.9)$$

Table 7.3: Vapour pressure measurements for Acetone

P ±0.013 /kPa	T ±0.02 /K	ΔP/ kPa		ΔP%	
		Lit[a]	Lit[b]	Lit[a]	Lit[b]
29.15	297.09	-0.08	-0.25	-0.26	-0.86
40.33	304.75	-0.01	-0.27	-0.02	-0.66
49.96	310.09	0.01	-0.31	0.03	-0.62
60.09	314.84	0.11	-0.29	0.18	-0.48
70.04	318.92	0.18	-0.28	0.25	-0.40
79.94	322.54	0.28	-0.24	0.35	-0.30
89.76	325.80	0.36	-0.22	0.40	-0.25
99.26	328.70	0.40	-0.24	0.40	-0.24
			$\%\Delta P_{AAD}$	0.24	0.48

[a]Dortmund Data Bank (2011)
[b]Poling *et al.* (2001)

Table 7.4: Vapour pressure measurements for Ethyl Acetate

P ±0.013 /kPa	T ±0.02 /K	ΔP/ kPa		ΔP%	
		Lit[a]	Lit[b]	Lit[a]	Lit[b]
18.24	305.95	0.01	0.00	0.04	0.02
28.15	315.71	0.18	0.14	0.63	0.51
38.00	322.99	0.25	0.20	0.67	0.53
47.88	328.86	0.40	0.33	0.83	0.70
			$\%\Delta P_{AAD}$	0.54	0.44

[a]Dortmund Data Bank (2011)
[b]Poling *et al.* (2001)

Table 7.5: Vapour pressure measurements for 1-Hexene

P/kPa	T ±0.02 /K	ΔP/ kPa		ΔP%	
		Lit[a]	Lit[b]	Lit[a]	Lit[b]
40.00±0.013	310.10	-0.06	-0.13	-0.15	-0.33
60.00±0.013	321.02	0.08	-0.03	0.14	-0.05
80.00±0.013	329.33	0.22	0.09	0.28	0.12
100.00±0.15	336.16	0.29	0.19	0.29	0.19
140.00±0.15	347.13	0.27	0.31	0.19	0.22
180.00±0.15	355.85	0.30	0.60	0.17	0.34
220.00±0.15	363.16	0.45		0.20	
260.00±0.15	369.53	0.49		0.19	
300.00±0.15	375.25	0.06		0.02	
340.00±0.15	380.38	-0.11		-0.03	
			$\%\Delta P_{AAD}$	0.17	0.21

[a]Dortmund Data Bank (2011)
[b]Poling *et al.* (2001)

Table 7.6: Vapour pressure for N-methyl pyrrolidone-2

P/kPa	T ±0.02 /K	ΔP/ kPa			ΔP%		
		Lit[a]	Lit[b]	Lit[c]	Lit[a]	Lit[b]	Lit[c]
3.09±0.005	371.30	-0.02	0.02	0.01	-0.80	0.77	0.18
5.00±0.005	382.60	-0.06	0.02	0.00	-1.16	0.43	0.01
6.00±0.005	386.85	-0.02	0.08	0.06	-0.31	1.29	0.94
6.94±0.005	390.65	-0.07	0.05	0.03	-0.94	0.70	0.40
8.00±0.005	394.35	-0.10	0.04	0.02	-1.19	0.50	0.25
10.00±0.005	400.15	-0.09	0.08	0.07	-0.92	0.84	0.68
20.00±0.013	420.05	-0.40	0.05	0.07	-2.00	0.26	0.36
				$\%\Delta P_{AAD}$	1.09	0.67	0.44

[a]Dortmund Data Bank (2011)
[b]Component Plus (2010)
[c]Aspen Plus® (2010)

Table 7.7: Vapour pressure measurements for 1-propanol

P/kPa	T ±0.02 /K	ΔP/ kPa		ΔP%	
		Lit[a]	Lit[b]	Lit[a]	Lit[b]
19.94±0.013	332.14	0.14	0.16	0.73	0.80
39.94±0.013	347.63	-0.16	-0.05	-0.41	-0.13
59.94±0.013	357.05	-0.19	0.02	-0.32	0.04
79.94±0.013	364.13	-0.19	0.11	-0.23	0.14
89.94±0.013	367.13	-0.17	0.15	-0.19	0.17
99.94±0.013	369.89	-0.22	0.12	-0.22	0.12
109.94±0.15	372.39	-0.09	0.25	-0.08	0.23
119.94±0.15	374.82	-0.44	-0.10	-0.36	-0.08
139.94±0.15	379.06	-0.41	-0.13	-0.29	-0.09
159.94±0.15	382.84	-0.37	-0.19	-0.23	-0.12
179.94±0.15	386.26	-0.37	-0.34	-0.20	-0.19
199.94±0.15	389.39	-0.34	-0.53	-0.17	-0.26
219.94±0.15	392.30	-0.46		-0.21	
240.00±0.15	394.96	-0.13		-0.06	
260.00±0.15	397.45	0.08		0.03	
280.00±0.15	399.78	0.44		0.16	
300.00±0.15	402.10	-0.26		-0.09	
320.00±0.15	404.15	0.48		0.15	
340.00±0.15	406.29	-0.61		-0.18	
360.00±0.15	408.23	-0.72		-0.20	
380.00±0.15	410.05	-0.34		-0.09	
			$\%\Delta P_{AAD}$	0.21	0.11

[a]Aspen Plus® (2010)
[b]Poling *et al.* (2001)

Table 7.8: Vapour pressure measurements for 2-Butanol

P ±0.013 /kPa	T ±0.02 /K	ΔP/ kPa		ΔP%	
		Lit[a]	Lit[b]	Lit[a]	Lit[b]
40.00±0.013	349.52	0.20	0.37	0.51	0.92
80.00±0.013	366.07	0.66	0.92	0.82	1.15
120.00±0.15	376.86	0.78	1.40	0.65	1.17
160.00±0.15	385.09	0.57	1.88	0.35	1.17
200.00±0.15	391.89	-0.37	1.99	-0.18	0.99
238.50±0.15	397.53	-1.82	1.87	-0.76	0.78
			$\%\Delta P_{AAD}$	0.38	0.75

[a]Dortmund Data Bank (2011)
[b]Aspen Plus (2010)

7.6.Gas Chromatograph operating conditions and calibrations

A Shimadzu 2010 gas chromatograph was utilized for all systems analysis under operating conditions summarized in Table 7.10. The GC calibration curves were completed using the area ratio method of Raal and Mühlbauer (1998) as described in section 6.4. The calibration graphs for all systems were fitted to linear equations except for the 1-hexene and N-methyl pyrrolidone-2 (NMP) that exhibited a best fit to a quadratic equation. The calibrations curves and combined standard uncertainties for all binary systems measured are presented in Figures 7.10-7.15 and listed in Table 7.9 respectively.

Table 7.9: Experimental mole fraction uncertainties for the binary systems measured.

	u_c (x) / mole
Cyclohexane (1) and ethanol (2)	±0.005
1-propanol (1) and 2-butanol (2)	±0.006
1-hexene (1) + N-methyl pyrrolidone-2 (NMP) (2)	±0.008

Table 7.10: Operating conditions for the Shimadzu 2010 gas chromatograph

System	Ethanol and Cyclohexane	1-Hexene and N-methyl pyrrolidone-2 (NMP)	1-Propanol and 2-Butanol
Carrier gas	Helium	Helium	Helium
Carrier gas flow ($ml.min^{-1}$)	35	205	30
Injector temperature (^oC)	250	30	250
Column used	Porapak Q	Porapak Q	Porapak Q
Temperature Control Mode	Isothermal	Isothermal	Isothermal
Oven Temperature (^oC)	240	220	238
Column Length (m)	4	3	4
ID(mm)	2.2	2.2	2.2
Material	Stainless Steel	Stainless Steel	Stainless Steel
Mesh Range	80/100	80/100	80/100
Detector type	TCD	TCD	TCD
Detector Temperature (^oC)	240	320	250
Current (mA)	90	62	105
Elution Time (min)			
Cyclohexane	5.539		
Ethanol	1.765		
1-Hexene		0.662	
N-methyl pyrrolidone-2		4.096	
1-Propanol			3.240
2-Butanol			4.330

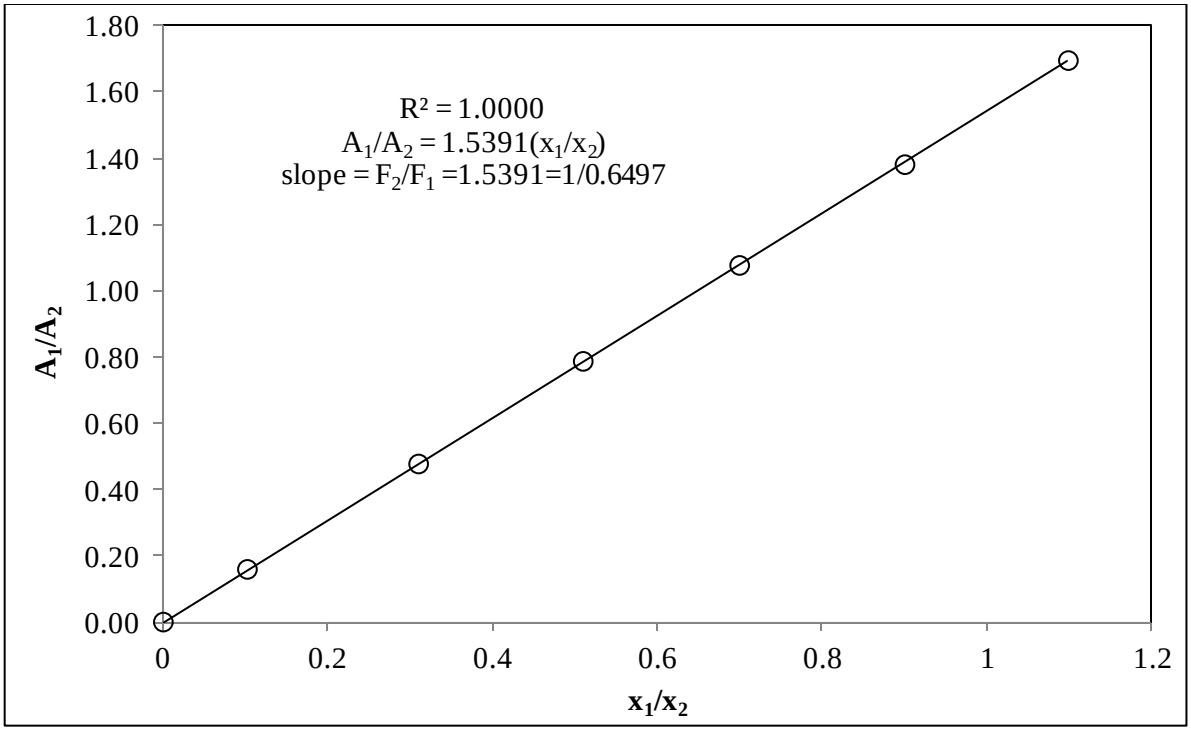

Figure 7.10: TCD calibration for the cyclohexane (1) and ethanol (2) system (Ethanol rich region)

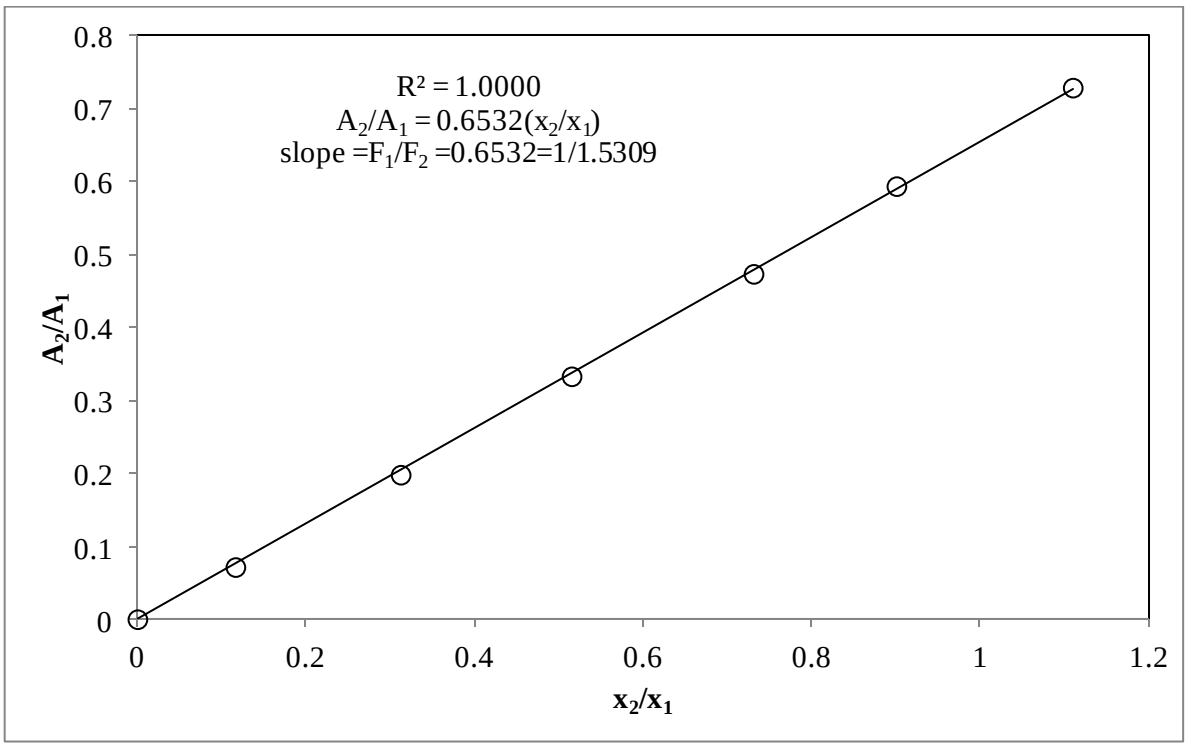

Figure 7.11: TCD calibration for the cyclohexane (1) and ethanol (2) system (Cyclohexane rich region)

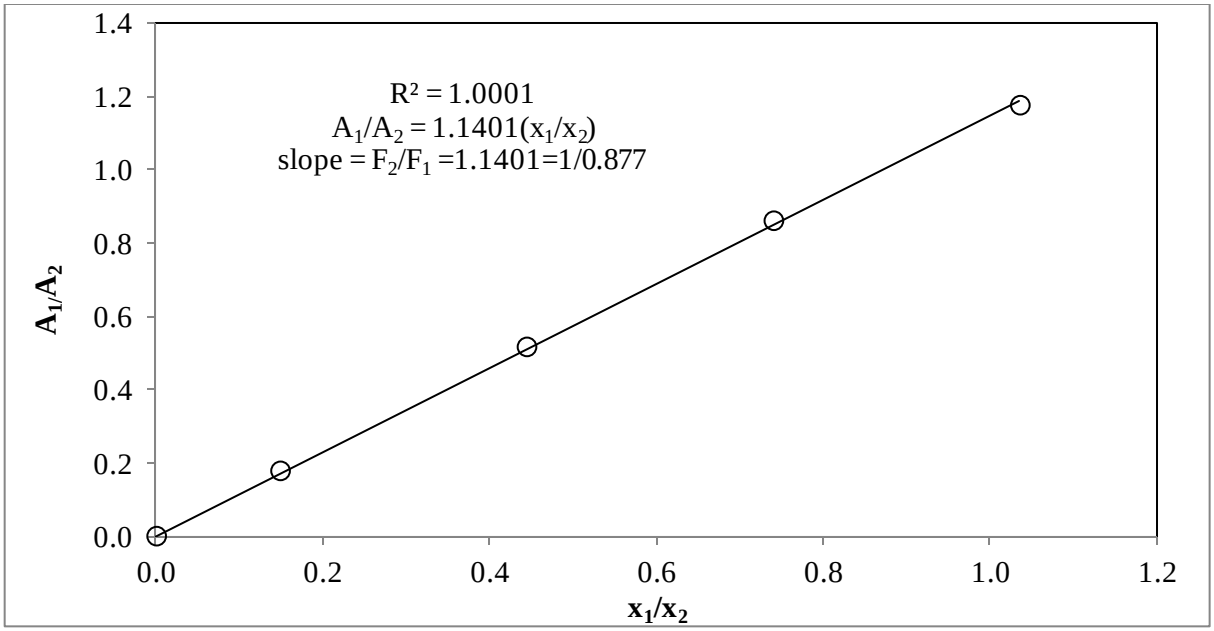

Figure 7.12: TCD calibration for the 1-propanol (1) and 2-butanol (2) system (1-propanol rich region)

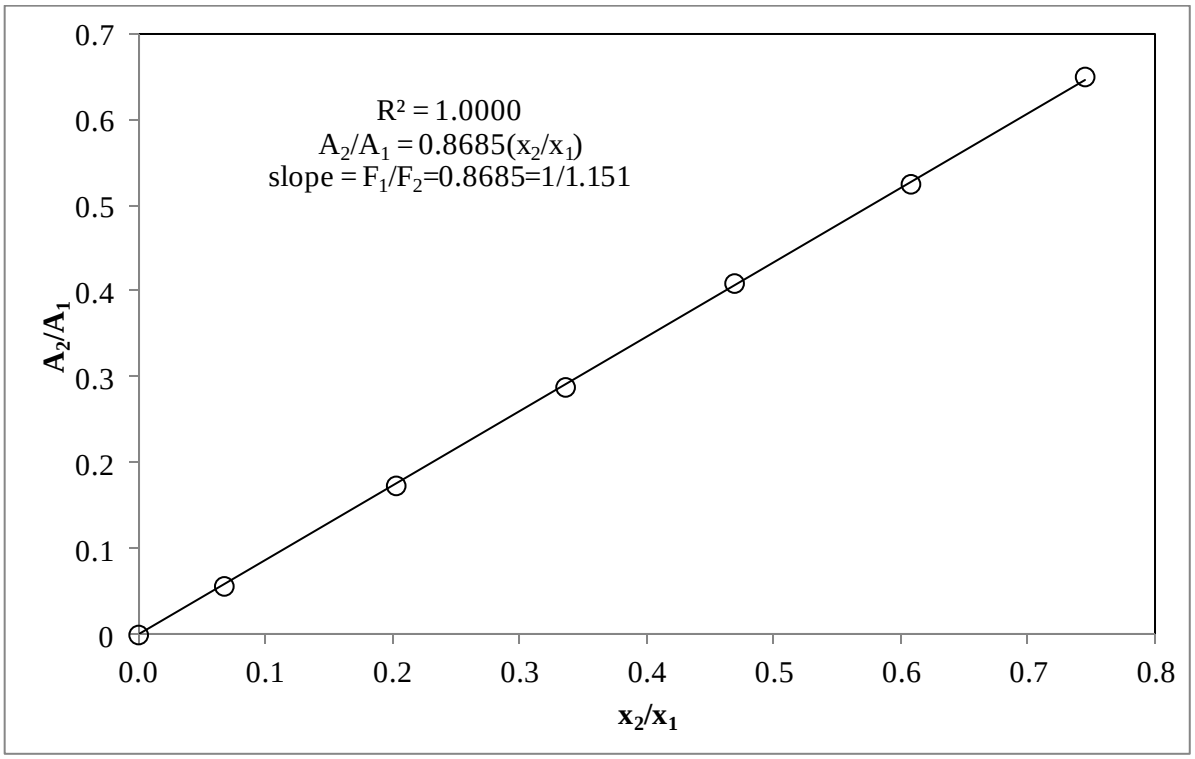

Figure 7.13: TCD calibration for the 1-propanol (1) and 2-butanol (2) system (2-butanol rich region)

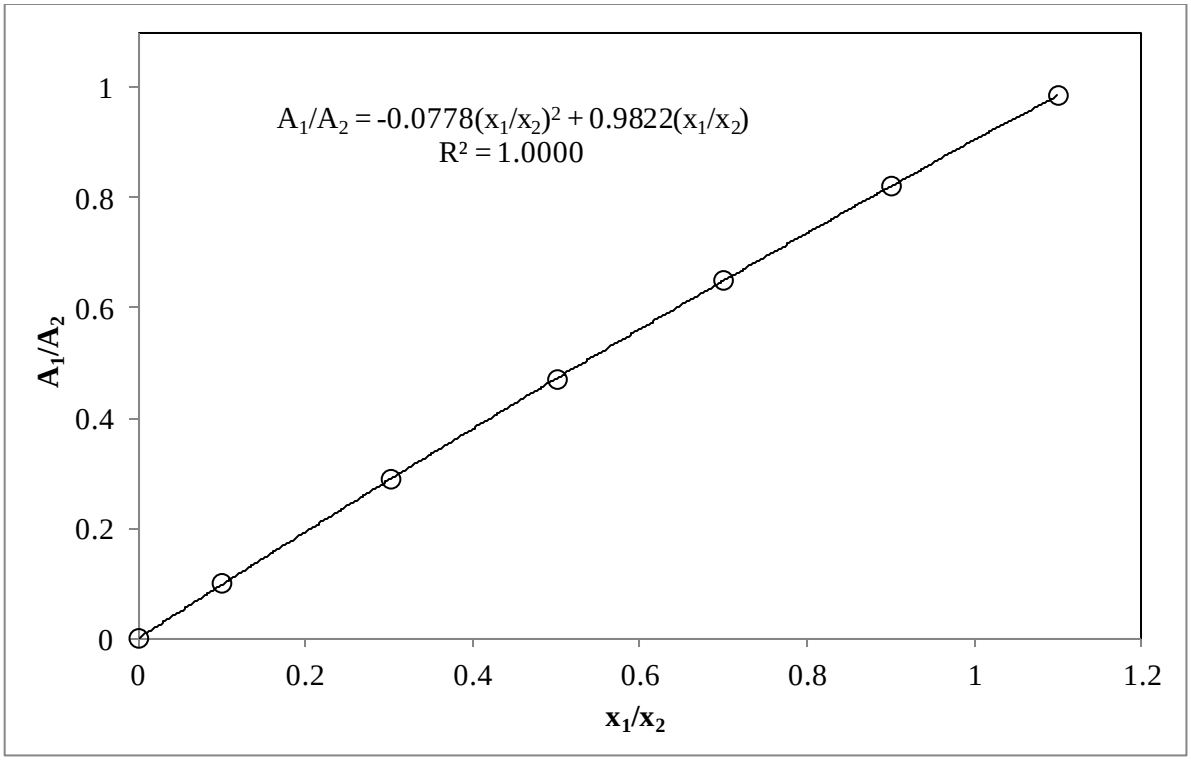

Figure 7.14: TCD calibration for the 1-hexene (1) + N-methyl pyrrolidone-2 (NMP) (2) system (1-hexene rich region)

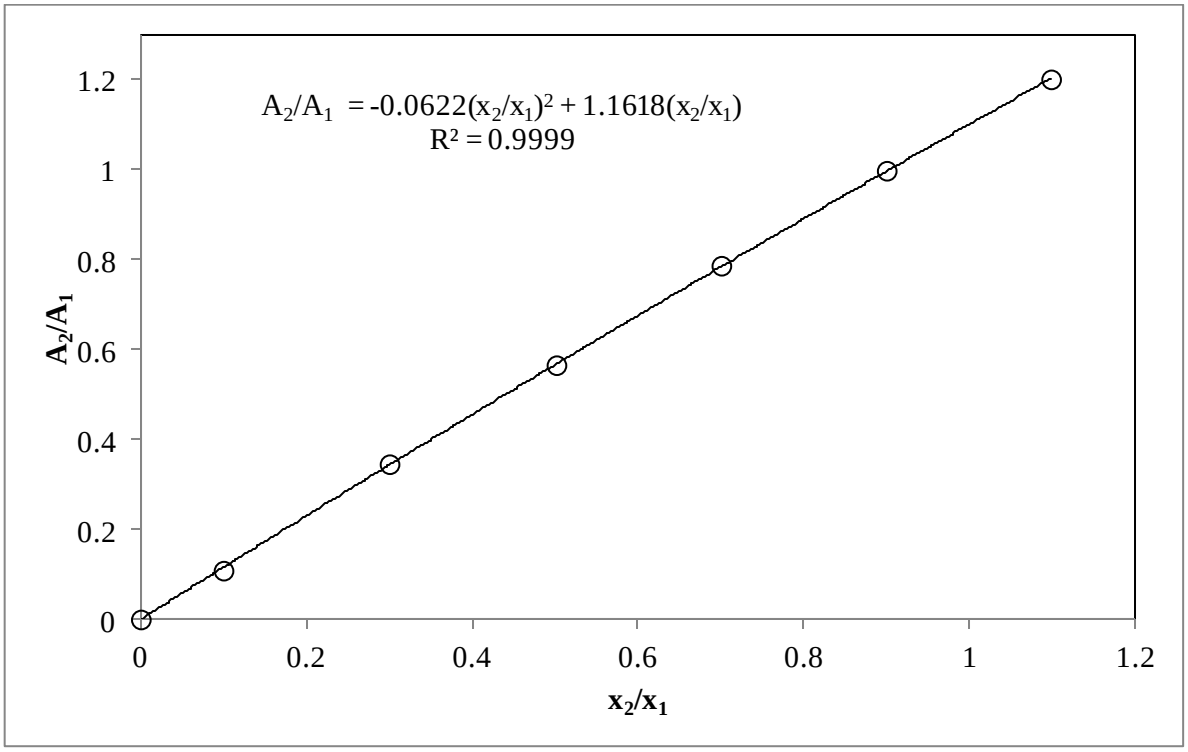

Figure 7.15: TCD calibration for the 1-hexene (1) + N-methyl pyrrolidone-2 (NMP) (2) system (NMP) rich region)

7.7.Binary Vapour-Liquid Equilibrium Results

7.7.1. Results for the system: Cyclohexane (1) and ethanol (2)

Measurements for the cyclohexane (1) and ethanol (2) system were undertaken at 40kPa and compared to the published data of Joseph *et al.*, (2001). The experimental VLE data are listed in Table 7.11 and the T-x_1-y_1 and x_1-y_1 plots are presented in Figure 7.16 and Figure 7.17 respectively.

The figures illustrate excellent conformity to literature data indicating success in the semi-automation process for isobaric measurement and correct experimental techniques.

Table 7.11: Vapour-liquid equilibrium data for the cyclohexane (1) and ethanol (2) system at 40 ± 0.013 kPa.

T ±0.02 / K	x_1	y_1
329.64	0.000	0.000
329.41	0.001	0.013
328.98	0.004	0.034
328.14	0.009	0.073
327.28	0.014	0.112
325.39	0.028	0.195
324.32	0.038	0.245
322.52	0.056	0.316
321.05	0.076	0.371
319.85	0.095	0.398
318.90	0.117	0.449
316.49	0.201	0.535
315.35	0.320	0.580
314.90	0.513	0.608
314.84	0.613	0.620
314.81	0.867	0.656
316.03	0.943	0.683
317.84	0.979	0.744
318.86	0.985	0.774
321.85	0.987	0.869
323.47	0.993	0.915
325.40	0.999	0.983
325.92	1.000	1.000

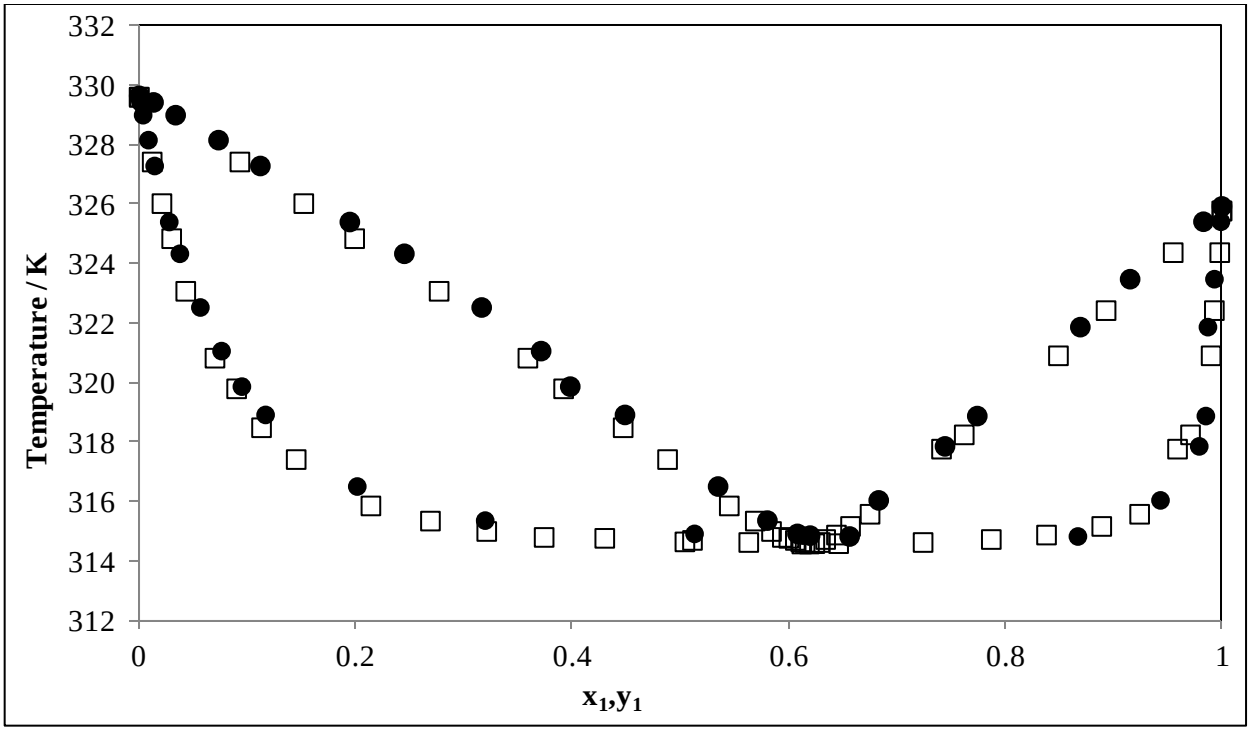

Figure 7.16: T-x_1-y_1 plot for the cyclohexane (1) and ethanol (2) system at 40±0.013 kPa. ● , Experimental data; □ , Joseph *et al*. (2001)

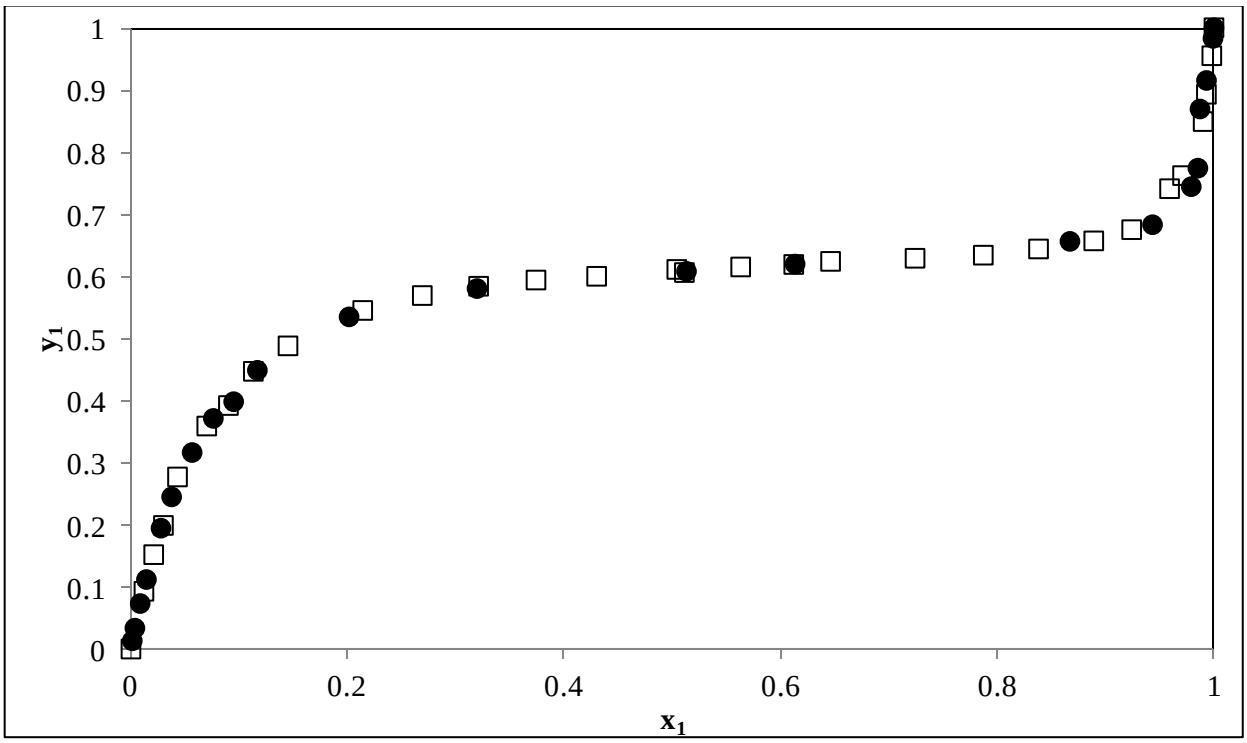

Figure 7.17: x_1-y_1 plot for the cyclohexane (1) and ethanol (2) system at 40±0.013 kPa. ● , Experimental data; □ , Joseph *et al*. (2001).

7.7.2. Results for the system: 1-hexene (1) + NMP (2)

Vapour-liquid equilibrium data were measured at two isotherms namely 363.61 K and 373.15 K for this system. The isotherm at 363.61 K, was previously published by Fischer and Gmehling (1995), however the measurement of P-y data was not included. The isotherm at 373.15 K can be regarded as new data.

The experimental VLE data points are tabulated in Table 7.12 to 7.13 and the P-x_1-y_1 and x_1-y_1 plots are presented in Figure 7.18 to 7.21. The excellent correlation to the literature data of Fischer and Gmehling (1995) at 363.61 K indicates a successful semi-automation for isothermal VLE measurements.

Table 7.12: Vapour-liquid equilibrium data for the 1-hexene (1) + N-methyl pyrrolidone-2 (NMP) (2) system at 363.61 ± 0.02 K

P / kPa	x_1	y_1
2.09 ± 0.005	0.000	0.000
2.19 ± 0.005	0.003	0.001
24.21 ± 0.013	0.019	0.910
33.80 ± 0.013	0.031	0.958
82.80 ± 0.013	0.097	0.978
111.43 ± 0.15	0.158	0.986
147.69 ± 0.15	0.278	0.990
151.26 ± 0.15	0.295	0.990
155.95 ± 0.15	0.330	0.990
165.90 ± 0.15	0.417	0.992
172.11 ± 0.15	0.467	0.992
175.92 ± 0.15	0.494	0.990
183.71 ± 0.15	0.583	0.991
187.27 ± 0.15	0.631	0.992
192.72 ± 0.15	0.700	0.993
198.65 ± 0.15	0.784	0.994
204.90 ± 0.15	0.859	0.995
213.83 ± 0.15	0.945	0.999
224.00 ± 0.15	1.000	1.000

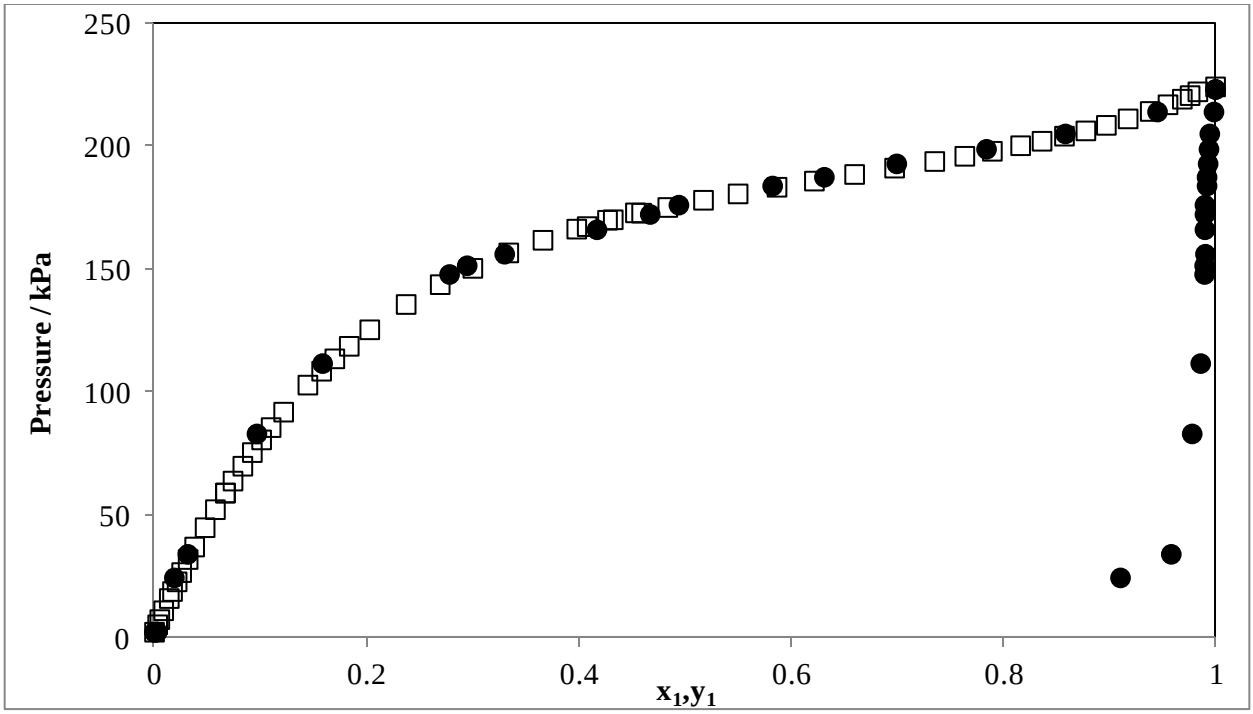

Figure 7.18: P-x_1-y_1 plot for the 1-hexene (1) + NMP (2) system at 363.61± 0.02 K ● , Experimental data; □ , Fischer and Gmehling, 1995 (P-x_1 data only).

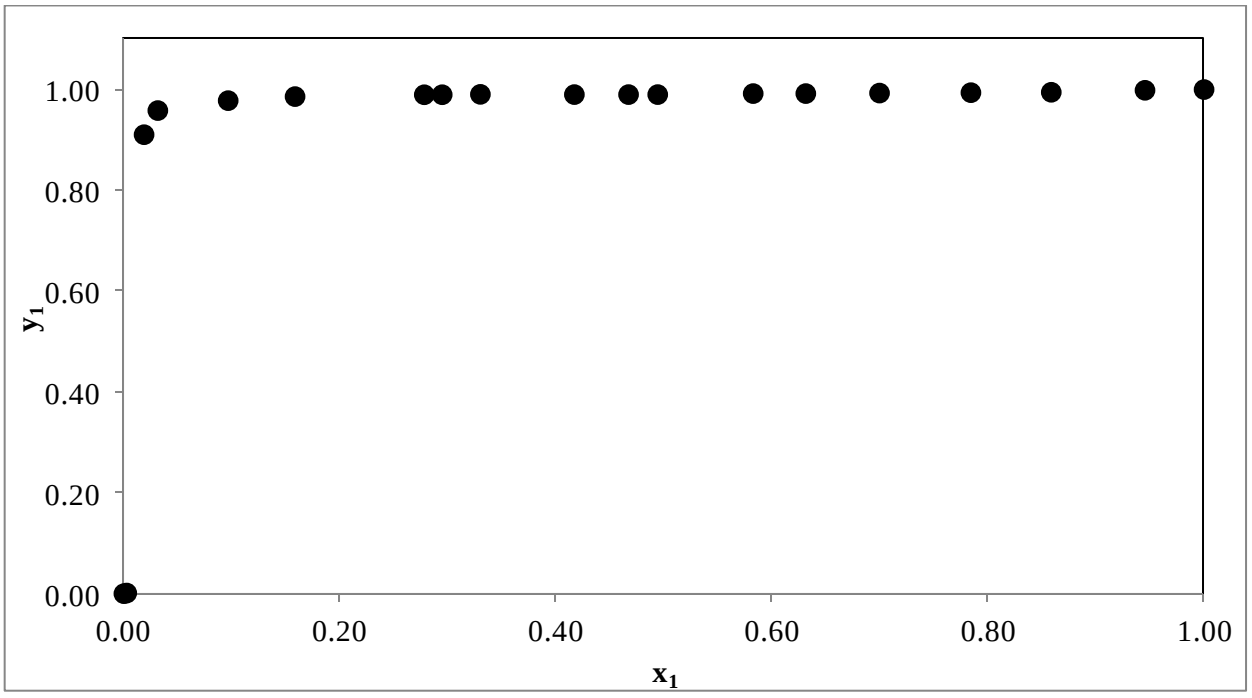

Figure 7.19: x_1-y_1 plot for the 1-hexene (1) + NMP (2) system at 363.61± 0.02 K ● , Experimental data.

Table 7.13: Vapour-liquid equilibrium data for the 1-hexene (1) + N-methyl pyrrolidone-2 (NMP) (2) system at 373.15 ± 0.02 K

P / kPa	x_1	y_1
5.10 ± 0.005	0.000	0.000
5.20 ± 0.005	0.003	0.001
9.21 ± 0.005	0.005	0.883
45.15 ± 0.013	0.033	0.967
107.98 ± 0.15	0.107	0.984
150.33 ± 0.15	0.178	0.988
176.00 ± 0.15	0.251	0.987
197.10 ± 0.15	0.348	0.988
211.18 ± 0.15	0.401	0.993
217.65 ± 0.15	0.430	0.993
225.38 ± 0.15	0.510	0.990
235.77 ± 0.15	0.607	0.990
240.12 ± 0.15	0.651	0.991
247.03 ± 0.15	0.718	0.992
256.78 ± 0.15	0.801	0.995
263.58 ± 0.15	0.863	0.998
275.17 ± 0.15	0.951	0.999
285.15 ± 0.15	1.000	1.000

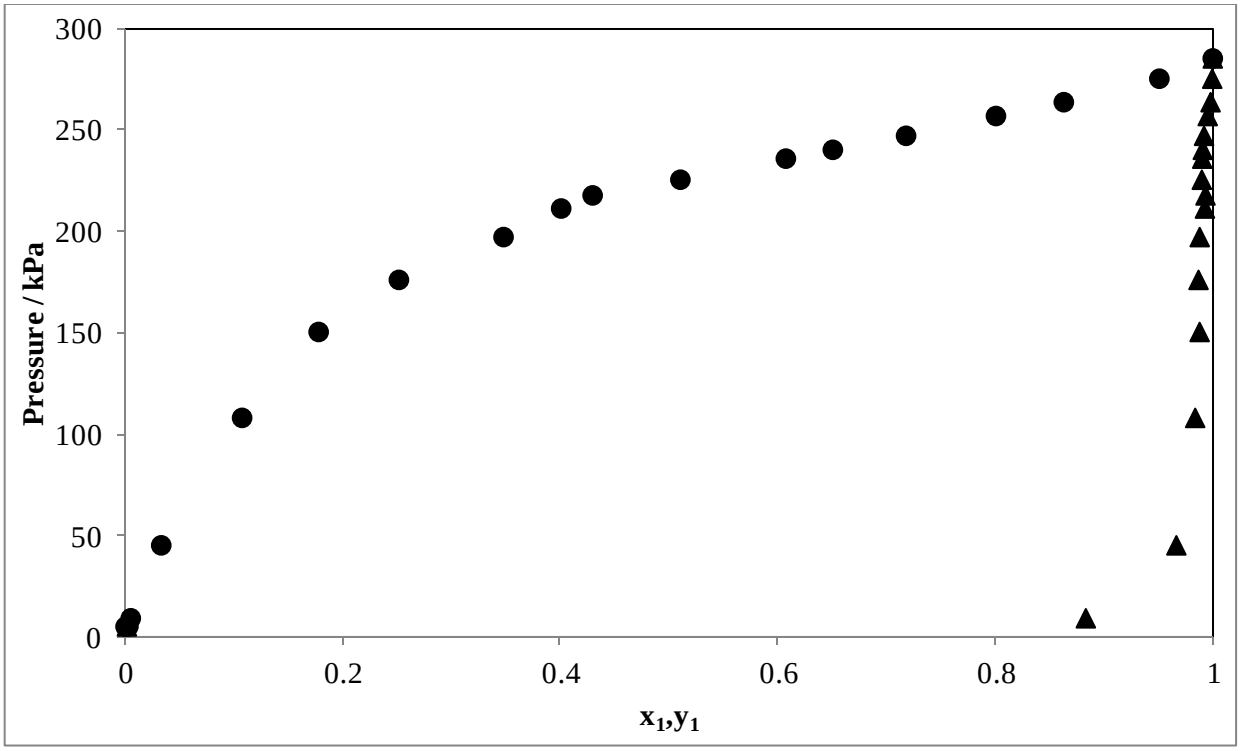

Figure 7.20: P-x1-y1 plot for the 1-hexene (1) + NMP (2) system at 373.15 ± 0.02 K

● , x_1 and ▲ , y_1 experimental data

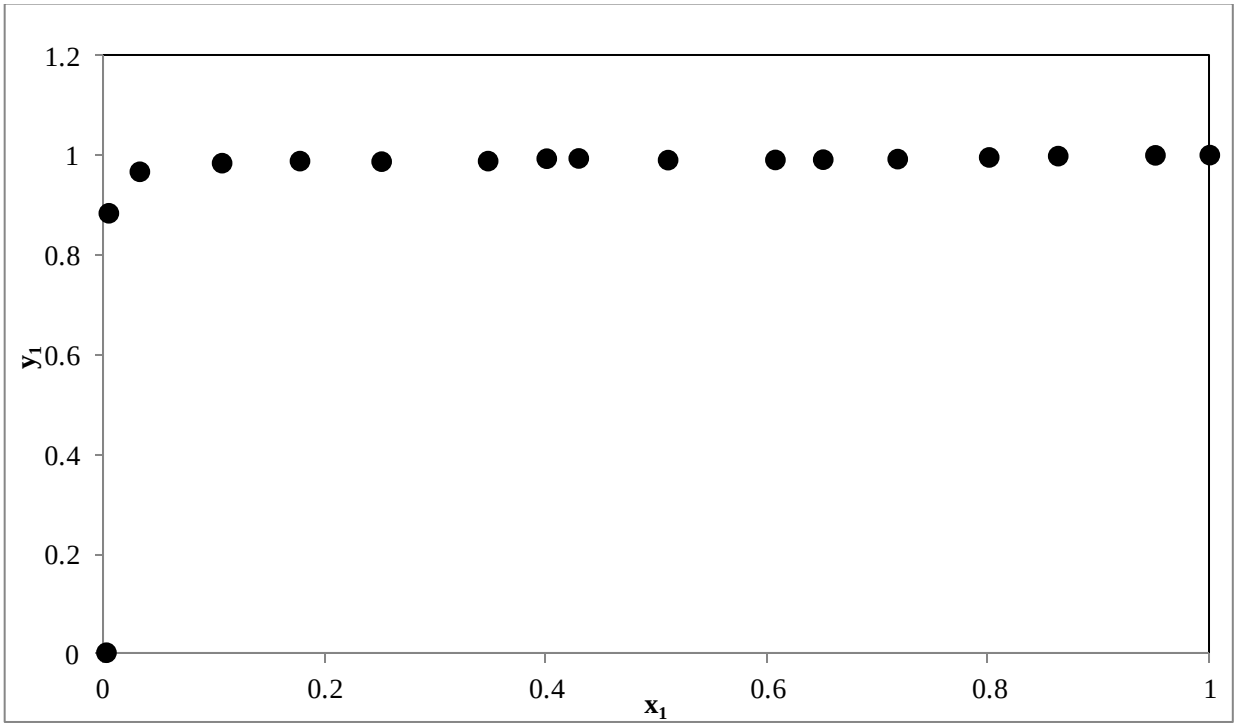

Figure 7.21: x_1-y_1 data for the 1-hexene (1) + NMP (2) system at 373.15 ± 0.02 K

● , Experimental data.

7.7.3. Results for the system: 1-propanol (1) and 2-butanol (2)

This binary system was measured at 393.15 K by Reddy (2009) using a dynamic stainless steel VLE apparatus and is presented for comparison.

The experimental VLE data are tabulated in Table 7.14 and the P-x_1-y_1 and x_1-y_1 plots are illustrated in Figure 7.22 to 7.23 respectively. The poor correlation observed to the literature data of Reddy (2009) is discussed in section 8.2.

Table 7.14: Vapour-liquid equilibrium data for the 1-propanol (1) and 2-butanol (2) system at 393.15 ± 0.02 K

P ± 0.15 / kPa	x_1	y_1
207.41	0.000	0.000
208.45	0.059	0.064
211.39	0.209	0.223
216.02	0.416	0.436
217.23	0.469	0.490
218.56	0.561	0.582
220.66	0.652	0.670
221.98	0.734	0.751
223.48	0.823	0.836
225.00	0.906	0.913
226.58	0.975	0.977
227.58	1.000	1.000

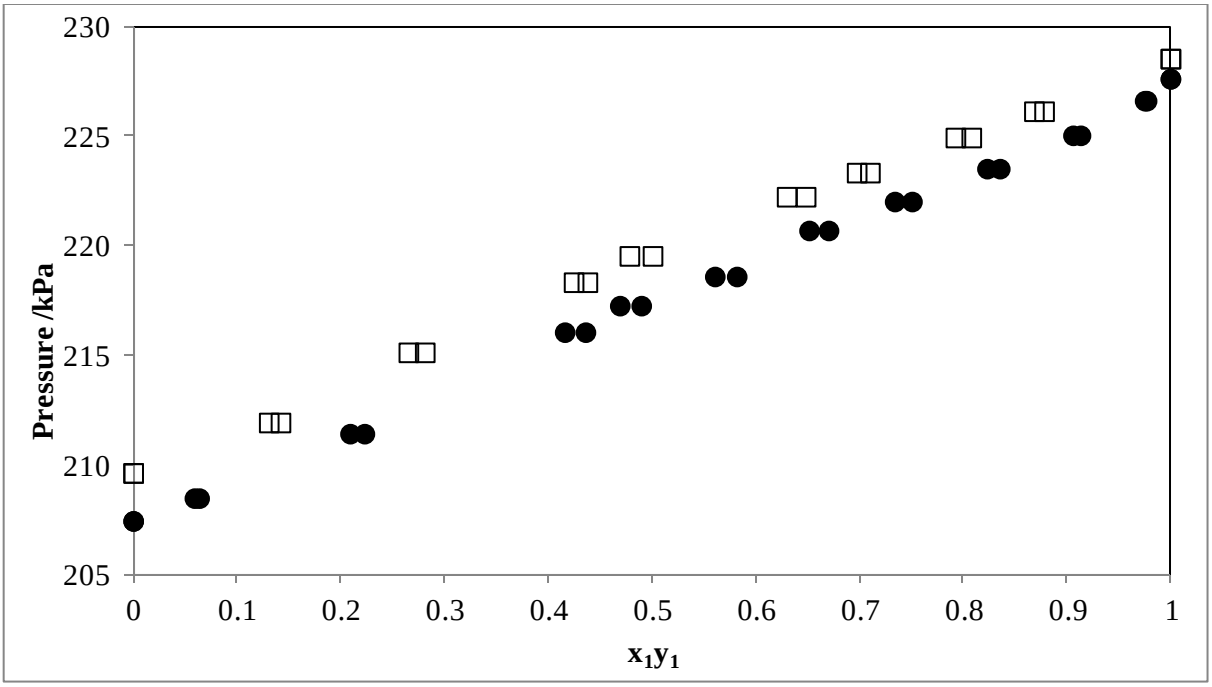

Figure 7.22: P-x_1-y_1 data for the 1-propanol (1) and 2-butanol (2) system at 393.15 ±0.02 K. ● , Experimental data; □ , Reddy (2001)

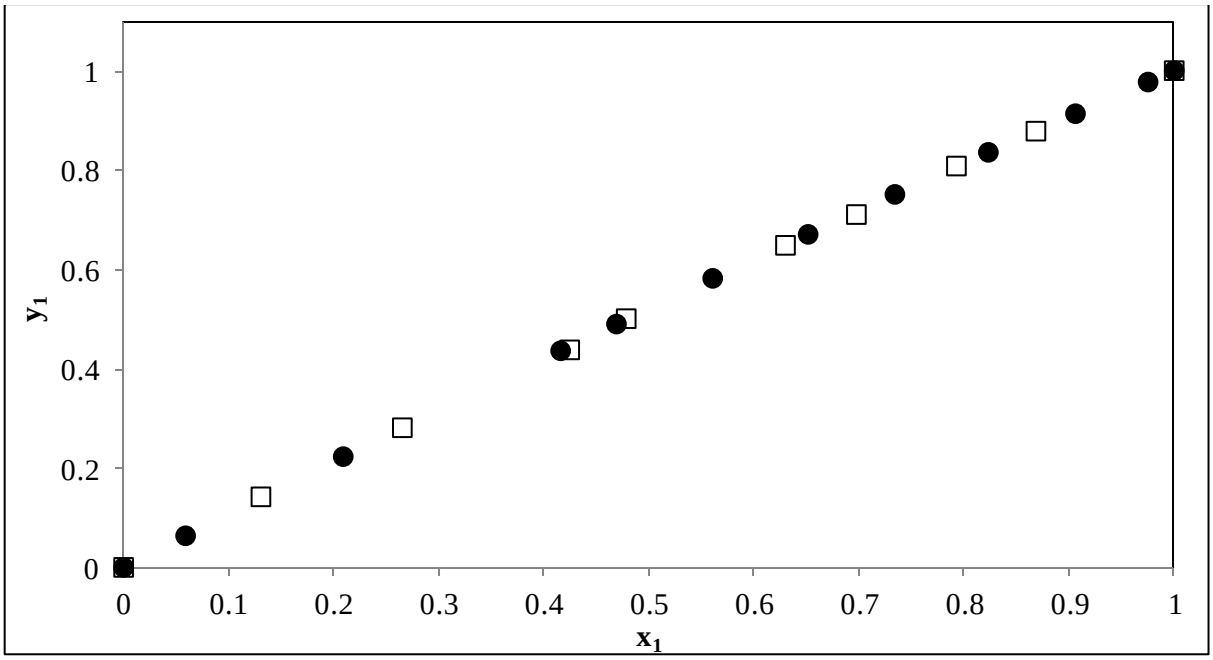

Figure 7.23: x_1-y_1 data for the 1-propanol (1) and 2-butanol (2) system at 393.15 ±0.02 K. ● , Experimental data; □ , Reddy (2001)

8. Data Analysis and Discussion

The analysis of the experimental data using the thermodynamic techniques described in Chapter 2 is presented in this chapter. The measured vapour pressure data sets were correlated to the Antoine and Wagner equations. The measured VLE data were regressed using both the combined and direct methods available in Aspen Plus®. Furthermore the experimental results were subjected to thermodynamic consistency testing to check its integrity.

8.1.Equipment Operation

The VLE glass still was tested to a pressure of 500kPa, in a stepwise pressurizing process using nitrogen. Table 8.1 lists the operating limits tested within this project.

Table 8.1: Equipment Operating Constraints

	Operating Conditions	
Pressure range tested (Under Nitrogen)	kPa	0 - 500
Pressure range tested (During VLE operation)	kPa	0 - 400
Maximum tested temperature	K	453.15
Temperature control deviation	K	±0.015
Pressure control deviation	kPa	±0.03

8.2.Pure Component: Vapour pressures

The functionality and reliability of the assembled equipment and the semi-automated LabVIEW program was initially tested measuring the vapour pressure of acetone and ethyl-acetate. The excellent correlation to literature data (Poling *et al.*, 2001) and to a lesser extent the data available from the Dortmund Data Bank (2011) for both of these chemicals (shown in Tables 7.3 and 7.4) indicates successful vapour pressure measurement using the equipment and software.

The average absolute pressure difference from literature data ($\%\Delta P_{AAD}$) for the chemicals investigated were less than 1%, the exception being for NMP when compared to Dortmund Data Bank (2011) as per Table 7.6. However the alternate literature sources Component Plus (2010) and Aspen Plus® (2011) for this chemical, exhibit average absolute pressure difference of 0.67% and 0.44% respectively. The

Aspen Plus® uses a four parameter Wagner equation (Reid *et al.*, 1988) compared to Dortmund Data Bank (2011) which uses the three parameter Antoine equation for vapour pressures. Further the Antoine coefficients from the Dortmund Data Bank (2011) literature source did not perfectly suit the experimental pressure range being investigated.

The vapour pressure data were correlated to the Antoine equation and Wagner equation (Reid *et al.*, 1988). The Antoine equation is given by:

$$\ln P(kPa) = A + \frac{B}{T(K) + C} \tag{8.1}$$

The "3-6" form of the Wagner equation (Reid *et al.*, 1988) is given by:

$$\ln \frac{P(kPa)}{P_C} = \frac{Ax + Bx^{1.5} + Cx^3 + Dx^6}{1 - x} \tag{8.2}$$

where, $x = \left(1 - \frac{T(K)}{T_C}\right)$, P is pressure in kPa, T is temperature in K, and T_C, P_C are critical properties for temperature and pressure respectively.

Table 8.2: Regressed Antoine equation parameters

Component	A	B	C	$\%\Delta P_{AAD}$ (kPa)	Temperature Range (K)
Acetone	14.370	-2773.55	-44.96	0.019	297.00 - 328.70
Ethyl Acetate	13.540	-2442.92	-76.29	0.049	305.95 - 328.86
1-hexene	13.770	-2629.02	-49.30	0.046	310.10 - 380.38
NMP	11.402	-2204.86	-157.18	0.333	297.09 - 419.46
1-propanol	16.359	-3666.28	-58.02	0.307	332.14 - 410.05
2-butanol	14.054	-2389.65	-118.98	0.049	349.52 - 397.53

$$\ln P(kPa) = A + \frac{B}{T(K) + C}$$

Table 8.3: Regressed Wagner (Reid *et al.*, 1988) equation parameters

Component	A	B	C	D	$\%\Delta P_{AAD}$ (kPa)	Temperature Range (K)
Acetone	-8.438	3.61	-6.52	6.143	0.0203	297.00 - 328.70
Ethyl Acetate	-41.191	80.69	-124.96	259.945	0.0000	305.95 - 328.86
1-hexene	-6.916	0.49	-1.91	-6.852	0.0424	310.10 - 380.38
NMP	-22.276	31.26	-32.06	11.342	0.345	297.09 - 419.46
1-propanol	-10.486	7.06	-25.63	105.632	0.1437	332.14 - 410.05
2-butanol	-11.368	9.16	=27.24	71.787	0.0139	349.52 - 397.53

$$\ln\frac{P(kPa)}{P_C}=\frac{Ax+Bx^{1.5}+Cx^3+Dx^6}{1-x}\ ,\ x=\left(1-\frac{T(K)}{T_C}\right)$$

The calculated average absolute pressure deviations for both the Antoine and Wagner (Reid *et al.*, 1988) equations were less than 1% for all investigated chemicals, indicating excellent model fitting of vapour pressures. The Wagner equation (Reid *et al.*, 1988) provided better correlation to pure component vapour pressures as anticipated. The Wagner equation (Reid *et al.*, 1988) is a four parameter equation, which is capable of representing experimental vapour pressure data for reduced temperatures, T_r ranging from zero to the chemical's critical point (Malanowski and Anderko, 1992). Reddy (2009) advices that the Wagner equation (Reid *et al.*, 1988) can be safely used to extrapolate outside the experimental data. The objective function employed for regressing the vapour pressure data is given by

$$Objective\quad function\quad =\sum_i\left(P_i^{\exp}-P_i^{calc}\right)^2 \tag{8.3}$$

The regression was completed using the computer programming platform MATLAB®, with built-in function (*fminsearch*).

8.3.Binary vapour-liquid equilibrium reduction

The measured VLE data was regressed using both the combined and direct reduction techniques, described in section 2.7. The software platform selected to accomplish this was Aspen Plus®, an excellent industrial process design simulation tool.

Aspen Plus® is equipped with a comprehensive thermodynamic database that is available for regression and process simulation calculations. The flexibility of Aspen Plus®, allows for user defined thermodynamic model inputs and promotes simulation robustness.

The Aspen Plus® thermodynamic model abbreviation conventions have been adapted for convenience and presented in Table 8.4.

Table 8.4: Thermodynamic model abbreviations

Thermodynamic Models	**Abbreviation**
Peng Robinson (1976) equation of state with the Wong Sandler (1992) mixing rule which includes the NRTL activity coefficient model.	PR-WS (NRTL)
Soave-Redlich-Kwong (1972) equation of state with the Wong Sandler (1992) mixing rule which includes the NRTL activity coefficient model.	SRK-WS (NRTL)
Hayden and O'Connell (1975) virial equation of state (vapour phase) with the NRTL activity coefficient.	HOC-NRTL
Hayden and O'Connell (1975) virial equation of state (vapour phase) with the Wilson activity coefficient.	HOC-WIL

The bubble-point pressure and bubble-point temperature type objective functions were employed for minimizing the error between experimental and model values for isothermal and isobaric measurements respectively (see section 2.8). The Britt-Luecke algorithm with maximum-likelihood objective function available in Aspen Plus® provided the best convergence and excellent parameter estimation. The Deming method was selected for the initialization process or approximate solution method.

The Predictive-Soave-Redlich-Kwong (PSRK) available in Aspen Plus® was initially employed to predict the behavior of the new systems being investigated. Deviations between the prediction and the measured data were observed indicating the group interaction parameters for the systems investigated may not be appropriate for the temperature range. The predictions however provided a guide/estimate for the

maximum pressures that could be exerted by the systems over the entire composition range especially considering that the equipment was tested only to 500 kPa.

8.3.1. Modeling of the 1-hexene (1) and NMP (2) binary system

This binary system was measured at two isotherms namely 363.61 and 373.15 K. Fischer and Gmehling (1995) measured P-x_i data on a static apparatus at 363.61 K only, therefore the P-y_i data at this isotherm and at 373.15 K performed within this project constitutes new data.

The adjustable binary interaction parameters for the different models are presented in Table 8.5. The ΔP_{AAD} and Δy_{AAD} for all models are very small, with the highest error being 0.006 for both, indicating good model fit. The PR-WS (NRTL) model provides the best fit to the VLE data at both isotherms. Figures 8.1 to 8.8 provide graphical comparison of the models fit to the VLE data set.

Twu and Coon (1996) stated that the Wong-Sandler (1992) mixing rule provides excellent correlation abilities for nonideal systems which is evident with the results presented. Both cubic equation of state models combined with the Wong Sandler (1992) mixing rule provided superior fit to VLE data.

NMP has polar and associative properties (Fischer and Gmehling, 1995) that are enhanced with an increase in temperatures leading to greater deviations. This is supported with the results presented in Table 8.5 that depict a trend of increasing deviations with increasing temperatures.

The literature review, Chapter2, describes the recommendations and applications which many researchers adopt when using the NRTL model with respect to the non-randomness α_{12} parameter. The consideration around this parameter is whether to regress or fix during regression calculations. Upon computation and analysis of both options, the preferred option was the regression of the α_{12}. The results for the regressed α_{12} are presented in Figures 8.1 to 8.4, while results for using a α_{12} of 0.4567 (fixed) recommended by (Fischer and Gmehling, 1995) are presented in Appendix C.

The comparison of the two options for an isothermal temperature of 363.61 K, reveals higher ΔP_{AAD} and Δy_{AAD} of 0.002 and 0.001 using a α_{12} of 0.4567 than the regression of this parameter.

Flashing did occur at low pressures during experimental investigations. 1-Hexene has a significantly lower boiling temperature than that of NMP, requiring a very low condenser temperature. Therefore, during the vapour circulation in the equilibrium still, the cold condensed fluid encourages flashing within the boiling chamber. However the integrity of the results was conserved by ensuring that more data points were measured in the region were flashing occurred and that sufficient agitation was provided in the boiling chamber.

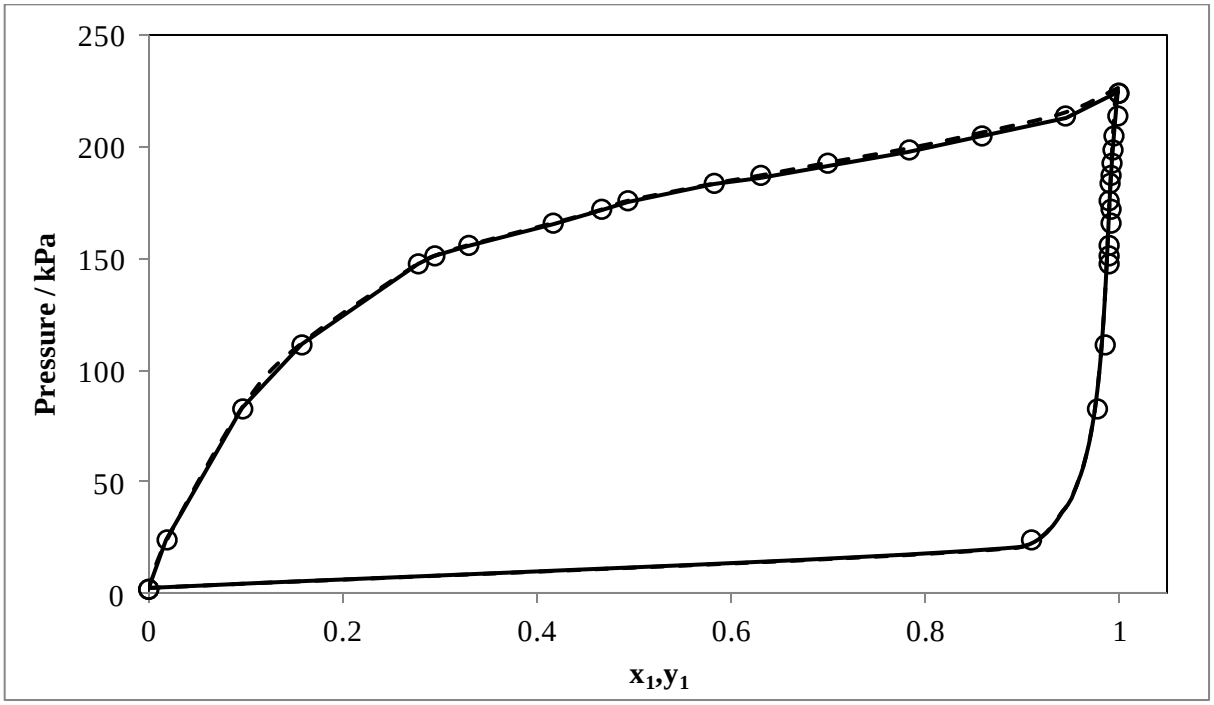

Figure 8.1: P-x_1-y_1 plot for the 1-hexene (1) + NMP (2) system at 363.61± 0.02 K
○, Experimental data; ——, PR-WS-NRTL; - - -, SRK-WS-NRTL

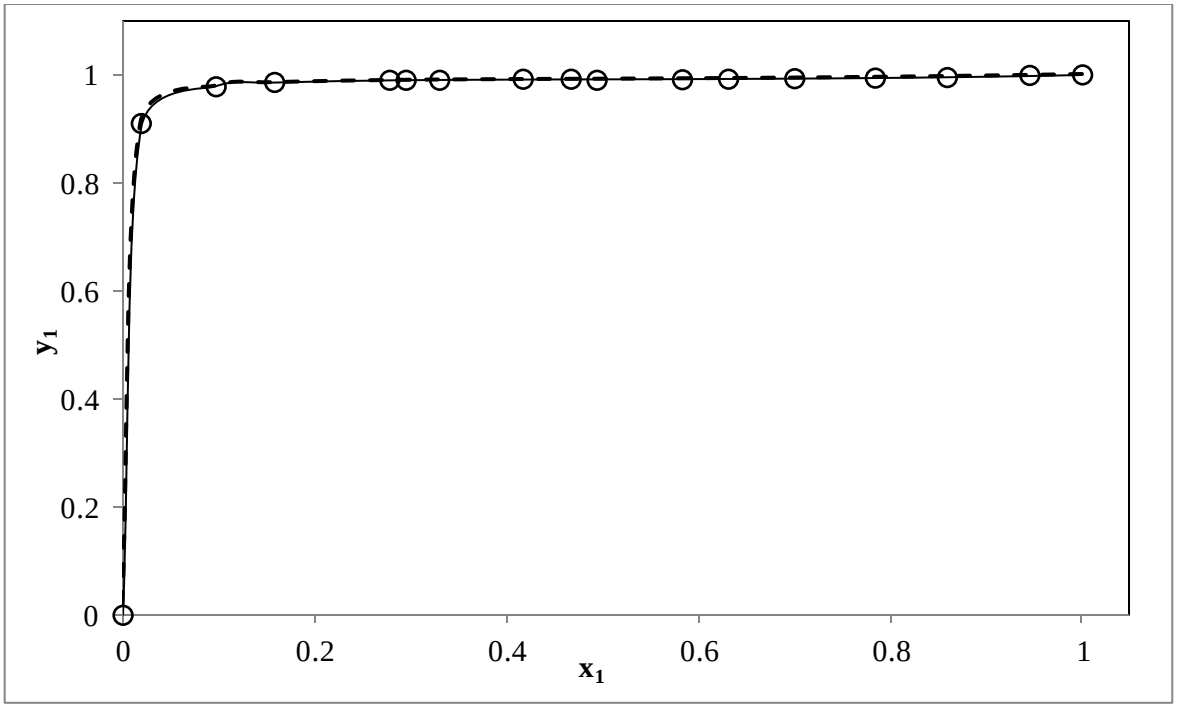

Figure 8.2: y-x plot for the 1-hexene (1) + NMP (2) system at 363.61± 0.02 K

○ , Experimental data; ——, PR-WS-NRTL; - - - , SRK-WS-NRTL.

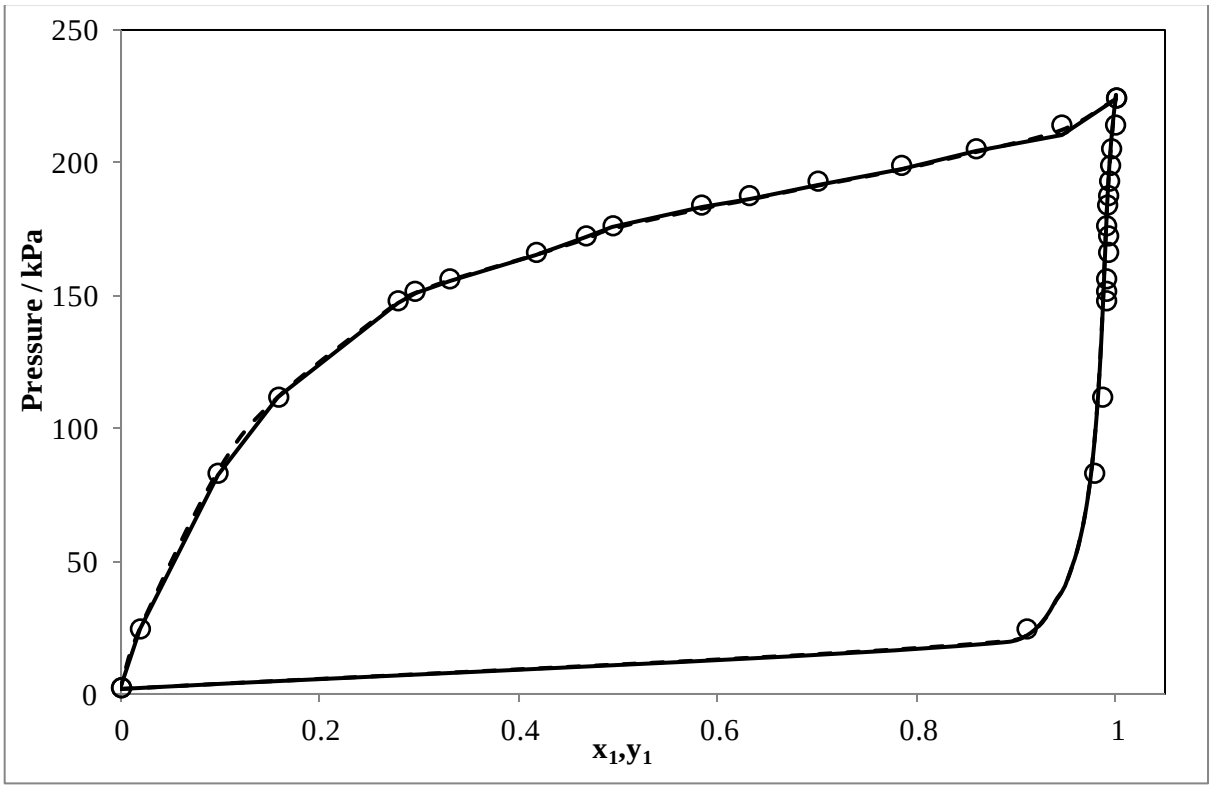

Figure 8.3: P-x_1-y_1 plot for the 1-hexene (1) + NMP (2) system at 363.61± 0.02 K

○ , Experimental data; ——, HOC-WIL; - - - , HOC-NRTL.

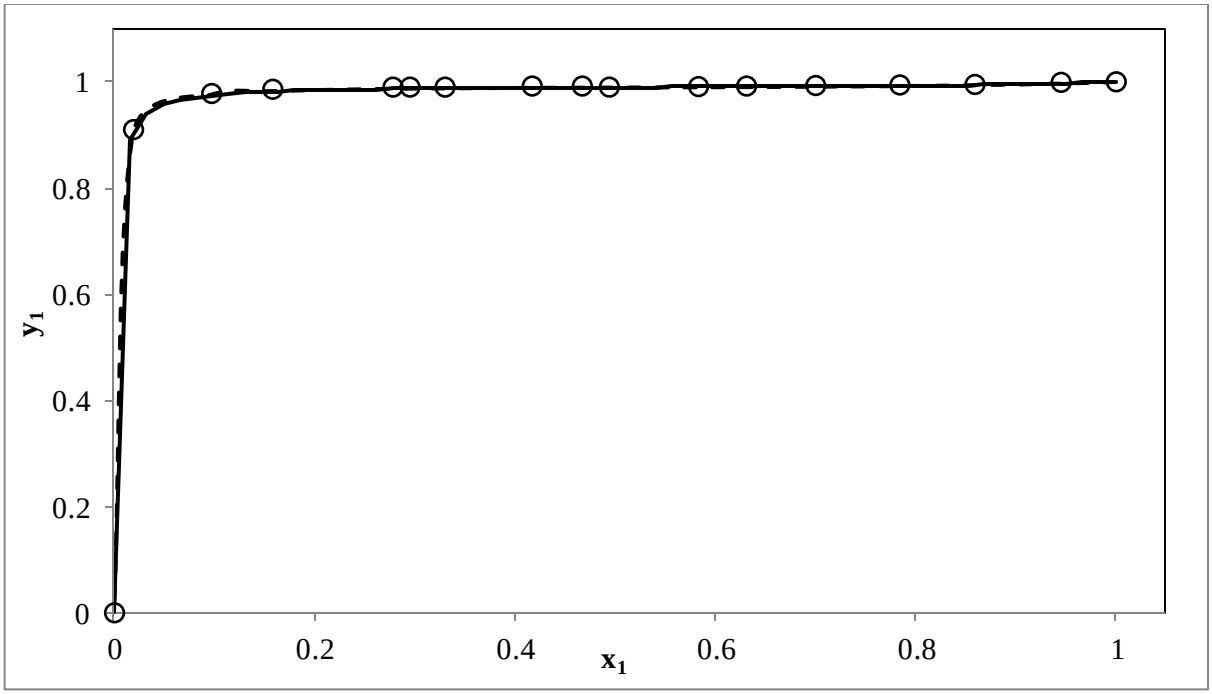

Figure 8.4: y-x plot for the 1-hexene (1) + NMP (2) system at 363.61± 0.02 K

○ , Experimental data; ——, HOC-WIL; - - - , HOC-NRTL.

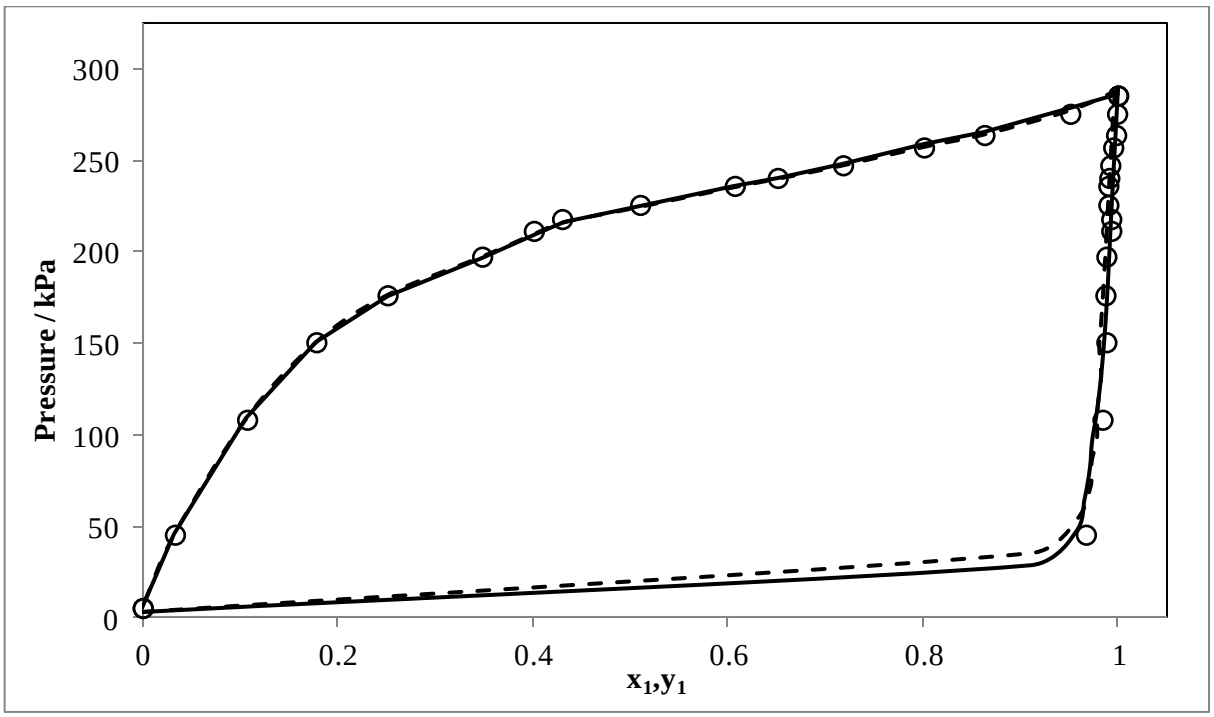

Figure 8.5: P-x_1-y_1 plot for the 1-hexene (1) + NMP (2) system at 373.15 ±0.02 K

○ , Experimental data; ——, PR-WS-NRTL; - - - , SRK-WS-NRTL.

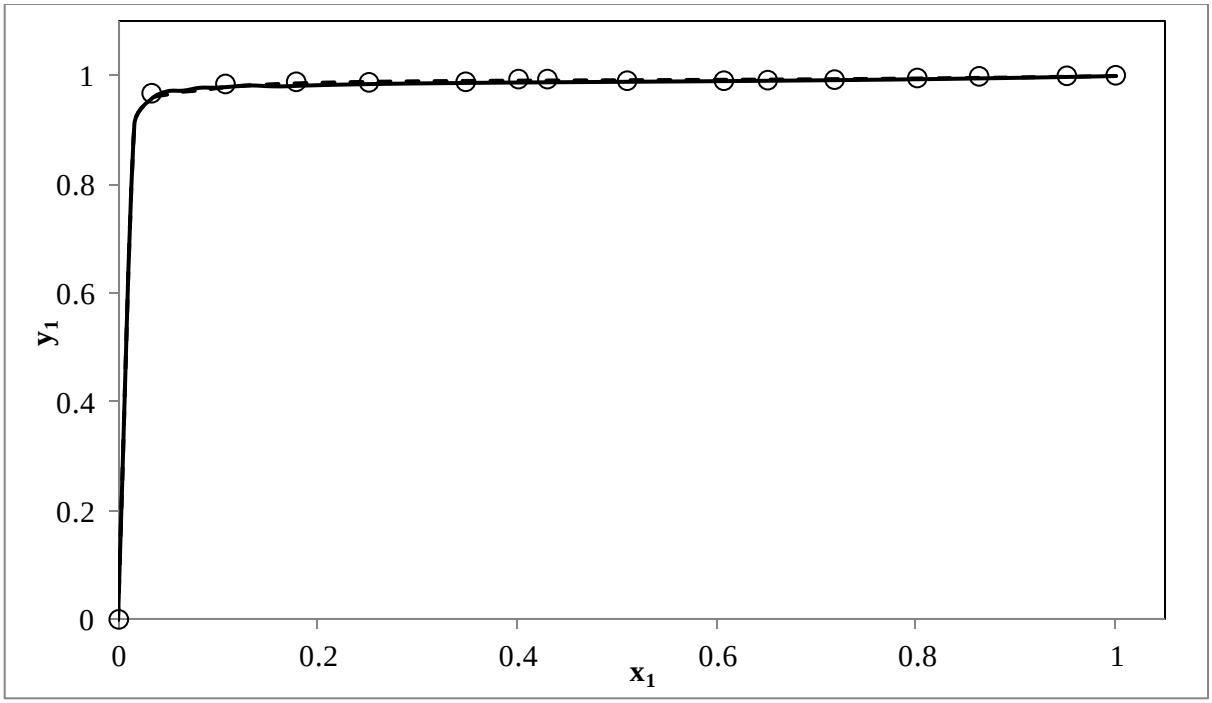

Figure 8.6: y-x plot for the 1-hexene (1) + NMP (2) system at 373.15± 0.02 K

○ , Experimental data; ——, PR-WS-NRTL; - - - , SRK-WS-NRTL.

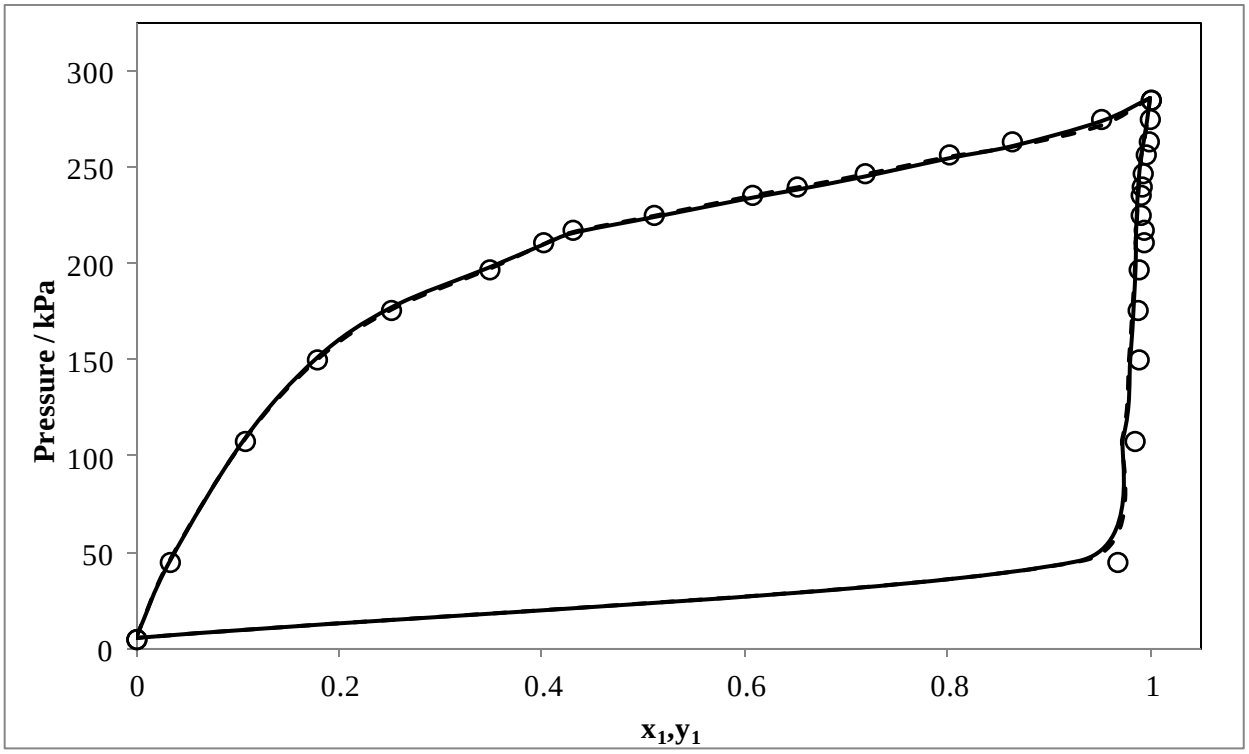

Figure 8.7: P-x_1-y_1 plot for the 1-hexene (1) + NMP (2) system at 373.15± 0.02 K

○ , Experimental data; ——, HOC-WIL; - - - , HOC-NRTL.

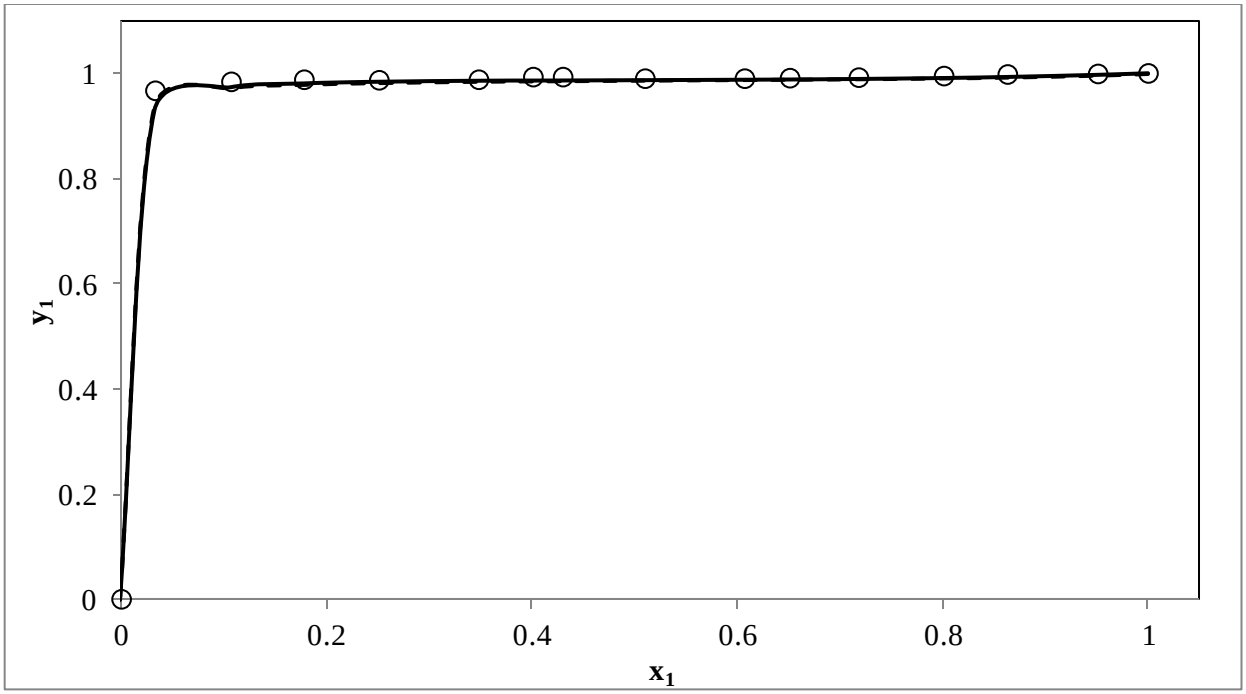

Figure 8.8: y-x plot for the 1-hexene (1) + NMP (2) system at 373.15± 0.02 K

○ , Experimental data; ——, HOC-WIL; - - - , HOC-NRTL.

Table 8.5: Modeling analysis for the 1-hexene (1) + NMP (2)

	PR-WS(NRTL)		SRK-WS(NRTL)		HOC-NRTL	
T (K)	363.61	373.15	363.61	373.15	363.61	373.15
k_{ij}	0.970	0.967	0.950	0.990	-	-
α_{12}	0.365	0.200	0.200	0.200	0.396	0.415
b_{ij} ***(J.K/kmol)***	390.701	985.661	198.032	148.201	420.092	416.252
b_{ji} ***(J.K/kmol)***	364.061	614.281	428.452	475.872	364.631	377.631
ΔP_{AAD}	0.003	0.006	0.003	0.005	0.003	0.006
Δy_{AAD}	0.001	0.004	0.001	0.004	0.002	0.006

	HOC-WIL	
T (K)	363.61	373.15
b_{ij} ***(J.K/kmol)***	-263.389	-266.581
b_{ji} ***(J.K/kmol)***	-592.272	-583.872
ΔP_{AAD}	0.003	0.006
Δy_{AAD}	0.002	0.006

b_{ij} and b_{ji} are the binary energy parameters used in Aspen Tech®, equivalent to Δg_{ij} / R (NRTL) and $\Delta\lambda_{ij}$ / R (Wilson), k_{ij} is the Wong Sandler (1996) mixing parameter,

$$\Delta P_{AAD} = \frac{1}{n}\sum_{i}^{n}\frac{P_i^{Exp} - P_i^{Lit}}{P_i^{Exp}} \quad \Delta y_{AAD} = \frac{1}{n}\sum_{i}^{n}\frac{P_i^{Exp} - P_i^{Lit}}{P_i^{Exp}}$$

Table 8.6: Modeling analysis for the 1-hexene (1) + NMP (2) at 363.61 (fixed α_{12} parameter of 0.4567)

	PR-WS(NRTL)	SRK-WS(NRTL)	HOC-NRTL
T (K)	363.61	363.61	363.61
k_{ij}	0.99	0.970	-
α_{12}	0.4567	0.4567	0.4567
b_{ij} ***(J.K/kmol)***	440.601	265.022	430.564
b_{ji} ***(J.K/kmol)***	462.561	555.322	354.232
$\Delta \mathbf{P_{AAD}}$	0.005	0.005	0.006
$\Delta \mathbf{y_{AAD}}$	0.002	0.002	0.002

b_{ij} and b_{ji} are the binary energy parameters used in Aspen Tech®, equivalent to $\Delta g_{ij} / R$ (NRTL), k_{ij} is the Wong Sandler (1996) mixing parameter, $\Delta P_{AAD} = \frac{1}{n}\sum_{i}^{n} \frac{P_i^{Exp} - P_i^{Lit}}{P_i^{Exp}}$

$$\Delta y_{AAD} = \frac{1}{n}\sum_{i}^{n} \frac{P_i^{Exp} - P_i^{Lit}}{P_i^{Exp}}$$

Thermodynamic consistency testing was performed to assess the quality of the measured VLE data as described in section 2.8. Tables 8.7 and 8.8 presents a summary of the point and direct test analysis for isothermal results at 363.61 K and 373.15 K respectively.

Although the direct test has been completed it does not reflect the true quality of the measured data. The binary system of 1-hexene and NMP measured at low to medium pressures displays associative properties introducing deviations from Raoult's Law for the liquid phase.

The point test is regarded as reflecting the quality of the measurements since it is a model independent test. As mentioned in Chapter 2, the absolute average vapour phase deviations must not exceed 0.01 ($\Delta \mathbf{y_{AAD}} \leq 0.01$) for the measured data to be regarded as consistent. The point test approach is to identify potentially erroneous measured points individually and remove them progressively until the point test criterion is met.

All models passed the point test for both isotherms upon exclusion of two points as per Table 8.7 and Table 8.8. The excellent fitting of the measured data of this work and the literature data of Fischer and Gmehling (1995), shown in Figure 7.18, indicates the accuracy of measurements and efficiency of the equipment

Table 8.7: Consistency Test results for the 1-hexene (1) + NMP (2) at 363.61 ±0.02 K

Data points removed for point test				
P / kPa	**x1**		**y1**	
2.19 ± 0.005	0.003		0.001	
33.80 ± 0.013	0.031		0.958	
Point test with selected points				
	PR-WS (NRTL)	**SRK-WS (NRTL)**	**HOC-NRTL**	**HOC-WIL**
Total data Points	17	17	17	17
ΔP_{AAD}	0.004	0.003	0.003	0.004
Δy_{AAD}	0.000	0.001	0.002	0.002
Direct Test				
RMSD	0.264	0.166	0.330	0.342
Direct Test Index	10	7	10	10

$$\Delta P_{AAD} = \frac{1}{n}\sum_{i}^{n}\frac{P_i^{Exp} - P_i^{Lit}}{P_i^{Exp}}, \quad \Delta y_{AAD} = \frac{1}{n}\sum_{i}^{n}\frac{P_i^{Exp} - P_i^{Lit}}{P_i^{Exp}},$$

$$RMSD = \sqrt{\frac{\sum_{i=1}^{n}\left(\ln\frac{\gamma_1^{Exp}}{\gamma_2^{Exp}} - \ln\frac{\gamma_1^{Calc}}{\gamma_2^{Calc}}\right)^2}{n}}$$

Table 8.8: Consistency Test results for the 1-hexene (1) + NMP (2) at 373.15 ±0.02 K

Data points removed for point test				
P / kPa	**x1**		**y1**	
5.20 ± 0.005	0.003		0.001	
9.21 ± 0.005	0.005		0.883	
Point test with selected points				
	PR-WS (NRTL)	**SRK-WS (NRTL)**	**HOC-NRTL**	**HOC-WIL**
Total data Points	16	16	16	16
ΔP_{AAD}	0.006	0.006	0.007	0.006
Δy_{AAD}	0.003	0.003	0.006	0.006
Direct Test				
RMSD	0.321	0.697	0.598	0.603
Direct Test Index	10	10	10	10

$$\Delta P_{AAD} = \frac{1}{n}\sum_{i}^{n}\frac{P_i^{Exp} - P_i^{Lit}}{P_i^{Exp}}, \quad \Delta y_{AAD} = \frac{1}{n}\sum_{i}^{n}\frac{P_i^{Exp} - P_i^{Lit}}{P_i^{Exp}},$$

$$RMSD = \sqrt{\frac{\sum_{i=1}^{n}\left(\ln\frac{\gamma_1^{Exp}}{\gamma_2^{Exp}} - \ln\frac{\gamma_1^{Calc}}{\gamma_2^{Calc}}\right)^2}{n}}$$

8.3.2. Modeling results for the 1-propanol (1) and 2-butanol (2) binary system

The vapour-liquid equilibrium data for this system was measured at 393.15 K. This isotherm has been measured by Reddy (2009) using a stainless steel dynamic equilibrium still.

The regressed adjustable interaction parameters for all models are presented in Table 8.9. Figures 8.9 to 8.14 provide illustration of model fitting to VLE data. In general, all models fitted the VLE data well with the highest deviations for ΔP_{AAD} and Δy_{AAD} being

0.002 and 0.009 respectively. The PR-WS-NRTL model provided the best fit for this alkanol + alkanol system.

Both of these compounds have similar boiling points and molecular interactions therefore one can expect close to ideal behaviour (Reddy, 2009). However being an n-alkanol and iso-alkanol system it exhibits isomer interaction effects and hydrogen-bonding interactions between the molecules (Li et al., 2000, Reddy, 2009).

In chapter 7, Figure 7.22 compares the measured VLE data to the available literature data of Reddy (2009). Although the measured and literature P-x_1 and P-y_1 curves are similar in trend, a clear discrepancy regarding the values for the measured pressure is observable. There is an average pressure bias of 1.2 kPa between the literature data of Reddy (2009) and the data measured in this work, over the entire composition range. The equipment of Reddy (2009) has reported uncertainties of ±0.09 kPa for $P \leq 150$kPa and ±0.4 kPa for $P \geq 150$ kPa for pressure and 0.08 K for temperature. These uncertainties are much larger compared to the uncertainties of this equipment of ±0.005 kPa for $P \leq 10$kPa, ±0.013 kPa for $10 < P \leq 100$kPa and ±0.15 $P > 100$ kPa for pressure and ±0.02 K for temperature as presented in Table 7.2.

Reddy (2009) emphasised that the design and operation of the pulley driven magnetic stirrers within the reboiler chamber presented a challenge. He elaborated that inefficient agitation within the boiling chamber could lead to poor quality VLE data. The material of construction of the still used was stainless steel which has properties of low thermal conductivity leading to non-ideal thermal response especially at elevated temperatures. This limitation was highlighted by researchers Harris (2004) and Reddy (2009) as inherent and unavoidable.

The thermodynamic consistency test results for this binary system are presented in Table 8.10. The PR-WS (NRTL), HOC-NRTL, and HOC-WIL models achieved a direct test index of 2, indicating high quality VLE data. The SRK-WS (NRTL) model had the worst direct test index of 5. A satisfactory pass for the point test with all points included was achieved for all models used.

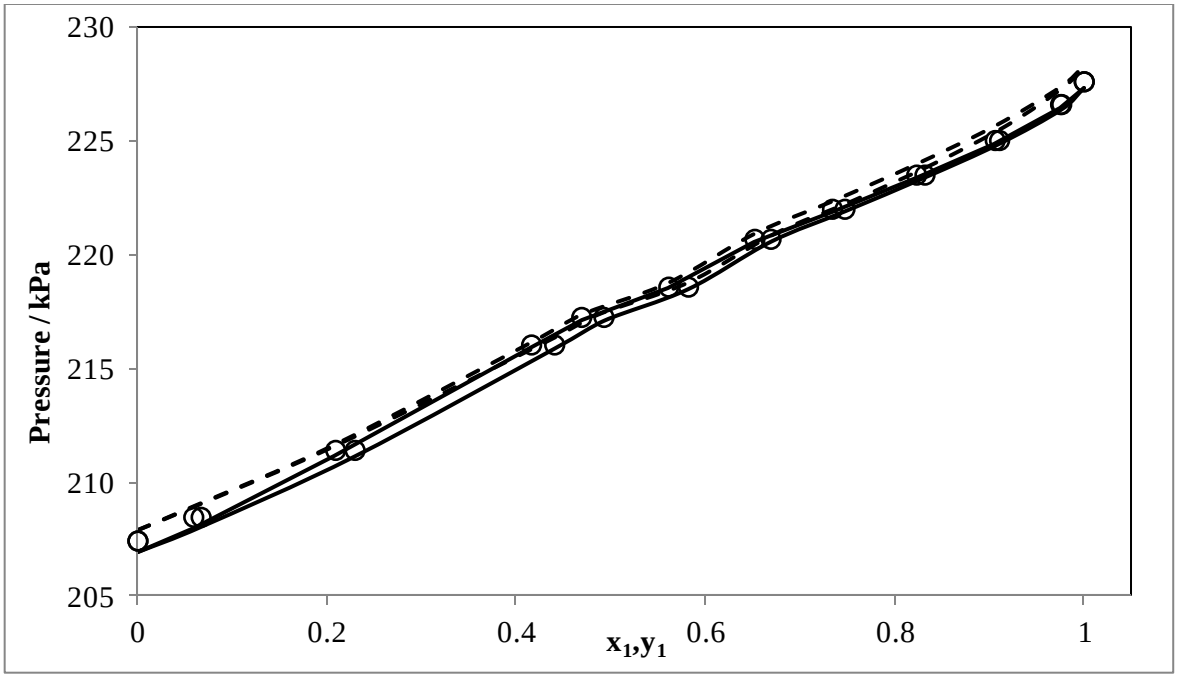

Figure 8.9: P-x_1-y_1 plot for the 1-propanol (1) and 2-butanol (2) system at 393.15±0.02 K, ○, Experimental data; ——, PR-WS-NRTL; - - - , SRK-WS-NRTL.

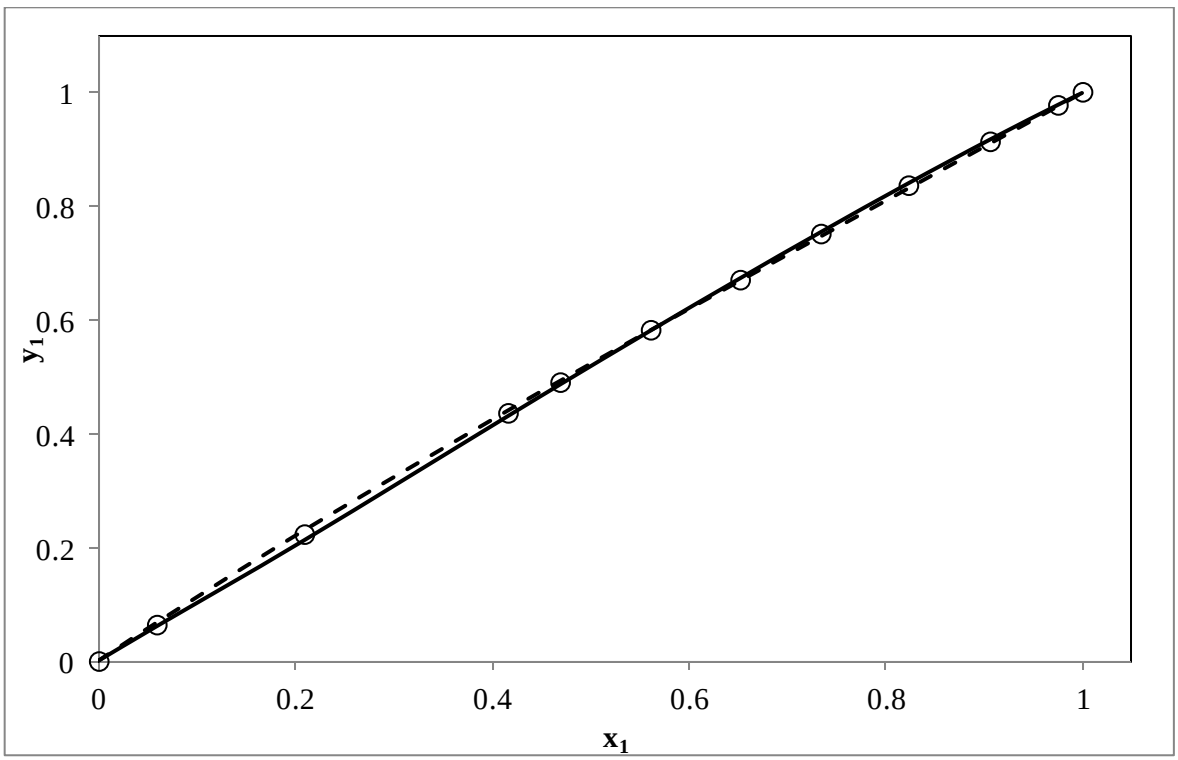

Figure 8.10: y-x plot for the 1-propanol (1) and 2-butanol (2) system at 393.15 ±0.02 K ○, Experimental data; ——, PR-WS-NRTL; - - - , SRK-WS-NRTL.

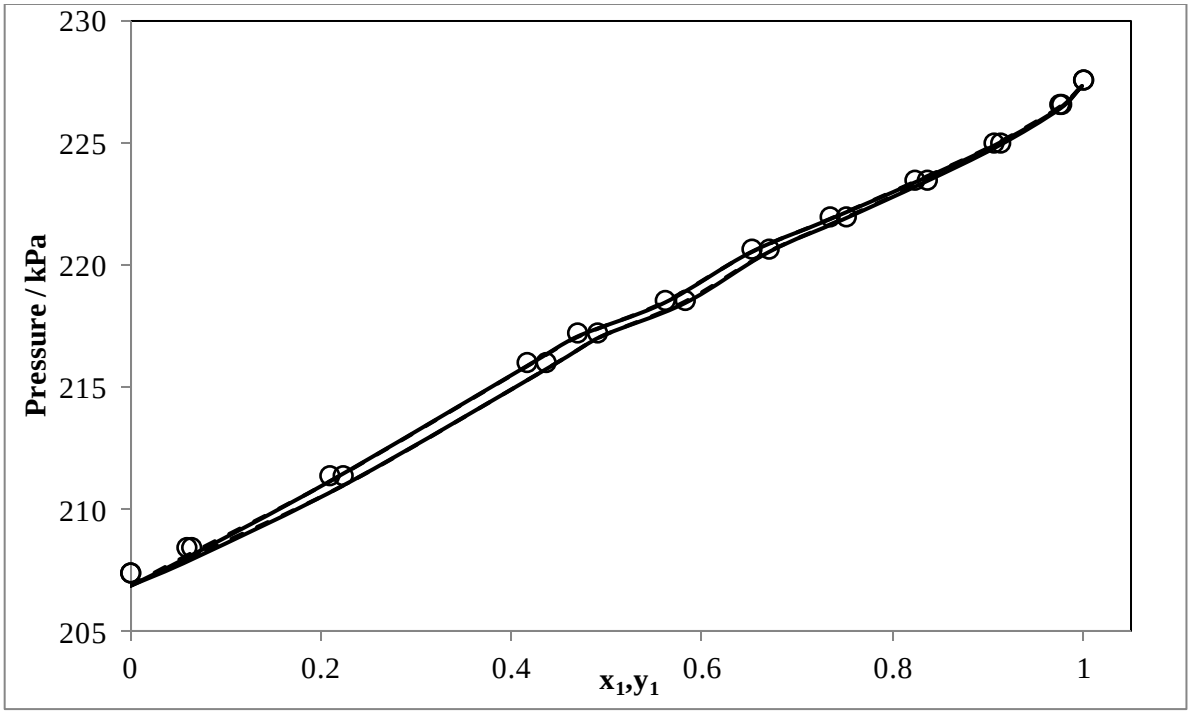

Figure 8.11: P-x_1-y_1 plot for the 1-propanol (1) and 2-butanol (2) system at 393.15±0.02 K, ○, Experimental data; ——, HOC-WIL; - - -, HOC-NRTL.

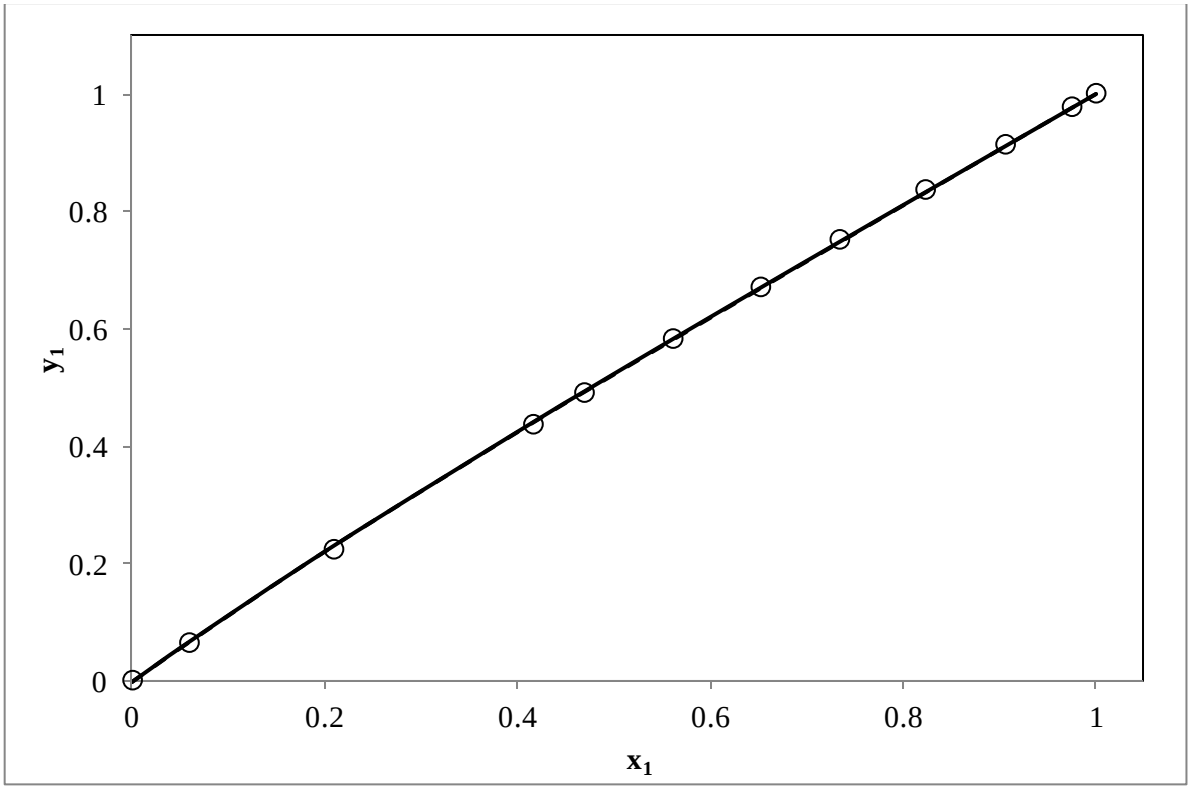

Figure 8.12: y-x plot for the 1-propanol (1) and 2-butanol (2) system at 393.15± 0.02 K ○, Experimental data; ——, HOC-WIL; - - -, HOC-NRTL.

Table 8.9: Modeling analysis for the 1-propanol (1) and 2-butanol (2)

	PR-WS(NRTL)	SRK-WS(NRTL)	HOC-NRTL	HOC-WIL
T (K)	393.15	393.15	393.15	393.15
k_{ij}	0.420	0.400	-	-
α_{12}	0.1	0.214	0.672	-
b_{ij} ***(J.K/kmol)***	-201.110	-110.552	-60.319	-201.381
b_{ji} ***(J.K/kmol)***	250.365	105.933	90.532	168.802
ΔP_{AAD}	0.001	0.002	0.001	0.001
Δy_{AAD}	0.008	0.009	0.009	0.009

b_{ij} and b_{ji} are the binary energy parameters used in Aspen Tech®, equivalent to Δg_{ij} / R (NRTL) and $\Delta\lambda_{ij}$ / R (Wilson), k_{ij} is the Wong Sandler (1996) mixing parameter,

$$\Delta P_{AAD} = \frac{1}{n}\sum_{i}^{n}\frac{P_i^{Exp} - P_i^{Lit}}{P_i^{Exp}} \quad \Delta y_{AAD} = \frac{1}{n}\sum_{i}^{n}\frac{P_i^{Exp} - P_i^{Lit}}{P_i^{Exp}}$$

Table 8.10: Consistency Test results for the 1-propanol (1) and 2-butanol (2) at 393.15 ±0.02 K

All data points were used for point test				
	PR-WS (NRTL)	**SRK-WS (NRTL)**	**HOC-NRTL**	**HOC-WIL**
Total data Points	12	12	12	12
ΔP_{AAD}	0.001	0.002	0.001	0.001
Δy_{AAD}	0.009	0.01	0.01	0.010
Direct Test				
RMSD	0.0266	0.1212	0.0274	0.0343
Direct Test Index	2	5	2	2

$$\Delta P_{AAD} = \frac{1}{n}\sum_{i}^{n}\frac{P_i^{Exp} - P_i^{Lit}}{P_i^{Exp}}, \quad \Delta y_{AAD} = \frac{1}{n}\sum_{i}^{n}\frac{P_i^{Exp} - P_i^{Lit}}{P_i^{Exp}},$$

$$RMSD = \sqrt{\frac{\sum_{i=1}^{n}\left(\ln\frac{\gamma_1^{Exp}}{\gamma_2^{Exp}} - \ln\frac{\gamma_1^{Calc}}{\gamma_2^{Calc}}\right)^2}{n}}$$

9. Conclusions

The modified dynamic glass equilibrium still of Joseph *et al.* (2001) has been successfully commissioned for performing semi-automated precise measurements of VLE data at low to medium pressures. The commissioned apparatus consists of the central dynamic glass still and auxiliary equipment allowing for digital measurement and control of VLE data. The commissioned equipment achieved very acceptable pressure and temperature control to within ± 0.03 kPa and ±0.015 K respectively.

The efficiency and accuracy of performing vapour pressure measurements has been greatly improved and unlike previously it requires little or no human intervention. The vapour pressure measurements of acetone, ethyl acetate, 1-hexene, NMP, 1-propanol and 2-butanol were performed. The vapour pressure data were correlated to the Antoine and Wagner (Reid *et al.*, 1988) equations to obtain model parameters, with the greatest average absolute difference in pressure being less than 1%.

The equipment was tested for both isobaric and isothermal operation by the measurements of test systems cyclohexane (1) + ethanol (2) at 40 kPa (Joseph *et al.*,2001) and 1-hexene (1) + NMP (2) at 363.61 K (Fischer and Gmehling, 1995) respectively. The results reveal good agreement with literature data.

The isothermal data sets for 1-hexene (1) + NMP (2) at 363.61 K and 1-propanol (1) and 2-butanaol (2) at 393.15 K are regarded as new VLE data. The systems were modeled using both direct and combined methods. The VLE data were modeled using the Hayden and O'Connell (1975) with NRTL and Wilson liquid activity coefficient models. The Soave Redlich Kwong (1972) and Peng-Robinson (1976) cubic equations of state with the Wong Sandler (1992) mixing rule incorporating the NRTL activity coefficient model were also used to regress the measured data.

It was shown that the PR-WS (NRTL) model provided the best fit for the 1-hexene (1) and NMP (2) binary system. The reported errors of ΔP_{AAD} and Δy_{AAD} were 0.003 and 0.001 respectively for this system. The PR-WS (NRTL) model also provided the best fit for the 1-propanol (1) and 2-butanol (2) binary system yielding errors of 0.001 and 0.008 for ΔP_{AAD} and Δy_{AAD} respectively.

The thermodynamic consistency was checked using the direct test of Van Ness *et al.* (1973) and the point test of Van Ness (1995). All measured data were found to be thermodynamically consistent; however the direct test results for the 1-hexene (1) + NMP (2) system has been neglected as the direct test is not suitable for chemicals like NMP that have associative properties.

10. Recommendations

It is suggested that the external heating of the equilibrium chamber be included in the LabVIEW program. The designed program for the external heaters should be linked to the internal heaters to ensure no temperature gradients within the boiling chamber. This improvement was not implemented as it required an additional Delta programmable power supplier (0-75V, 0-2A) which was not initially budgeted for.

The solenoid valves used for pressure control operate fully open or close. An analysis on the appropriate valve characteristic to achieve and maintain better process stability should be completed. Alternatively, it is recommended to automate the operation of manual valves V5 and V6 installed on the nitrogen cylinder and vacuum pump pressure lines respectively as per Figure 4.2. These upstream throttling valves prevent large pressure variances across the solenoid valves especially since the solenoid are unable to open partially.

The developed isothermal and isobaric processes are regarded as semi-automatic. The user needs to re-initialize the LabVIEW program with identified plateau region conditions; this should be automated to increase efficiency.

The direct analysis of the vapour phase composition through the use of a direct injection by GC, this avoids the difficulties during vapour sampling.

The NMP and 1-hexene system has associative, self-associative and polar effects. Letcher *et al*., (1998) recommends the use of the Flory-Benson-Treszczanowicz (FBT) or the Extended Real Association Solution (ERAS) to best describe system containing NMP.

The 1-propanol (1) and 2-butanol (2) system exhibits isomer interaction effects and hydrogen-bonding interactions. Associative models such as Perturbation-Chain Statistical Associating Fluid Theory (PC-SAFT) should be employed to represent the mentioned interactions between 1-propanol and 2-butanol.

11. References

Abbott, M.M, and Van Ness, H.C, (1975), "*Vapour Liquid Equilibrium: Part 3-Data Reduction with Precise Expressions for* G^E," American Institute of Chemical Engineering Journals, Vol.21, Pg.62-71

Abbott, M.M (1986), "*Low pressure vapour phase equilibria: Measurement of VLE*," Fluid Phase Equilibria, Vol.29, Pg.193-207

Abu Zalata, M.K (2012), "*Pulse-Width-Modulation DC Chopper using LabView Software*," Faculty of Engineering Technology Al-Balqa, Applied University Amman, Jordon

Åkesson, B (2001), "*Concise International Chemical Assessment Document 35: N-Methyl-2-Pyrrolidone*," Department of Occupational and Environmental Health, University Hospital, Lund, Sweden.

Alia, M.A.K and Abu Zalata, M.K (2004), "*A closed loop temperature control system by utilizing a Labvew Custome-design PID Controller,*" Faculty of Engineering Technology Al-Balqa, Applied University Amman, Jordon

ASPEN Plus ® Simulation Package, (2010), Aspen Technology, Inc

Bell, S (1999), "*A Beginner's Guide to Uncertainty of Measurement*," National Physical Laboratory, Teddington, Middlesex, United Kingdom, Issue 2.

Birch, K (2003), "*An Intermediate Guide to Estimating and Reporting Uncertainty of Measurement in Testing*," British Measurement and Testing Association, Teddington, Middlesex, United Kingdom, TW11 0NQ.

Component Plus, (2011), *Pure Component Database Manager*, Component Plus Software Package Version 5.1.2600 Service Pack 3 Build 2600, United States.

Clifford, S.L (2003), "*Low-Pressure Vapour-Liquid Equilibrium and Molecular Simulation of Carboxylic acids,*" MSc. Eng. Thesis, University of Kwa Zulu Natal, Durban, South Africa

Davila, M.J, Trusler J.M, Aparicio S, Alcalde R, Garcia and Leal (2006), "*Thermodynamic Properties of NMP/methanol over a Wide Temperature and Pressure Range*" Department of Chemical Engineering and Chemical Technology, Imperial college of Science, Technology and Medicine, London, UK

Eitelberg, E, (2000), "*Control Engineering: Course Notes*", University of Kwa Zulu Natal, Durban, South Africa

Fischer, K and Gmehling, J, (1995), "*Vapor-liquid equilibria, activity coefficients at infinite dilution and heats of mixing of N-methyl pyrrolidone-2 with C5 orC6*

hydrocarbons and for hydrocarbon mixtures," Fluid Phase Equilibria, Vol.119, Pg.113-130.

Focke, W, (2004), "*Excess Gibbs Energy of Binary Liquid Mixtures and the Wong-Sandler Postulate*s" Dept. Of Chemical Engineering, Istitute of Applies Materials, Unveristy of Pretoria, South Africa, DOI 10.1002/aic.10222, Vol. 50, No. 12

Hala, E.J, Pick, V. Fried and O. Vilim, (1967), "V*apour-Liquid Equilibrium*" Second Edition, Pergamon Press, Oxford.

Harris, R.A, (2004), "*Robust Equipment for the Measurement of Vapour-Liquid Equilibrium at High Temperatures and High Pressures,*" Phd. Eng. Thesis, University of Kwa Zulu Natal, Durban, South Africa

Hayden, J.G, and O'Connell, J.P, (1975), "*A Generalised Method for Predicting Second Virial Coefficients*," Industrial and Engineering Chemistry. Process Design and Development, Vol.14, Pg.209-216.

Hirawan, R, (2007), "*Development of a thermodynamic for the purification of 1-hexene*" MSc. Eng. Thesis, University of Kwa Zulu Natal, Durban, South Africa

Iwarere, S, (2009), "*Measurement of Phase Equilibria for Oxygenated Hydrocarbon Systems,*" MSc. Eng. Thesis, University of Kwa Zulu Natal, Durban, South Africa

Joseph, MA, Ramjugernath, D and Raal, JD, (2001), "*Phase Equilibrium Properties for Binary Systems with Diacetyl from a Computer Controlled Vapour-Liquid Equilibrium Still*," Fluid Phase Equilibria, Vol.182, Pg. 157-176.

Letcher, T.M, Domanska, U, and Mwenesongole, E, (1998), "*The excess molar volumes of N-methyl- 2-pyrrolidone + an alkanol or a hydrocarbon) at 298.15 and application of the Flory-Benson-Treszczanowicz and the Extended Real Association Solution theories,*" Department of Chemistry and Applied Chemistry, University of Kwa Zulu Natal, Durban, South Africa, Fluid Phase Equilibria, Vol.149, Pg.323-337.

Lyondell Chemical company, "*N-Methyl-2-Pyrrolidone,*" Member of the LyondellBasell group companies. Available online from: http://www.lyondellbasell.com/techlit/techlit/2313.pdf

Marquadt, D.W, (1963), "*An Algorithm for Least-Squares Estimation of Non-Linear Parameters,*" Journal. Society of Industrial and Applied Mathematics,Vol.11, Pg.431-441.

Marsh, K.N, (1989), "*New methods of vapour-liquid-equilibria measurements,*" Fluid Phase Equilibria, Vol.52, Pg.169-180.

Moodley, K, (2012), "*Automation of Static-Synthetic Apparatus for Vapour Liquid Equilibrium Measurement,*" MSc. Eng. Thesis, University of Kwa Zulu Natal, Durban, South Africa

Nagahama, K, (1996), "*VLE measurements at elevated pressures for process development*," Fluid Phase Equilibria, Vol.116, Pg.361-372.

Narasigadu, C, (2006), "*Phase Equilibrium Investigation of the Water and Acetonitrile Solvent with Heavy Hydrocarbons,*" MSc. Eng. Thesis, University of Kwa-Zulu Natal, Durban, South Africa

National Instruments, (2002), "*Labview Basics Introduction*" Course Manual, United States of America.

Ndlovu, M, (2005), "*Development of Dynamic Still for Measuring Low Pressure Vapour-Liquid-Liquid Equilibria (Systems of Partial Liquid Miscibility),*" MSc. Eng. Thesis, University of Kwa-Zulu Natal, Durban, South Africa

Oliver, N, Fischer, K and Gmehling, J, (1995), "*Vapor-Liquid Equilibria and Enthalpies of Mixing for the Binary System Water + N-methyl-2-pyrrolidone in the Temperature Range 80-140°C,*" Journal of Chemical Engineering Data, American Chemical Society, Vol.41, Pg.1434-1438.

Pillay, C.J (2009), "*Binary Vapour-Liquid Equilibria for Oxygen Containing Compounds,*" MSc. Eng. Thesis, University of Kwa Zulu Natal, Durban, South Africa

Prausnitz, J.M,(1969), "*Molecular Thermodynamics of Fluid Phase Equilibria*" , 1th Edition, Prentice Hall Inc, Canada.

Prausnitz, J.M, Anderson, T.F, Grens, E.A, Eckert, C.A, O'Connell, J.P (1980), "*Computer Calculations for Multi-component Vapor-Liquid and Liquid-Liquid Equilibria,*" Prentice Hall Englewood Cliffs, NJ

Raal, J.D and Mühlbauer, A.L (1998), "*Phase Equilibria: Measurement and Computation,*" Taylor and Francis, Bristol.

Ralf, D, Peper, S and Fonseca J.M.S (1972), "*High-pressure fluid-phase equilibria: Experimental methods and systems investigated (2000-2004),*" Fluid Phase Equilibria, Vol.288, Pg. 1-54.

Reddy, P, (2006), "*Development of a Novel Apparatus for the Measurement of Vapour-Liquid Equilibria at Elevated Temperatures and Moderate Pressures,*" PhD. Eng. Thesis, University of Kwa Zulu Natal, Durban, South Africa

Redlich, O. and Kister, A.T (1948), "*Algebraic Representation of Thermodynamic Properties and Classification of Solutions,*" Industrial and Engineering Chemistry, Vol.40, Pg.345-348.

Redlich, O. and Kwong, J.N.S (1949), "*On Thermodynamics of Solutions V: An Equation of State. Fugacities of Gaseous Solutions,*" Chemical Reviews, Vol.44, Pg.233-244.

Reid, C.R, Prausnitz, J.M and Polling, B.E (1988), "*Properties of Gases and Liquids,*" 4th Edition, McGraw Hill Book Company, Singapore.

Renon, H and Prausnitz, J.M (1968), "*Local Compositions in Thermodynamics Excess Functions for Liquid Mixtures,*" American Institute of Chemical Engineering Journals, Vol.14, Pg.135-144.

Seader, JD and Henley, EJ, (2006), "*Separation Process Principles*" 2th Edition, John Wiley and Sons, USA.

Smith, JM, Van Ness, HC and Abbott, MM, (2005), "*Introduction to Chemical Engineering Thermodynamics*" 7th Edition, McGraw-Hill, New York

Smith, JM, Van Ness, HC and Abbott, MM, (2001), "*Introduction to Chemical Engineering Thermodynamics,*" 6th Edition, McGraw-Hill, New York.

Soave, G (1972), "*Equilibrium Constants from a modified Redlich-Kwong Equation of State,*" Chemical Engineering Science, Vol.27, Pg.1197-1203.

Stryjek, R and Vera, J.H. (1986), "*PRSV: An Improved Peng- Robinson Equation of State for Pure Compounds and Mixtures,*" The Canadian Journal Chemical Engineering, Vol.64, Pg.323-333.

Budavari, S and O'Neil, M.J (1989), "*The Merck Index: An encyclopaedia of chemicals, drugs and biological,*" 52th Edition, Merck and Co., Inc, Rahway, N.J.U.S.A

Tsonopoulos, C (1974), "*An Empirical Correlation of the Second Virial Coefficients,*" American Institute of Chemical Engineers Journals, Vol.20, Pg.263-272.

Twu, C.H and Coon J.E (1996), " *CEOS/A^E Mixing Rules Constrained by vdW Mixing Rule and Second Virial Coefficient,*" American Institute of Chemical Engineering Journals, Vol.42, Pg.3212-3222.

Uusi-Kyyny, P., Pokki, J.-P., Aittamaa, J. and Liukkonen, S., Vapor Liquid Equilibrium for the Binary Systems of 2-Methyl-2-propanol + 2,4,4-Trimethyl-1-pentene at 333 K and 348 K and 2- Butanol + 2,4,4-Trimethyl-1-pentene at 360 K, *J. Chem Eng Data* **46** (2001) 686-691

Van der Waals, J.D (1873), "*On the Continuity of the Gaseous and Liquid States,*" Doctoral Dissertation, University Leiden.

Van Laar, J.J (1910), "*The Vapour Pressure of binary mixtures,*" Zeitschrift feur Physik Chemie, Vol.72, Pg.723-751 (Given in Walas, 1985).

Van Ness, HC, (1995), "*Thermodynamics in the Treatment of Vapor/Liquid Equilibrium (VLE) Data*," Pure and Applied Chemistry, Vol.67, Pg.859-872.

Walas, S.M (1985), " *Phase Equilibrium in Chemical Engineering,*" Butterworth, Boston.

Wilson, G.M (1964), "*Vapour-Liquid Equilibrium, A New Expression for the Excess Free Energy of Mixing*," Journal of American Society, Vol.86, Pg.127-130.

Weast,R.C (1972), "*Handbook of Chemistry and Physics*," 52th Edition published by the Chemical Rubber CO, Cranwood, Parkway, Cleveland.

Wong, D.S.H and Sandler, S.I (1992), "*A Theoretically Correct Mixing Rule for Cubic Equation of State vapour-Liquid Equilibrium, A New Expression for the Excess Free Energy of Mixing*," American Institute of Chemical Engineers Journals, Vol.10, Pg.660-665.

Yerazunis, S, Plowright, J.D and Smola, F.M (1964), "*Vapour-Liquid Equilibrium Determination by a New Apparatus*," American Institute of Chemical Engineers Journals, Vol.10, Pg.660-665.

Appendix A

A.1. Soave-Redlich-Kwong (SRK) Equation of State

$$P = \frac{RT}{V-b} - \frac{a(T,\omega)}{V(V+b)} \tag{A1.1}$$

where T is the absolute temperature, P and R, are pressure and universal gas constant respectively and V the molar volume. The *a* constant is a function of temperature and represents force of attraction between molecules while the *b* constant corrects for volume (Iwarere, 2009) and is temperature independent.

$$a\ (T,\omega) = a_c \alpha\ (T,\omega) \tag{A1.2}$$

$$a_c = 0.42747\left(\frac{R^2 T_c^2}{P_c}\right) \tag{A1.3}$$

$$b = 0.08664\left(\frac{RT_c}{P_c}\right) \tag{A1.4}$$

$$T_r = \frac{T}{T_c} \tag{A1.5}$$

The alpha function, $\alpha(T,\omega)$

$$\alpha(T,\omega) = \left[1+\kappa\ \left(1-T_r^{0.5}\right)\right]^2 \tag{A1.6}$$

with κ being a quadratic function of acentric factor ω, by the following equation

$$\kappa = 0.480 + 1.574\omega - 0.176\omega^2 \tag{A1.7}$$

Equation (A4.1) can be expressed in terms of compressibility as follows

$$Z^3 - Z^2 + Z(A - B - B^2) - AB = 0 \tag{A1.8}$$

where

$$A = \frac{aP}{R^2T^2} \tag{A1.9}$$

$$B = \frac{bP}{RT} \tag{A1.10}$$

$$Z = \frac{PV}{RT} \qquad \text{(A1.11}$$

The solution of Z in equation (A1.8) will produce either one or three real roots. For the solution that produces three real roots, the largest of the three real roots corresponds to the compressibility factor of the vapour and smallest of the three real roots corresponds to the compressibility factor of the liquid.

Pure component fugacity coefficient is calculated as follows:

$$\ln \phi = Z - 1 - \ln(Z - B) - \frac{A}{B} \ln\left[\frac{Z + B}{Z}\right] \qquad \text{(A1.12)}$$

A.2. Peng-Robinson (PR) Equation of State

$$P = \frac{RT}{V - b} - \frac{a(T, \omega)}{V(V + b) + b(V - b)} \qquad \text{(A2.1)}$$

The *b* constant adjusts for molecular size and is temperature independent while the *a* constant is temperature dependent and relates to the intermolecular forces of attraction.

$$a(T, \omega) = a_c \alpha\ (T, \omega) \qquad \text{(A2.2)}$$

$$a_c = 0.45724\left(\frac{R^2 T_c^2}{P_c}\right) \qquad \text{(A2.3)}$$

$$b = 0.07780\left(\frac{RT_c}{P_c}\right) \qquad \text{(A2.4)}$$

$$\kappa = \kappa_0 + \kappa_1\left(1 + T_r^{0.5}\right)\left(0.7 - T_r\right) \qquad \text{(A2.5)}$$

$$\kappa_0 = 0.378893 + 1.4897153\omega - 0.17131848\omega^2 - 0.0196554\omega^3 \qquad \text{(A2.6)}$$

Equation (A4.11) can be expressed in terms of compressibility as follows

$$Z^3 - (1 - B)Z^2 + (A - 3B^2 - 2B)Z - (AB - B^2 - B^3) = 0 \qquad \text{(A2.7)}$$

In the same manner, for a binary system the solution of Z in equation (A2.7) will produce either one or three roots. The largest of the three real roots corresponds to the vapour and the smallest of the three roots corresponds to the liquid.

The pure component fugacity coefficient can be calculated as follows:

$$\ln\phi = (Z-1) - \ln(Z-B) - \frac{A}{2\sqrt{2}B}\ln\left[\frac{Z+(1+\sqrt{2})B}{Z+(1-\sqrt{2})B}\right] \quad \text{(A2.8)}$$

Peng-Robinson (1976) also included a set of mixing rules:

$$a_m = \sum_i \sum_j x_i x_j a_{ij} \quad \text{(A2.9)}$$

$$a_{ij} = (1-\delta_{ij})(a_i a_j)^{0.5} \quad \text{(A2.10)}$$

$$b_m = \sum_i x_i b_i \quad \text{(A2.11)}$$

The δ_{ij} is the binary interaction parameter determined empirically for each unique binary system. The parameter is determined from regression of vapour-liquid data and it should be noted that $\delta_{ij} = \delta_{ji}$. A discussion on application of mixing rules will be covered in section 2.4.

A.3. Wong-Sandler Mixing Rules

For the Soave-Redlich-Kwong Equation of state (Naidoo, 2004)

$$\ln\hat{\phi}_i = -\ln\left[\frac{P(V-b_m)}{RT}\right] + \frac{1}{b_m}\left(\frac{\partial n b_m}{\partial n_i}\right)\left(\frac{PV}{RT}-1\right) + \left(\frac{a_m}{b_m RT}\right)\left[\frac{1}{a_m}\left(\frac{1}{n}\frac{\partial n^2 a_m}{\partial n_i}\right) - \frac{1}{b_m}\frac{\partial n b_m}{\partial n_i}\right]\ln\left[\frac{V}{V+b_m}\right] \quad \text{(A3.1)}$$

Peng-Robinson Equation of state (Naidoo, 2004)

$$\ln\hat{\phi}_i = -\ln\left[\frac{P(V-b_m)}{RT}\right] + \frac{1}{b_m}\left(\frac{\partial n b_m}{\partial n_i}\right)\left(\frac{PV}{RT}-1\right) + \frac{1}{2\sqrt{2}}\left(\frac{a_m}{b_m RT}\right)\left[\frac{1}{a_m}\left(\frac{1}{n}\frac{\partial n^2 a_m}{\partial n_i}\right) - \frac{1}{b_m}\frac{\partial n b_m}{\partial n_i}\right]\ln\left[\frac{V+(1-\sqrt{2})b_m}{V+(1+\sqrt{2})b_m}\right] \quad \text{(A3.2)}$$

To evaluate of the fugacity coefficient obtained from the equation of state requires the partial derivative of the a_m and b_m parameters stated below:

$$\left(\frac{\partial n b_m}{\partial n_i}\right) = \frac{1}{(1-D)}\left(\frac{1}{n}\frac{\partial n^2 Q}{\partial n_i}\right) - \frac{Q}{(1-D)^2}\left(1-\frac{\partial n D}{\partial n_i}\right) \quad \text{(A3.3)}$$

$$\left(\frac{1}{n}\frac{\partial n^2 a_m}{\partial n_i}\right) = RT\left(D\frac{\partial n b_m}{\partial n_i} + b\frac{\partial n D}{\partial n_i}\right) \quad \text{(A3.4)}$$

Further the partial derivatives of Q and D are provided below:

$$\left(\frac{1}{n}\frac{\partial n^2 Q}{\partial n_i}\right) = 2\sum_j x_j\left(b-\frac{a}{RT}\right)_{ij} \quad \text{(A3.5)}$$

$$\left(\frac{\partial nD}{\partial n_i}\right) = \frac{a_i}{b_i RT} + \frac{\ln \gamma_i^{\infty}}{c} \tag{A3.6}$$

The constant c is specific to the cubic equation of state chosen:

$$c = -\ln(2) \qquad \text{Soave-Redlich-Kwong} \tag{A3.7}$$

$$c = \frac{1}{\sqrt{2}} \ln\left(\sqrt{2} - 1\right) \qquad \text{Peng-Robinson} \tag{A3.8}$$

$$\ln \gamma_i^{\infty} = \frac{1}{RT} \frac{\partial n A_{\infty}^{E}}{dn_i} \tag{A3.9}$$

Thus allowing predictions of high pressure vapour-liquid equilibrium from low pressure vapour-liquid equilibrium, furthermore any expression for excess Gibbs free energy can be substituted for excess Helmholtz free energy at constant temperature shown below (Raal and Mühlbauer, 1998):

$$\overline{G}^{E}(T, P = 1\,bar, x) = \overline{A}^{E}(T, P = 1\,bar, x) = \overline{A}^{E}(T, P = high, x) \tag{A3.10}$$

In this study the NRTL Gibbs excess energy model was selected to describe A^E as follows:

$$\frac{A_{\infty}^{e}}{RT} = \sum_i x_i \left(\frac{\sum_j x_j \tau_{ji} g_{ji}}{\sum_k x_k g_{ki}} \right) \tag{A3.11}$$

$$\ln \gamma_i^{\infty} = \frac{\sum_j x_j \tau_{ji} g_{ji}}{\sum_k x_k g_{ki}} + \sum_j \frac{x_j g_{ij}}{\sum_k x_k g_{kj}} \left(\tau_{ij} - \frac{\sum_l x_l \tau_{lj} g_{lj}}{\sum_k x_k g_{ki}} \right) \tag{A3.12}$$

The cross parameter are calculated as follows:

$$\left(b - \frac{a}{RT}\right)_{ij} = \frac{\left(b_i - \frac{a_i}{RT}\right) + \left(b_j - \frac{a_j}{RT}\right)}{2} \left(1 - k_{ij}\right) \tag{A3.13}$$

The adjustable parameter k_{ij} in equation (A3.13) is acquired through the regression of binary vapour-liquid equilibrium experimental data. The use of the NRTL Gibbs excess energy model also brings additional parameters, bringing the overall number of interaction parameters used to four.

Appendix B

Coefficients for Equation 4.1

$$\tau \frac{\partial y}{\partial t} + y(t) = kF(t) \tag{B.1}$$

Laplace Transform, y(0) = 0

$$Y(s)[\tau s + 1] = kF(s) \tag{B.2}$$

$$\frac{Y(s)}{F(s)} = k\left[\frac{1}{\tau s + 1}\right] \tag{B.3}$$

Solve by the Trapezoidal Method (Eidelberg, 2001)

$$s = \left(\frac{2}{\Delta t}\right)\left[\frac{z-1}{z+1}\right] \tag{B.4}$$

$$F(z) = \frac{z+1}{z\left[1+\frac{2\tau}{\Delta t}\right] - \tau\left(\frac{2}{\Delta t}\right) + 1} \tag{B.5}$$

Use

$$\alpha = \frac{2\tau}{\Delta t} \tag{B.6}$$

$$F(z) \Rightarrow \frac{T(z)}{T_m(z)} = \frac{z+1}{z[1+\alpha] + (1-\alpha)} \tag{B.7}$$

$$T\left[z(1+\alpha)\right] + T(1-\alpha) = T_m(z+1) \tag{B.8}$$

Transform

$$(1+\alpha)T(i+1)+T(i)(1-\alpha)=T_m(i+1)+T_m(i) \tag{B.9}$$

Trapezoidal Method $T_m(i+1)\cong T_m(i)$

$$T(i+1) = \frac{2}{1+\alpha}T_m(i)+\left(\frac{\alpha-1}{1+\alpha}\right)T(i) \tag{B.10}$$

Substitute

$\alpha = \frac{2\tau}{\Delta t}$ τ = 120 sec Δt = 8 sec

Results in Equation 4.1

$$T(i+1)=\frac{2}{31}T(i-1)+\frac{29}{31}T(i)$$

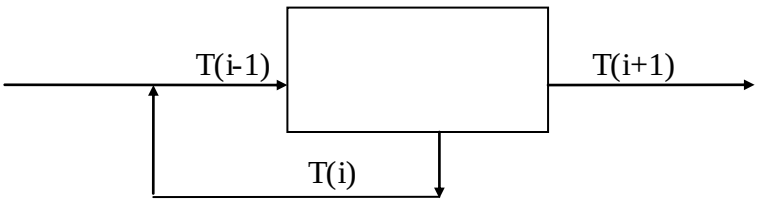

Appendix C

C.1. Fixed NRTL α_{ij} non-randomness parameter

Fischer and Gmehling (1995) has recommended using a fixed α_{12} parameter of 0.4567 for the 1-hexene (1) + NMP (2) binary system. This alternative was only performed for an isothermal temperature of 363.61 K and the comparison is shown in Figures C.1 to C.5

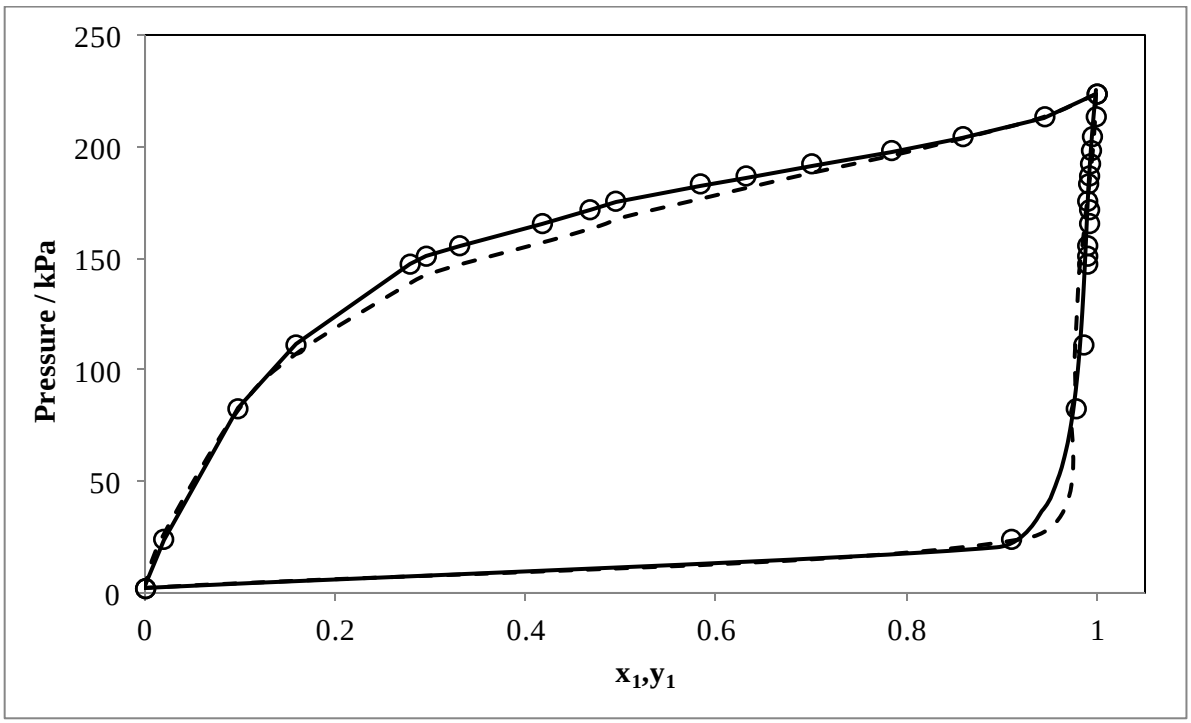

Figure C.1: P-x_1-y_1 plot for the 1-hexene (1) + NMP (2) system at 363.61± 0.02 K ○ , Experimental data; ——, PR-WS-NRTL (Regressed); - - - - , PR-WS-NRTL (fixed α_{12} = 0.4567)

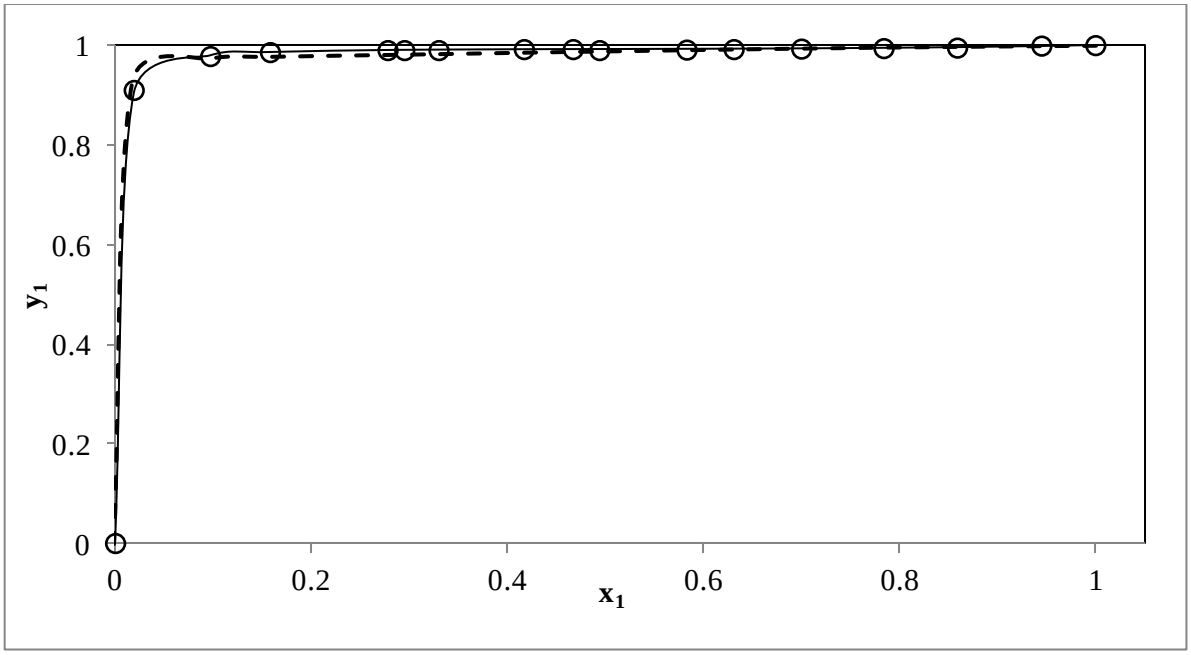

Figure C.2: y-x plot for the 1-hexene (1) + NMP (2) system at 363.61± 0.02 K
○ , Experimental data; ——, PR-WS-NRTL (Regressed); - - - - , PR-WS-NRTL (fixed α_{12} = 0.4567)

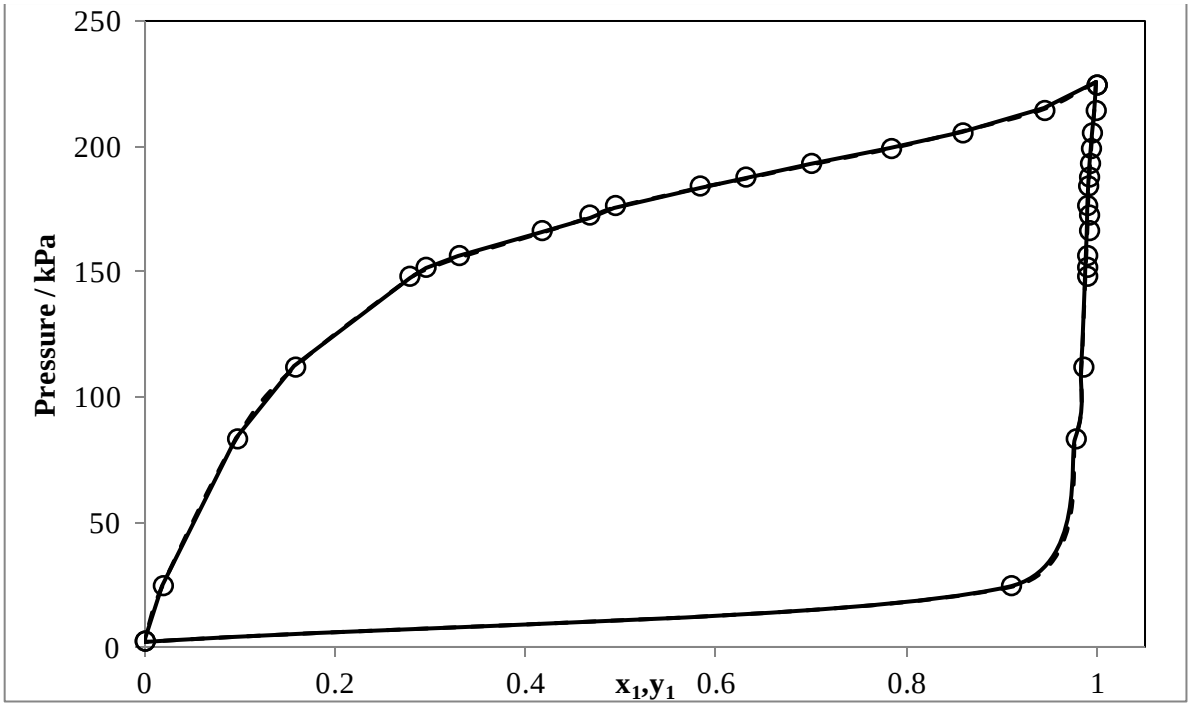

Figure C.3: P-x_1-y_1 plot for the 1-hexene (1) + NMP (2) system at 363.61± 0.02 K
○ , Experimental data; ——, SRK-WS-NRTL (Regressed); - - - , SRK-WS-NRTL (fixed α_{12} = 0.4567)

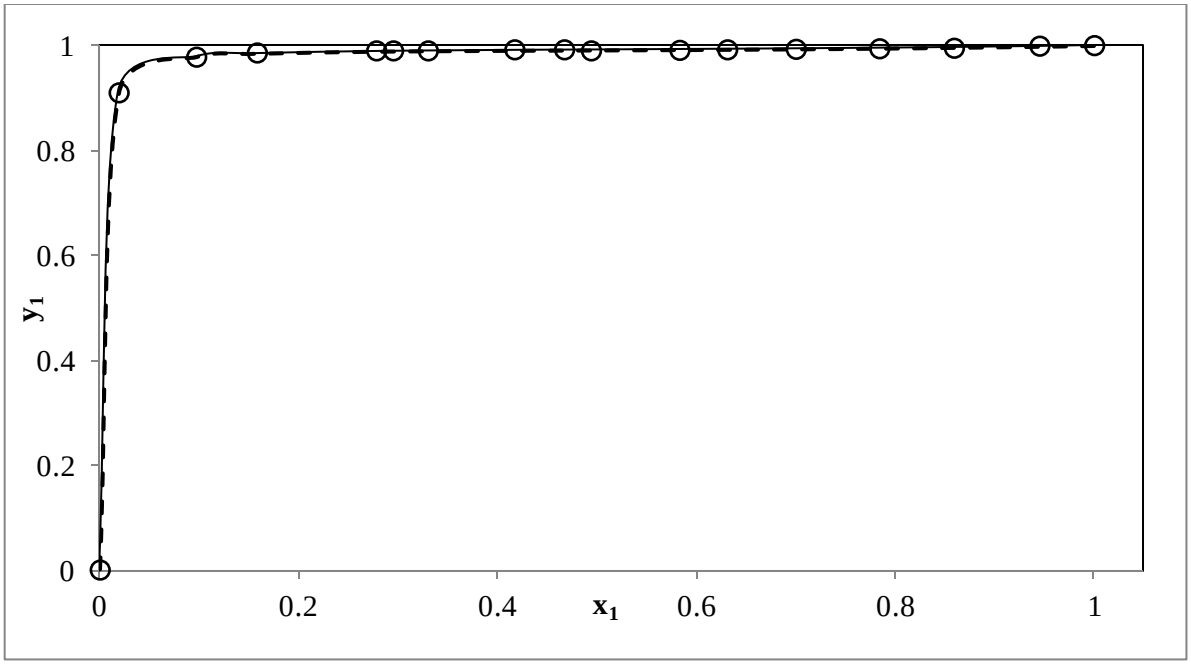

Figure C.4: y-x plot for the 1-hexene (1) + NMP (2) system at 363.61± 0.02 K ○ , Experimental data; ——, SRK-WS-NRTL (Regressed); - - - - , SRK-WS-NRTL (fixed α_{12} = 0.4567)

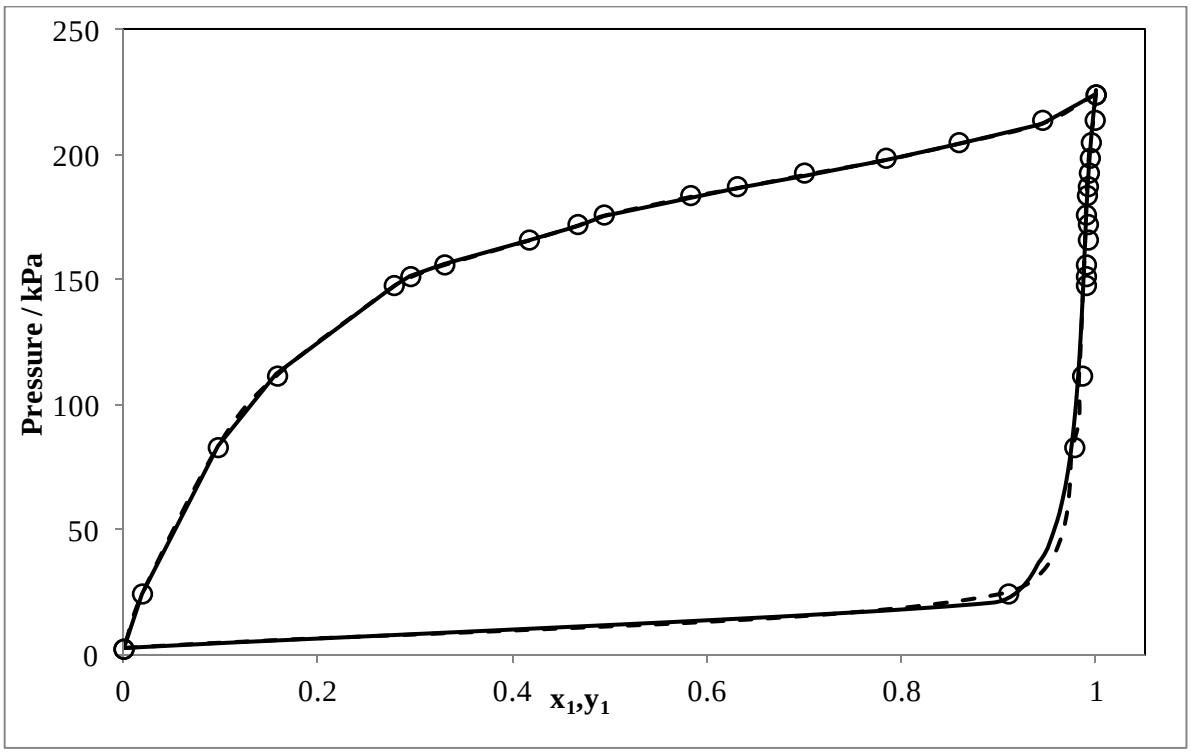

Figure C.5: P-x_1-y_1 plot for the 1-hexene (1) + NMP (2) system at 363.61± 0.02 K ○ , Experimental data; ——, HOC-NRTL (Regressed); - - - -, HOC-NRTL (fixed α_{12} = 0.4567)

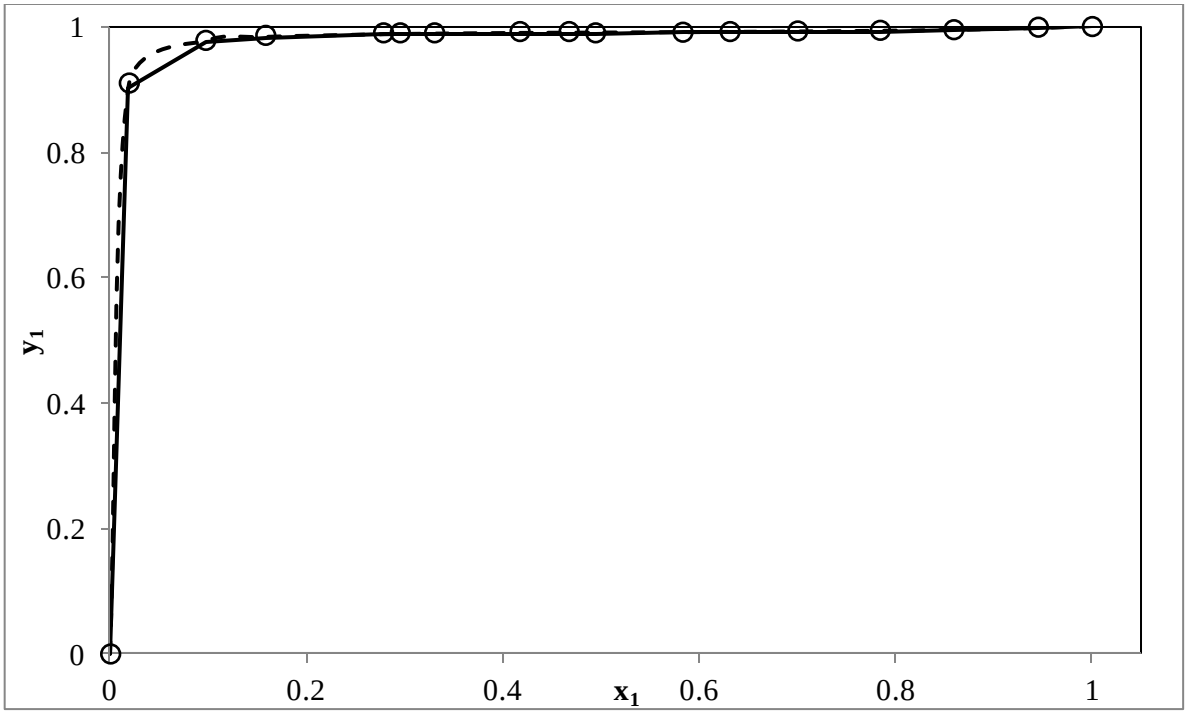

Figure C.6: y-x plot for the 1-hexene (1) + NMP (2) system at 363.61± 0.02 K

○ , Experimental data; ——, HOC-NRTL (Regressed); - - - -, HOC-NRTL (fixed α12 = 0.4567)